Departamento de Biología Molecular

Facultad de Ciencias

Universidad Autónoma de Madrid

In vivo role of DNA polymerases lambda and mu in Genome Stability

ANA AZA MONTOYA

Licenciada en Biotecnología

Directores: **Prof. Luis Blanco Dávila**
Dra. Gloria Terrados Aguado

Madrid 2014

Memoria presentada por Ana Aza Montoya, Licenciada en Biotecnología, para optar al Grado de Doctora en Biociencias Moleculares por la Universidad Autónoma de Madrid.

El trabajo recogido en esta memoria ha sido llevado a cabo en el Centro de Biología Molecular 'Severo Ochoa' (CSIC/UAM), bajo la supervisión del Prof. Luis Blanco Dávila, y la co-dirección de la Dra. Gloria Terrados Aguado.

Fdo: Luis Blanco Dávila

Fdo: Gloria Terrados Aguado

A mis padres

A mi hermano

"I may not have gone where I intended to go, but I think I have ended up where I needed to be."
- Douglas Adams-

"The fool doth think he is wise, but the wise man knows himself to be a fool."
-William Shakespeare-

RESUMEN

El mantenimiento de la estabilidad genómica es crítico para la supervivencia celular y una fiel transmisión del material genético a las células hijas. Las roturas de doble cadena de DNA (DSB) son una de las lesiones más tóxicas y mutagénicas que pueden experimentar las células humanas. Una única rotura puede dar lugar a una pérdida de más de 100 millones de pares de bases de información genética, mientras que una rotura no reparada o reparada incorrectamente en células de mamífero puede originar translocaciones cromosómicas y carcinogénesis. Dos de las principales vías implicadas en reparación de roturas de doble cadena son: Unión de extremos no homólogos (NHEJ) y la recombinación homóloga (HR). En la reparación de DNA por NHEJ, la homología en la secuencia está ausente o se da solo en unos pocos nucleótidos.

Existen evidencias que sostienen que la DNA polimerasa λ y la DNA polimerasa *μ*, ambas miembros de la familia de polimerasas X en mamíferos, tienen papeles no redundantes en NHEJ, debido a sus diferentes grados de complementariedad que pueden aceptar como micro homología.

En esta tesis se ha continuado el estudio bioquímico de las propiedades de Pol*μ*. Proponemos un modelo de expansión de dinucleótidos mediado por Pol*μ* en función del contexto de secuencia. En este modelo Pol*μ* requiere diferentes substratos de DNA, incluidos aquellos que pueden mimetizar los intermediarios de NHEJ. Además, nuestro estudio mecanístico señaló los residuos His329 y Arg387 de Pol*μ* humana como responsables de la regulación de la expansión de nucleótidos que ocurre durante las transiciones de reparación de DNA, o bien promoviendo o bien bloqueando, respectivamente, mediante polimeración iterativa.

Hemos demostrado que la ausencia de Pol*μ* puede provocar una reparación menos eficiente en NHEJ pero más conservadora en el cerebro de ratones de edad avanzada. Utilizando extractos de tejidos de ratones deficientes en Pol*μ* demostramos una reducción en la tasa de error en la síntesis en los ratones Pol$\mu^{-/-}$ cuando soportan lesiones de tipo 8oxoG.

Hemos estudiado la posible relación entre Polλ y la enfermedad de Huntington utilizando modelos murinos. La enfermedad de Huntington (HD) es un desorden neurodegenerativo autosómico dominante y progresivo causado por una expansión de repetición de poliglutamina en la región codificante del gen de la Huntingtina (Htt). Combinamos ratones R6/1(N-mutante Htt) con ratones deficientes de Polλ. El análisis somático de la expansión revela que Polλ está implicada en este proceso, ya que los ratones R6/1;Polλ-/- muestran una menor expansión somática de CAG e incluso lo transmiten a sucesivas generaciones. Además, el área de las inclusiones de huntingtina está reducida en los ratones R6/1;Polλ-/-, pero contrariamente a lo esperado, la prevención de esta expansión no disminuye la progresión de la enfermedad en características como la deficiencia motora o la pérdida de peso.

También hemos investigado y evaluado la contribución de las DNA polimerasas λ y *μ* en la reparación de DSB vía NHEJ en un contexto celular. Para ello, desarrollamos un modelo de ratón deficiente en ambas polimerasas, el cual era tanto viable como fértil. Obtuvimos fibroblastos embrionarios de ratón (MEFs) deficientes en Polλ, Pol*μ* o en ambas (Doble KO). Analizamos la sensibilidad de estos MEFs frente a diferentes drogas capaces de dañar el DNA: desde agentes oxidantes (TBH, H_2O_2) a análogos de nucleósidos utilizados en medicina como agente quimioterapéuticos (Citarabina, Fludarabina, Etopósido), así como su supervivencia frente a radiación ionizante. Los MEFs procedentes del doble KO son más sensibles a estos agentes de daño que los MEFs control procedentes de ratones silvestres, indicando una mayor inestabilidad genómica debido a la ausencia de estas dos polimerasas. Evaluamos el efecto del etopósido en nuestros MEFs a través del ensayo de formación de focos y citometría de flujo: los MEFs doble KO presentan un daño persistente en el DNA en tiempo y el ciclo celular se ve drásticamente afectado provocando un mayor arresto en G2/M. También analizamos la senescencia celular en estas células, observando que los MEFs doble KO entran en senescencia antes que los MEFs control.

Para entender más a fondo las diferencias estructurales y funcionales entre la Polλ y Pol*μ* humanas, que les permiten ser complementarias en su rol en reparación de DSB vía NHEJ, desarrollamos varias quimeras intercambiando dos dominios específicos: “Loop 1”, presente de manera específica en Pol*μ* y TdT confiriendo un rol muy importante a Pol*μ* tanto en NHEJ como en la actividad transferasa terminal, y un dominio “nail” presente en Polλ que interactúa con la hebra molde. En esta tesis hemos podido evaluar *in vivo* estas quimeras confirmando la importancia de estos residuos reconociendo la secuencia en el contexto de NHEJ. Demostramos también que la fosforilación de ciertos residuos específicos aumenta la actividad de las polimerasas λ durante NHEJ.

SUMMARY

The maintenance of genomic stability is critical for cell survival and the faithful transmission of genetic material to daughter cells. The DNA double strand break (DSB) is one of the most toxic and mutagenic DNA lesions experienced in human cells: a single DSB can potentially lead to loss of more than 100 million base pairs of genetic information, while unrepaired or incorrectly repaired DSBs in mammalian cells can lead to large chromosomal translocations and carcinogenesis. Two major pathways have evolved to repair DSBs: non-homologous end-joining (NHEJ) and homologous recombination (HR). In the DNA repair by NHEJ, sequence homology is absent or restricted to few nucleotides.

Evidences support that DNA polymerase λ and DNA polymerase *μ*, both members of the mammalian Pol X family, have complementary, non-redundant roles in NHEJ, due to their different degree of complementarity that they can accept as micro-homology.

I continued the biochemical study of the properties of Pol*μ*. We proposed a model for Pol*μ*-mediated dinucleotide expansion as a function of the sequence context. In this model, Pol*μ* requires an initial dislocation that must be subsequently stabilized, to generate large sequence expansions at different DNA substrates, including those that mimic NHEJ intermediates. Moreover, our mechanistic studies pointed at human Pol*μ* residues His329 and Arg387 as responsible for regulating nucleotide expansions occurring during DNA repair transactions, either promoting or blocking, respectively, iterative polymerization.

We have demonstrated that the absence of Pol*μ* could provoke a less efficient but more conservative NHEJ repair in the brain of old mice. By using tissue extracts from mice deficient in Pol*μ*, we demonstrated a reduced error-prone synthesis in the Pol*μ*-KO mice when tolerating 8oxoG lesions.

We've been working in the possible relationship between Polλ and Huntington's disease using mouse models. Huntington's disease (HD) is an autosomal dominant progressive and fatal inherited neurodegenerative disorder caused by a polyglutamine repeat expansion (CAG) in the coding region of the Huntingtin (Htt) gene. We combined R6/1(N-mutant Htt) mice with Polλ knockout mice. Analysis of somatic expansion reveals that Polλ is implicated in this process, since R6/1;Polλ$^{-/-}$ mice showed lower CAG repeat somatic expansion and even contraction transmitted to successive generations. In addition, the area of huntingtin inclusions is reduced in R6/1;Polλ$^{-/-}$ mice, but contrary to expect, prevention of this expansion does not preclude disease progression such as motor impairment or weight loss.

We have investigated and evaluated the contribution of DNA polymerases λ and *μ* in the repair of DSB via NHEJ in a cellular context. For thus, we have developed a mouse model deficient in both polymerases, which is viable and fertile. We have obtained Mouse Embryonic Fibroblasts (MEFs) deficient in ether Polλ, Pol*μ* or in both (Double KO). We analyzed the sensitivity of these MEFs to different drugs related to DNA damage: from oxidative agents (TBH, H_2O_2) to nucleoside analogous used in medicine as a chemotherapeutical agents (Cytarabine, Fludarabine, Etoposide). Ionizing radiation survival, a well-known agent that induces DNA damage, was also tested in these MEFs. Double KO MEFs are more sensitive to these drugs than wild type MEFs, indicating a major genetic instability due to the absence of both polymerases. We have evaluated the effect of etoposide (a drug which produces DSB) in our MEFs through foci assay and flow cytometry analysis: Double KO MEFs present persistent DNA damage in time and cell cycle is drastically affected provoking major arrest in G2/M. We also analyzed cell senescence in these MEFs. We observed that Double KO MEFs entry in senescence earlier than wt MEFs.

To further understand the structural and functional differences between human Polλ and Pol*μ* that allow them to be complementary in their role in DSB repair via NHEJ, we have developed various chimeras interchanging two specific domains: 'Loop 1', specifically present in Pol*μ* and TdT which confers an important role in Pol*μ*'s NHEJ and terminal transferase activity; and a 'nail' domain present in Polλ that interacts with the template strand. Here we evaluated *in vivo* these chimeras confirming the importance of these residues recognizing the sequence in NHEJ context. We have also demonstrated that the phosphorylation of specific residues enhances Polλ's activity during NHEJ.

TABLE OF CONTENTS

ABBREVIATIONS

8oxoG:	7,8-dihydro-8-oxoguanine
AraC:	Cytarabine
AML:	Acute myeloid leukemia
A-NHEJ:	Alternative NHEJ
ATM Ataxia:	Telangiectasia mutated
ATP:	Adenosine-5'-triphosphate
BER:	Base excision repair
BRCT:	BRCA1 C-terminal domain
C-NHEJ:	Classic NHEJ
dA:	Deoxyadenosine
dC:	Deoxycytidine
DDR:	DNA damage response
DK:	Double KO
DNA-PK:	DNA-dependent protein kinase
DNA-PKcs:	DNA-PK catalytic subunit
DSB:	Double strand break
KO:	Knock-out
IR:	Ionizing radiation
MEF:	Murine Embryonic Fibroblast
MMEJ:	Microhomology-mediated end joining
MMR:	Mismatch repair
NER:	Nucleotide excision repair
NHEJ:	Non homologous end-joining
Nt:	Nucleotide
P:	Phosphate
PARP-1:	Poly (ADP-ribose) polymerase-1
Polß:	DNA polymerase beta
Polλ:	DNA polymerase lambda
Polμ:	DNA polymerase mu
ROS:	Reactive oxygen species
SSB:	Single strand break
TBH:	Tert-Butyl hydroperoxide
TdT:	Terminal deoxynucleotidyl transferase
TLS:	Translesion synthesis

INTRODUCTION

Most living organisms maintain their genetic information through desoxirribonucleic acid (DNA). In order to maintain genomic stability, this information must be transmitted to daughter cells without any alteration. There are two main processes in charge of holding up genomic integrity: DNA replication and repair. DNA replication is the process by which DNA information is error-free duplicated and transmitted from one generation to another, whereas DNA repair involves diverse mechanisms that attempt to restore the DNA sequence when the latter is altered by different endogenous and exogenous damages produced continuously in living cells. When DNA replication faces damages that were not previously solved, certain 'tolerance' should be allowed to make the replication fork progress. In all these mechanisms: DNA replication, repair and damage tolerance the DNA polymerases play a fundamental role.

1 DNA polymerases

Just few years after J.D. Watson and F.H. Crick discovered the DNA anti parallel double helix structure (Watson and Crick 1953), Arthur Kornberg's group discovered the first DNA polymerase, DNA polymerase I (Pol I) from *E. coli* (Kornberg 1957). This DNA polymerase can synthesize DNA following the dictate of a template chain. This was a key aspect in the understanding of how DNA replication happens inside the cell and it also settled the basis for subsequent studies. At present, a bunch of DNA polymerases have been discovered, being involved not only in DNA replication and repair mechanisms, but also in DNA damage tolerance, recombination and mutagenic processes.

Every single polymerase described so far share a common basic structure: its right-handed folding with three main domains named 'fingers', 'palm', and 'thumb' (Ollis et al. 1985). There's only one polymerase lacking the finger domain, the African swine fever virus' DNA polymerase (Maciejewski et al. 2001; Oliveros et al. 1997; Showalter et al. 2001). The residues involved in catalysis are located in the palm domain. The finger domain contributes to bind both to the incoming nucleotide and to the template DNA base. The thumb domain plays an important role setting the DNA duplex in the right position. However, despite this general conformation, specific domains are needed to confer the specific function of each DNA polymerase. For example, there are polymerases with specific domains that confer additional activities such as 3'-5' exonuclease activity or deoxyribose-phosphate lyase activity, among others. There are also additional domains that favor protein or DNA interactions. Biochemically, polymerases can be distinguished by the number of nucleotides they are able to incorporate before dissociating from DNA (distributive polymerases, when these events are only a few; processive polymerases, when hundreds to thousands nucleotides are incorporated per single association event), or by their preferred substrate (template/primer, small gapped DNA, DNA with lesions…).

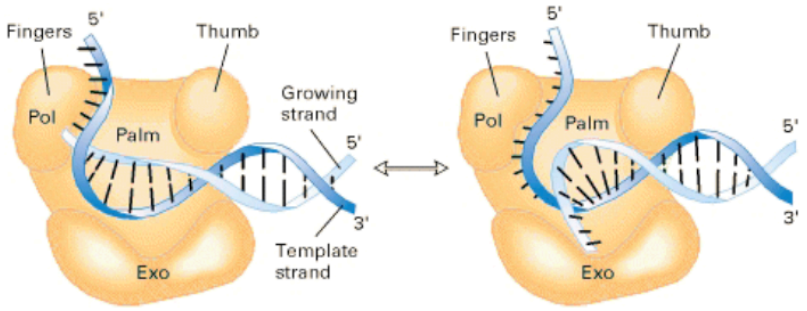

Figure 1. Replicative polymerases. Schematic representation of a replicative polymerase (orange) with exonuclease (exo) and polymerase (pol) domains, showing the correlation between the three subdomains of the polymerase and a right hand: fingers, palm and thumb. The double-stranded DNA substrate is shown in blue.

Finally, one of the fundamental differences among polymerases is their synthesis fidelity, the ability to select the correct nucleotide avoiding mispairs, deletions or insertions (Arana et al. 2008; Kunkel 2004, 2009). The most faithful polymerases are the replicatives, helped by their proof-reading 3'-> 5' exonuclease activity. On the other hand, some genes, as those coding the antigen receptors in B and T cells, require specific processes that modify the genetic information; in this case, specific polymerases with very low fidelity synthesis are crucial partners.

DNA polymerases are classified in families depending on their amino acid sequence similarity with the various polymerases described in *E. coli* (D. K. Braithwaite and Ito 1993; Ito and Braithwaite 1991). Family A consists of the polymerases homologues to *E.coli* Pol's I. Family B includes polymerases similar to *E.coli* Pol's II. Family C, absent in eukaryotes, is composed of *E.coli* Pol's III homologues (Burgers et al. 2001). Family D consists of DNA polymerases only present in Archeas (Cann and Ishino 1999). Family X contains polymerases that participate in DNA repair processes as well as in the generation of genome variability (Bebenek and Kunkel 2004). Finally, Family Y includes DNA polymerases able to synthetize through lesions present in DNA (Sale et al. 2012). Table 1 shows DNA polymerases known up to date.

Greek Name	HUGO name	Family	Proposed Function
Polγ (gamma)	POLG	A	Mitochondrial DNA replication/repair
Polθ (theta)	POLQ	A	TLS; SHM
Polν (nu)	POLN	A	TLS
Polα (alpha)	POLA	B	DNA replication; HR
Polδ (delta)	POLD1	B	DNA replication; NER; MMR; HR
Polε (epsilon)	POLE	B	DNA replication; NER; MMR; HR
Polζ (zeta)	POLZ	B	TLS
Polη (eta)	POLH	Y	TLS
Polι (iota)	POLI	Y	TLS
Polκ (kappa)	POLK	Y	TLS
	REV1	Y	TLS
Polβ (beta)	POLB	X	BER
Polλ (lambda)	POLL	X	Meiosis; BER; NHEJ; V(D)J
Polμ (mu)	POLM	X	SHM; NHEJ; V(D)J
	TDT	X	V(D)J
Polσ (sigma)	POLS	X	Sister Chromatid cohesion

Table 1. Families of human DNA polymerases. SHM: Somatic Hypermutation; HR: Homologous recombination; NER: Nucleotide Excision Repair; MMR: Mismatch repair; BER: Base Excision Repair; NHEJ: Non-homologous End Joining; TLS: Translesion synthesis; V(D)J: Antigen receptor gene rearrangement.

2 Human DNA polymerases involved in DNA repair

The cell constantly faces diverse damages as single-strand breaks (SSBs), double-strand breaks (DSBs), mismatches and intra or inter catenary cross-link (Fig. 2). In order to solve these situations, many different DNA damage response (DDR) mechanisms were developed to coordinate and detect DNA damage, accumulate repair factors where the lesion is located and finally to repair that lesion. DNA polymerases take part in all these processes (see Table 1), with a remarkable role that present of Family X DNA polymerases. In the following section we will discuss the repair processes and characteristics that present this family of DNA polymerases.

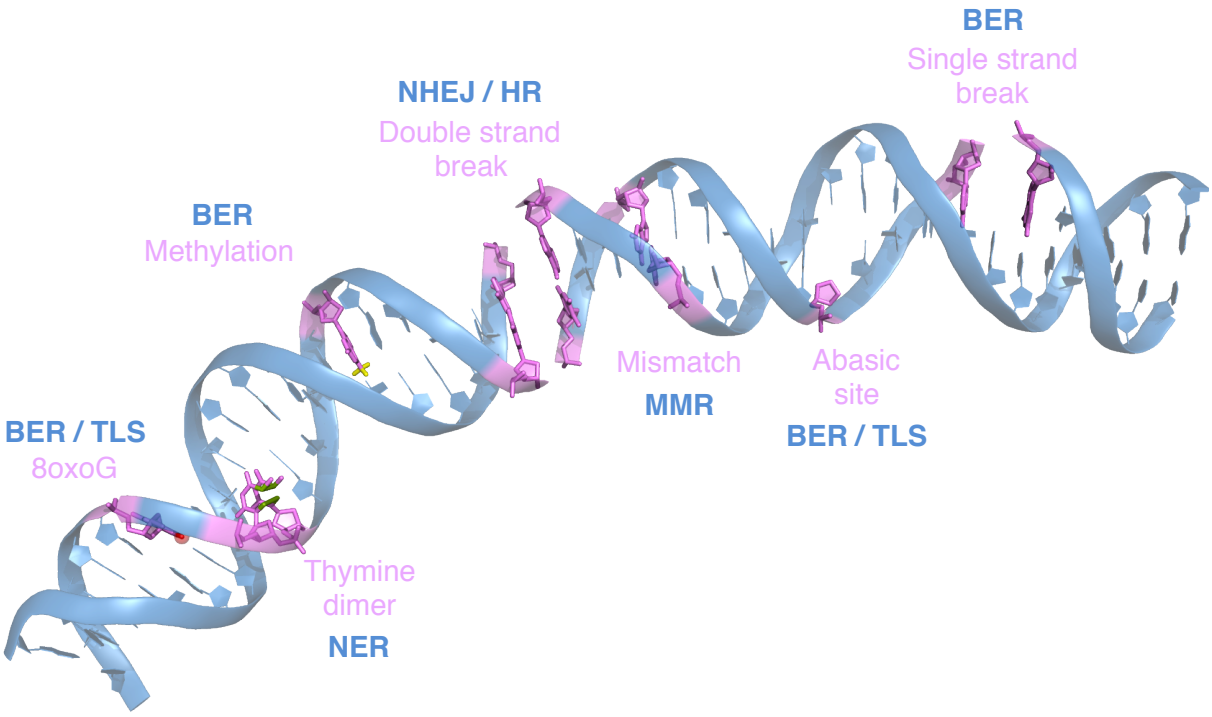

Figure 2. DNA lesions caused by different damaging agents that are targeted by several and repair and tolerance pathways. BER: Base Excision Repair; HR: Homologous recombination; NER: Nucleotide Escision Repair; MMR: Mismatch repair; NHEJ: Non-homologous End Joining; TLS: Translesion synthesis.

2.1 Nucleotide Excision Repair (NER)

The NER mechanism chiefly targets in the lesions that distort the DNA double helix, preferentially caused by UV light. This complicates replication and transcription processes. NER is classified in two subtypes: global genome NER targets lesions produced at any place in the genome, whereas transcription coupled NER targets to lesion encountered by the RNA polymerase during the transcription process. The difference among them consists of the enzymes that recognize the damage (de Laat et al. 1999). The rest of the process is common: the helicases open the double helix, damaged DNA is cut, and new DNA is synthesized by the replication machinery. Endonuclease ERCC1 is crucial during the process.

2.2 Mis-Match Repair (MMR)

This is one of the most important DDR mechanisms. It occurs mainly during DNA replication, when incorrect nucleotides are inserted or as a result of slippage produced by DNA polymerases creating small bubbles or protuberances in the double helix. Many enzymatic activities participate in this repair process that begins with the recognition of the error afterwards protein complexes are recruited to interact in turn with replicative factors. The DNA strand targeted for repair is the newly synthesized. Thus, the NER process removes the mismatch and the subsequent DNA resynthesis involves diverse proteins, such as Polymerases like Polε and Polδ, RPA, PCNA, or endonuclease FEN-1 (Schofield and Hsieh 2003).

2.3 Trans-lesion Synthesis (TLS)

During the S phase of the cell cycle the DNA template still contains different lesions that were not repaired before replication is initiated. If these lesions that change the normal geometry of the DNA (abasic sites, contiguous covalent bonds between bases, etc…) remain unsolved, they can result in a block of the replication machinery that can ultimately lead to cell death (Boudsocq et al. 2004). To overcome this barrier, a number of specialized trans-lesion synthesis (TLS) DNA polymerases have evolved to be recruited to the site of the lesion. These polymerases are not strictly repair enzymes, but involved in damage tolerance to allow cell survival. The TLS polymerases are capable of DNA synthesis opposite damaged DNA, after which the replicative DNA polymerase can continue normal DNA synthesis. These TLS polymerases are generally error prone and have been implicated in drug resistance in bacteria and in different forms of cancer in humans (Sale et al. 2012). These polymerases are grouped in the Y family (Polη, Polι, Polκ and REV1), except Polζ that belongs to B family (Prakash et al. 2005).

2.4 Base Excision Repair (BER)

This is the principal mechanism that repairs DNA lesions affecting DNA bases, as the presence of uracil in DNA, modification or spontaneous loss of DNA bases, oxidation, alkylation, deamination, or insertion of modified bases such as dUTP or 8-oxo.dGTP (Fortini et al. 2003). There are two well-known BER pathways in mammals: 'short patch' BER, where one nucleotide is replaced, and 'long patch' BER, which involves the synthesis of 2-8 nucleotides (Dogliotti et al. 2001). In both pathways, there is a specific DNA glycosidase that recognizes and excises the modified base leaving an abasic site in the DNA. APE endonuclease eliminates the 5' phosphodiester bond in the abasic site, leaving a nick in the 3'OH DNA and a 5' desoxirribose phosphate residue (dRP). In short patch BER, this residue is deleted thanks to a polymerase endowed with dRP lyase activity that removes the dRP and fills the gap left in the DNA. This dRP residue may be also removed by a glycosilase that possesses AP-lyase activity. In this case, Polynucleotide kinase (PNK) with its 5' DNA kinase and 3' DNA phosphatase activity, replaces the OH group and the P group in 3' and 5', respectively. Subsequently, the polymerase fills the gap and a ligase completes the process sealing the union (DNA ligase I or XRCC1/Ligase III complex).

Long patch BER acts when the dRP residue is modified (oxidized or reduced) and it can't be removed. In that moment, DNA synthesis associated to strand displacement is produced, generating a displaced single strand that will be removed by FEN1 endonuclease. Ligase ends the processes by sealing the nick between both chains.

There are several DNA polymerases involved in BER. Particularly, there is a Family X member, Polβ, which is specifically involved in this mechanism. This has been demonstrated *in vitro* and *in vivo* (Burgers et al. 2001; Kubota et al. 1996; Sobol et al. 1996). Polβ interacts with many proteins involved in this process such as AP-endonuclease (Bennett et al. 1997), DNA ligase I and the heterodimer XRCC1/DNA Ligase III (Caldecott et al. 1996). Taken together, all of these interactions

could facilitate the enzymatic steps involved in the process. Polβ also plays an important role in long patch BER, beggining with DNA synthesis and strand displacement in order to facilitate the labour of replicative polymerases. There are other polymerases involved in BER mechanism: Polλ belongs to Family X and presents dRP lyase activity (Garcia-Diaz et al. 2000; Garcia-Diaz et al. 2001), and Polι from Family Y, involved in a more specific BER process (Bebenek et al. 2001). Additionally, PolϒΥ (from Family A) is involved in BER in mitochondria.

2.5 Double Strand Break Repair (DSB)

DSBs may occur during physiological process such as replication or meiosis, due to external agents like IR (Morgan et al. 1996) or as a consequence of cellular metabolism (Karanjawala et al. 2002). This kind of lesions is strongly dangerous for the cell, as DSB may lead to the loss of genetic material or chromosomal rearrangements (translocations, inversions, deletions). All may result in tumor processes mediated by oncogene's activation or tumor-suppressor's genes inactivation, or cell death. Therefore, the ability to repair these strand breakages is essential to maintain genomic instability and cell survival. For this reason, Eukaryotic organisms have developed two different mechanisms: Homologous Recombination (HR) and Non-homologous End Joining (NHEJ). In mammals, non-homologous end joining occurs through all the cell cycle, whereas homologous recombination is restricted to S and G2 phase (Lieber 2008; Takata et al. 1998). It is known that both mechanisms can operate coordinately (Shrivastav et al. 2008).

2.6 Homologous Recombination (HR)

Homologous recombination is based in the existence of a second copy of the region be repaired. This region serves as a back-up template for DNA synthesis, allowing genomic integrity to be restored faithfully (West 2003). This process requires the processing of DNA ends by a 5'->3' endonuclease, generating fragments with 3'-protruding ssDNA where the repair proteins will bind. Replicative Protein A (RPA) removes secondary DNA structures allowing Rad51 and Rad52 binding. Rad55 and Rad57 interact with this nucleoprotein filament. Rad51 promotes the invasion of the sister chromatid allowing the interchange with the DNA homologous and the damage repair. Genomic stability is guaranteed thanks to this faithful mechanism.

2.7 Non Homologous End Joining (NHEJ)

During DNA repair by NHEJ, sequence homology between the two ends is either absent or restricted just to a few nucleotides. The proteins involved in this process do not recognize the DNA sequence, but the structure of the damaged DNA (Lieber et al. 2004). NHEJ can be a mutagenic process, contributing to genomic variability and also implicated in cellular processes such as antibody generation. This is the main repair process of DSBs in Eukarya, being operational during all the cell cycle.

The first step is the DNA break recognition by the Ku70/Ku80 heterodimer (Fig. 3). This binding impedes the DNA duplex degradation (Walker et al. 2001). Secondly, DNA-PK binds the DNA ends (Gottlieb and Jackson 1993), allowing the internalization of the Ku heterodimer and favoring the joining of both sides of the break through protein-protein interactions. (Chen et al. 2000; Yaneva et al. 1997). In most of the cases, the ends can not be joined directly; they have to be processed previously. Sequence analysis done in the break points have revealed that this processing requires the alignment of the ends through microhomologies (complementary sequences from 1 to 4 nucleotides) (Kramer et al. 1994; Roth and Wilson 1986). When there is no homology among the sequences, the system generates it through nucleases or DNA polymerases (T. E. Wilson and Lieber 1999). This enzymes are necessary sometimes to delete distortions or to fill gaps generated as a consequence of the alignment produced previously (Hefferin and Tomkinson 2005).

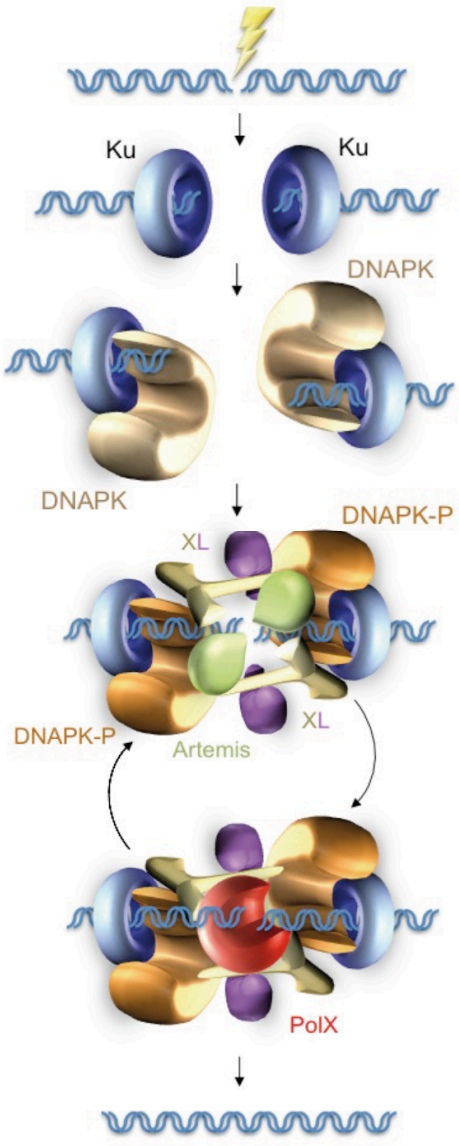

The proteins needed to process the ends are recruited by Ku/DNA-PK complex. Artemis 3'->5' exonuclease is phosphorylated by DNA-PK, and the polynucleotide kinase (PNK) may also intervene in the process (Chappell et al. 2002). If the processing is successful and the ends are compatible, XRCC4/ligase4 complex is recruited and DNA is ligated (Grawunder et al. 1997; Teo and Jackson 1997; T. E. Wilson et al. 1997).

Figure 3. Non-homologous end-joining pathway in eukaryotes. This pathway acts repairing damage-generated DSBs. The Ku70/80 heterodimer is the first protein factor to arrive at the site of the break and bind the DNA ends. The DNA PKcs is then recruited and forms a complex with Artemis. The phosphorylated Artemis acts as an endonuclease, generating ssDNA protruding regions at the ends, and after this the complex dissociates from the DNA. The X family DNA polymerases are then in charge of searching for microhomologies or generating them, as well as filling in the gaps generated. Finallly, the XRCC4/Ligase IV complex seals the break. (*Scheme from María José Martín Thesis*).

However, if the ends are non-compatible, a DNA polymerase will fill the gap generated after the alignment. Family X polymerases, Pol*μ* (Dominguez et al. 2000) and Polλ (Garcia-Diaz et al. 2000), participate in this process (Lee et al. 2004; Y. Ma et al. 2004; Mahajan et al. 2002; Ramsden 2011). Pol*μ* could generate connectivity in non-compatible ends through its terminal transferase activity (Juarez et al. 2006), whereas Polλ requires sequence complementarity in the ends to be joined (Ramsden 2011).

A similar factor to XRCC4 protein has been described in mammals in the past years, XLF (XRCCA-like factor) or Cernunnos, that interacts with XRRC/DNA ligase IV complex and promotes ends ligation (Ahnesorg et al. 2006; Hentges et al. 2006). In *S. cerevisae's,* the NHEJ mechanism involves the proteins Ku70/Ku80, MRX complex (Mre11-Rad50-Xrs2), DNA ligase IV (Dnl4), Nej1 (XLF homologous) and ScPolIV homologues to DNA-PK or Artemis (Daley et al. 2005) have not being identified. XRCC4, DNA-PK or Artemis were not identified in *S. pombe,* although the Ku70/Ku80 complex, Xlf1, DNA ligase 4 and SpPolIV have been involved in NHEJ in this organism (T. E. Wilson and Lieber 1999).

2.8 Alternative NHEJ

In the absence of some classical NHEJ factors (such as Ku, XRCC4 or DNA ligase IV) there is an alternative end-joining pathway that operates and DSBs: alternative NHEJ (alt-NHEJ) or microhomology-mediated end-joining (MMEJ). These events occasionally entail small deletions and the necessity of short sequence homologies at the break point (Grabarz et al. 2012; Guirouilh-Barbat et al. 2007; J. L. Ma et al. 2003; Mladenov and Iliakis 2011). MMEJ repair occurs in a proportion of V(D)J recombination events (Yan et al. 2007). Besides, it is also related to several carcinogenic processes, suggesting a role for MMEJ in translocation breakpoints in human cancers and chemotherapy resistance (Greenman et al. 2007; Hartlerode and Scully 2009).

3 X Family of DNA polymerases

X Family of DNA polymerases is composed by 4 members: TdT, Pol*μ*, Polβ and Polλ. Among their common characteristics is the involvement in DNA repair process, their small sized (monomeric) an their lack of a 3'->5' exonuclease activity; and they present distributive synthesis. All the members share a structural organization composed by Polβ core that comprehends an N-terminal region (8kDa domain) and the polymerization domain (31kDa). This core is formed by the domains finger, palm and thumb. Some of these family members present additional domains involved in different functions (Fig. 4) (Bebenek et al. 2003; Prasad et al. 1994; Ruiz et al. 2001).

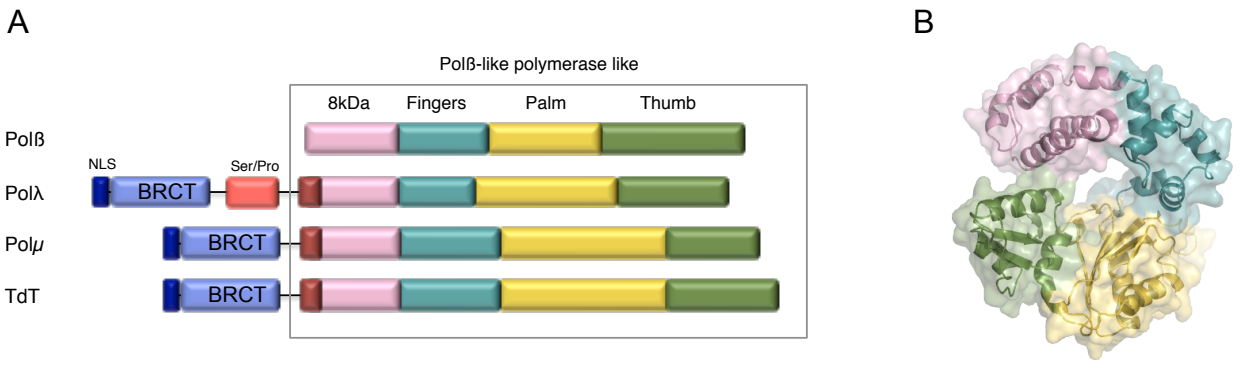

Figure 4. Modular organization of the family X polymerases. A) Schematic representation of the domains present in family X members. On the basic Polß-like domain scheme (8 kDa, fingers, palm and thumb) are shown the additional elements present in the other members (Ser/Pro rich region, nuclear localization sigal -NLS-, BRCT domain). **B)** Surface representation of Polß with the domains colored as they are in A.

3.1 Evolution of the X Family of DNA Polymerases

X Family members are present in all monophyletic taxa: Eukaria, Bacteria and Archea; even in virus whose genome is DNA (Oliveros et al. 1997). The high degree of conservation at primary and tridimensional structure suggests that their evolution comes from a common ancestor. Higher eukaryotes present more than one member of this X Family. In contrast, there are some organisms like *Caenorhabditis elegans* and *Drosohopila melanogaster* (Burgers et al. 2001) where Family X members have not been described. In yeast there is a single member from this family, Pol4. Both Pol4 from *S. cerevisae* (ScPol4) and *S. pombe* (SpPol4) present a core structure ß-like, additional domains such as BRCT and Ser/Pro, and both have dRP lyase activity (Bebenek et al. 2005; Gonzalez-Barrera et al. 2005). Based on sequence identity, we can argue that ScPol4 is Polλ's orthologous in humans (24% sequence identity) and ScPol4 is Pol*μ*'s orthologous (27% sequence identity).

The modular organization of different members of the X family (Fig. 5) highlights the existence of a conserved Polß-type core present from viruses to eukaryotes. African swine fever virus (ASFV) possesses the smallest version of this core that contains only the palm and thumb subdomains of the polymerase domain (Oliveros et al. 1997). Despite its small size, ASFV PolX presents AP-lyase activity, which supports a possible role in the viral BER pathway (Garcia-Escudero et al. 2003). During evolution, the members of the X family diverge by acquisition of additional domains involved in regulatory and/or enzymatic activities that keep a close relationship with their physiological function.

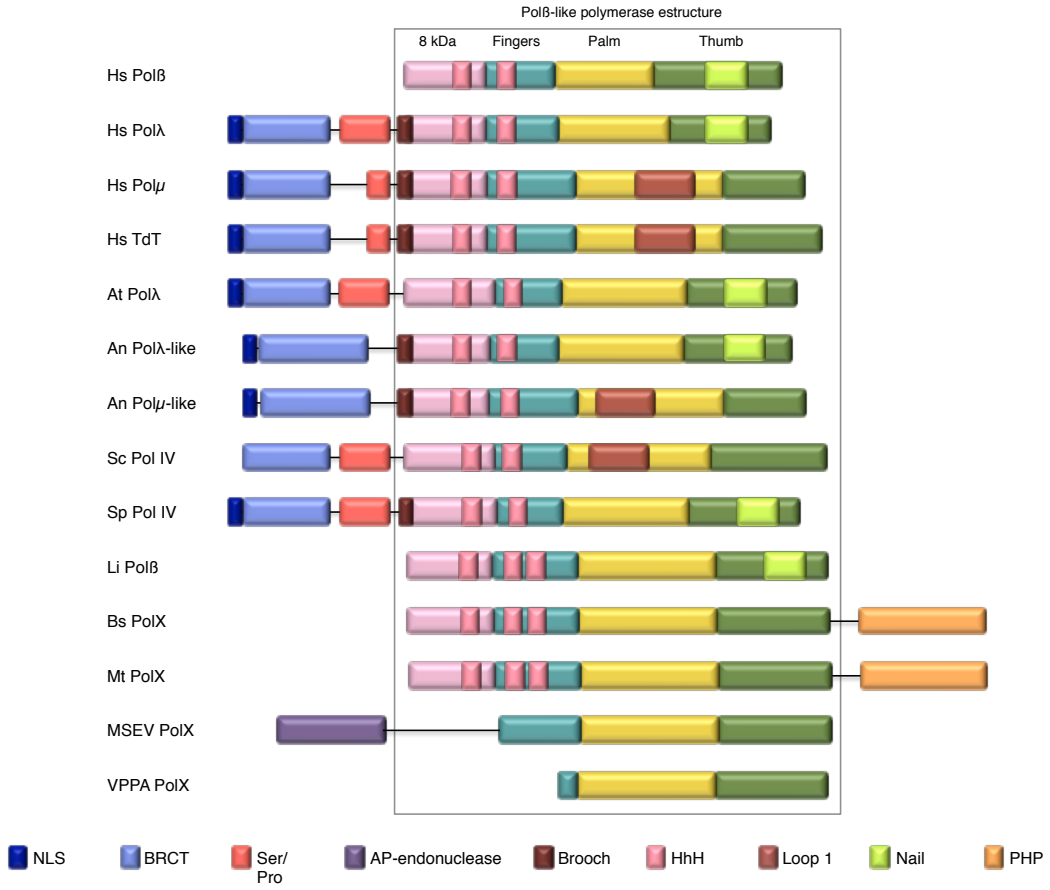

Figure 5. Modular organization of the family X polymerases. Schematic representation of the domains present in family X members from viruses to higher eukaryotes. Regarding the coloring of the 8 kDa domain, dark green represents dRP lyase-containing domains while bright green color indicates the lack of such activity. Sc: Saccharomyces cerevisiae; Sp: Schizosaccharomyces pombe; Li: Leishmania infantum; ASFV: African swine fever virus; Bs: Bacillus subtilis; Mthe: Methanobacterium thermoautotrophicum; Dr: Deinococcus radiodurans

BRCT domains are present in Pol4, Polλ, Polμ and TdT. This domain plays a role in processes such as V(D)J recombination and NHEJ repair, by recruiting Ku proteins to the site of the break (Tseng and Tomkinson 2002). The specificity of each polymerase to access a precise substrate may reside in the mild differences found in the amino acid sequence of each BRCT domain.

The 8 kDa domain hosts the dRP-lyase activity central in the BER pathway. Whereas Polß, a housekeeping DNA repair polymerase involved in the protection against oxidative damage, has lost

some accessory domains during evolution, the 8 kDa domain has been preserved in order to its essential function.

3.2 From the oldest member of the X family to the youngest: From Polλ to Polß

Polλ shares amino acid sequence similarity with Pol4 in yeast and also in plants (*Arabidopsis thaliana*). This suggests Polλ as the closest member to the common ancestor in X family (Fig. 6). Its many and diverse functions coincide with the different mechanisms that the ancestral polymerase necessarily would do. In this regard, the presence of a Ser/Pro-rich domain allows cell-cycle and DNA damage response (DDR) regulation of Polλ in processes like BER, NHEJ and V(D)J recombination. Taking this common ancestor as a starting point, the X Family has been specialized in diverse processes related to DNA repair. Among them, BER is carried out by Polß (although Polλ participates in certain situations); DSB by NHEJ carried out by Polλ and Pol*μ* depending on the break context and finally, V(D)J recombination performed by Polλ, Pol*μ* and TdT with non-redundant functions (Bertocci et al. 2006). This specialization through evolution confers to each one of these polymerases great efficiency in all biological process they participate.

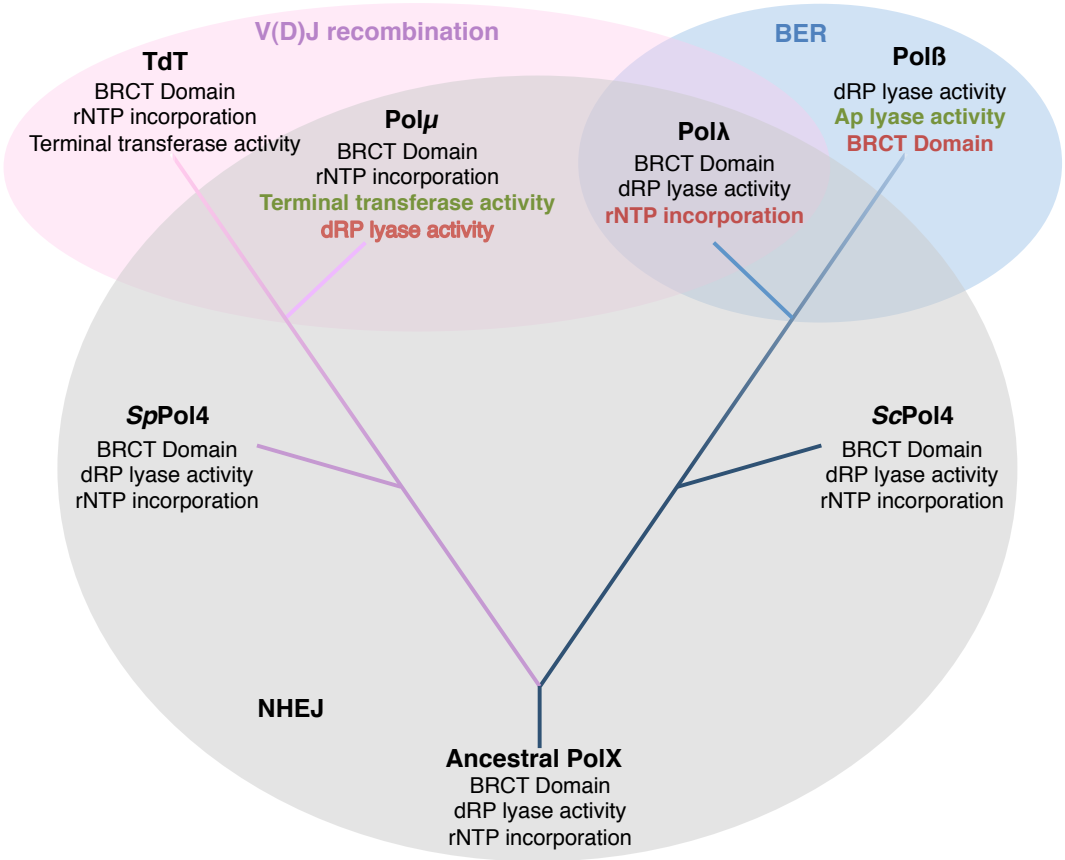

Figure 6. Evolution of family X polymerases. Red color indicates the loss of an activity or feature, green color indicates the gain of an activity or feature. See text for details.

Polλ, the oldest member of the family Polλ, presents not only the BRCT domain needed to interact with NHEJ factors, but also dRP-lyase activity for an efficient BER. Indeed, Polλ harbors a long nail motif involved in dealing with misaligned substrates and scrunching. The Ser/Pro domain is present only in Polλ and its *S.cerevisae* yeast homologue, pol IV. This region has been suggested to play a role in modulating the fidelity and participation of Polλ in many processes such as repair by BER, NHEJ and V(D)J recombination. Recent studies have shown that several serine residues in this region are modified by phosphorylation, thereby protecting Polλ from ubiquitin-dependent degradation and modulating its actitivity in the MutYH glicosylase-dependet BER pathway (Markkanen et al. 2011; Markkanen et al. 2012b).

In contrast, as a younger member of the family, Polß has lost most of these characteristics such as the BRCT and Ser/Pro-rich domains, but increases the contacts with the 5' phosphate DNA group, and developed both dRP-lyase and AP-lyase activities to increase its focus on short-patch BER repair. The lost of the BRCT domain does not allow Polß to be recruited to DNA DSBs, but, on the contrary, Polß has developed new protein interactions with other BER factors (Dianova et al. 2004; Gryk et al. 2002; Marintchev et al. 2000). As a housekeeping gene, Polß is unique in the family and lacks CDK phosphorylation sites.

3.3 The influence of Pol*μ* and TdT in generation of variability in the immune system

Although the phylogenetic branch corresponding to Pol*μ* and TdT appears in the phylogenetic tree sooner than Polß, the acquisition of terminal transferase activity corresponds to recent evolution, concurring with the development of V(D)J recombination in mammals.

TdT shares the common Polß-like core with 8 kDa, fingers, palm and thumb and the C-terminal BRCT domain. But TdT has lost the essential residues for the dRP-lyase activity, which also occurs in Pol*μ*. Both polymerases, TdT and Pol*μ*, are able to add nucleotides in the absence of a primer strand (Brissett et al. 2011). Whereas in Pol*μ* this situation benefits DSB repair, in TdT plays a physiological role in generating random nucleotide additions during recombination. Besides, they are both able to incorporate ribonucleotides (Boule et al. 2001; Nick McElhinny and Ramsden 2003; Ruiz et al. 2003).

Pol*μ* is more ancient in evolution than TdT. This means that the function of Pol*μ* has to be more general in DNA repair in NHEJ. However, the appearance of Pol*μ* in the phylogenetic tree of the X family could implicate the need of generating variability during development of the adaptive immune response as well as maintaining a DNA repair function. The presence of a flexible Loop1 supports the role of Pol*μ* in as a template-directed polymerase.

Despite their close amino acid sequence similarity and some common biochemical and structural characteristics, Pol*μ* is specialized in NHEJ repair whereas TdT function is limited to the generation of variability in immune system development.

Taking all this information together, it is suggested that there are very subtle biochemical and structural differences, which appear to be crucial for their separated cellular functions. As shown in

Fig. 7, a gradient of template dependency for each polymerase *in vitro* has been described, as they possess decreasing requirement for complementary sequence opposite the primer terminus and incoming triphosphate. While Polλ normally requires a template to fill gaps, Pol*μ* can direct template-independent synthesis across a DSB with no terminal microhomology (Nick McElhinny et al. 2005a).

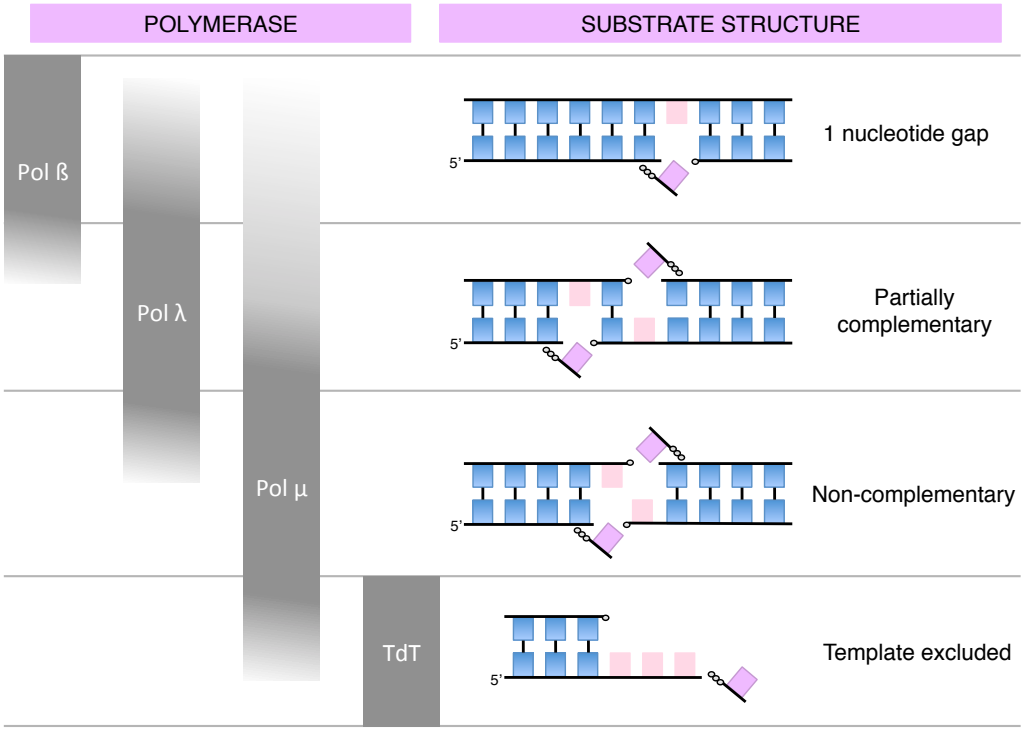

Figure 7. A gradient of template dependency of X family DNA polymerases. The spectrum of each of the vertebrate X family member (left) on various substrates (right) is shown, with decreasing dependency on template strand from top to bottom. Incoming nucleotide triphosphate, dark pink. Template nucleotide, light pink. The grey ball indicates the presence of a 5'-P group in the downstream strand of the substrate. *(Adapted from Ramsden and Asagoshi 2012)*

3.4 X family members have non-redundant roles and expression patterns

As mentioned before, The four members of the X family of polymerases became specialized in different processes of DNA synthesis associated with repair: BER, NHEJ and V(D)J recombination. Interestingly, there are slight differences in the biochemical properties that make all the members of this family highly specialized in their function, carrying out non-redundant tasks (Table 2).

Despite the fact that Polß is a housekeeping gene, the other members of the family present different expression patterns among tissues. Polß, the youngest member of the X family, is highly expressed in brain tissue (Hirose et al. 1989). Interestingly, as neuronal cells can suffer from a high level of oxidative lesions (Nakamura and Swenberg 1999; D. M. Wilson, 3rd and McNeill 2007) Polß would be required to minimize the accumulation of DNA damage in these cells. Polλ, on the other hand, is highly expressed in testis and in the fetal liver (Garcia-Diaz et al. 2000). Recently, it was reported that Polλ was expressed at high level in the respiratory epithelia suggesting a role in DNA repair processes against DNA damage caused by smoking (Ohba et al. 2009).

Pol X family member	Polβ	Polλ	Polμ	TdT
Template-dependent DNA polymerase	+	+	+	-
Template-independent activity DNA polymerase	-	+	+	+
Template-dependent RNA polymerase	+	-	+	-
Template-independent activity RNA polymerase	-	+	+	+
Synthesis of DNA *de novo*	-	+	+	+
dRP-lyase activity	+	+	-	-
Physiological functions	BER	BER; NHEJ	NHEJ; V(D)J recombination	V(D)J recombination

Table 2. Functional properties of X family DNA polymerases. BER: Base Excision Repair; NHEJ: Non-homologous End Joining; V(D)J: Antigen receptor gene rearrangement.

Contrary to Polß and its ubiquity, TdT expression is restricted to primary lymphoid tissues such as thymus or bone marrow. Pol*μ* is strongly expressed in lymphoid tissues in human too, but unlike TdT, basal expression of Pol*μ* is observed in a wide range of tissues, specifically in the brain (Dominguez et al. 2000).

Mouse models for each of the four polymerases were obtained in order to get direct evidence of their *in vivo* functions. Starting with Polß, a complete knock-out resulted unviable due to apoptosis of post-mitotic neurons as a consequence of defective DNA SSB repair (Sugo et al. 2000). The principal mediator of the apoptosis in Polß defective background was p53 (Sugo et al. 2004).

The knock-out mice show slower cellular proliferation, increased apoptosis, deficient gap-filling during BER and thus, chromosomal aberrations (Allinson et al. 2001). In summary, Polß plays an important role in meiosis, neuronal development, DNA repair and genomic stability.

In the case of Polλ, it was shown that these mice are viable and fertile, and lack diversity in the junctions in the heavy chain of the TCR receptors (Bertocci et al. 2006), indicating that Polλ might act before TdT during heavy chain rearrangement. Besides, it was demonstrated that Polλ has a role as a back-up in the absence of Polß in BER to protect cells from oxidative damage (E. K. Braithwaite et al. 2005a; E. K. Braithwaite et al. 2005b). In addition, Polλ is responsible for most of the error-free gapfilling in the presence of the 8oxoG lesion in DNA by an accurate repair pathway that is coordinated by the MutY glycosylase homologue (MutYH) and Polλ *in vitro* and *in vivo* (Maga et al. 2008; Markkanen et al. 2012a)

It was shown that in mice deficient for Pol*μ* are viable and fertile (Bertocci et al. 2002). Moreover, in the embryonic stage when TdT is not expressed, it was shown that Polμ is responsible for the observed N-additions at the post-gastrulation DJ_H joints during immunoglobulin gene rearrangements (Gozalbo-Lopez et al. 2009). It was also described that the antibody repertoire was drastically affected because the TCR receptors of B- and T- lymphocytes had fewer or none N-additions from the fetal to the adult animal (Gilfillan et al. 1993; Komori et al. 1993) being TdT responsible for 90% of the diversity of the α β TCR receptor repertoire (Cabaniols et al. 2001).

Moreover, Pol*μ* mice are defective in immunoglobulin light chain rearrangements compromising B cell differentiation and development of the bone marrow (Bertocci et al. 2003); defective in somatic hypermutation and V(D)J recombination (Lucas et al. 2005); hypersensitive to γ-irradiation due to a defective DSB repair also in non-hematopoietic tissues (Lucas et al. 2009a), and recently, it was shown that Pol*μ* deficiency increases resistance to oxidative damage and delays liver aging (Escudero et al. 2014). Taken together, all these results support multiple roles of Pol*μ* in the immune system during hematopoietic development, somatic hypermutation and class-switch recombination, and besides, in the contribution to DNA repair of DSB via the NHEJ pathway.

The differences mentioned among the members of the X family make them of special interest in the study of the non-redundant roles they might have. Moreover, the subtle differences between Polλ and Pol*μ* shown *in vitro* also support a non-redundant role of these enzymes in NHEJ, and whose *in vivo* significance is studied in this thesis. Determining the *in vivo* role of Pol*μ* and Polλ will help to elucidate one important piece of the machinery that repairs DNA damage.

OBJECTIVES

During the present PhD Thesis our fields of interest have been the following:

1. Study the behavior of Pol*μ* on iterative DNA sequences.

2. Analyzing the genomic instability in the double deficient murine model in DNA polymerases lambda and mu.

3. Study the role of DNA polymerases lambda and mu in DNA repair and damage tolerance.

4. Analysis of the effect of of DNA Polymerase λ on CAG somatic expansion in a Huntington´s disease murine model.

5. Study of the non-overlapping functions of DNA polymerases lambda and mu during NHEJ *in vivo*.

MATERIALS AND METHODS

1 Reagents

Ultrapure NTPs, dNTPs, ddNTPs, [α -32 P]dNTPs (3000 Ci/mmol) and [γ -32 P]ATP (3000 Ci/mmol) were purchased from GE Healthcare (USA). T4 polynucleotide kinase and purified TdT were obtained from New England Biolabs (Beverly, MA, USA). Polλ was obtained as described in(Garcia-Diaz et al. 2000). Polμ mutants, and were obtained as described in (Dominguez et al. 2000; Ruiz et al. 2001). Site directed mutagenesis and purification of Pol*μ* mutants H329G, R387K and R387A was done as described in (Andrade et al. 2009). Inorganic salts, acids, bases and organic compounds were delivered by Merck, Sigma and Fluka.

2 DNA Oligonucleotides used in DNA polymerization and NHEJ assays

DNA oligonucleotides were obtained from Isogen, Invitrogen, Sigma and Eurogentec. In each case, the indicated PAGE or HPLC-purified oligonucleotides were labeled at their 5' ends with [γ -32 P]ATP for detection during biochemical assays. Synthetic DNA oligonucleotides were obtained from Invitrogen:

D (5'-ACGACGGCCAGT) was used as downstream oligonucleotide;

$T(GAC)_2$ (5´-ACTGGCCGTCGT**CAGCAG**GTACTCACTGTGATC),

$T(GTC)_2$ (5'-ACTGGCCGTCGT**CTGCTG**GTACTCACTGTGATC),

$T(AAG)_2$ (5'-ACTGGCCGTCGT**GAAGAA**GTACTCACTGTGATC),

$T(CTT)_2$ (5'-ACTGGCCGTCGT**TTCTTC**GTACTCACTGTGATC),

$T(CAG)_2$ (5'-ACTGGCCGTCGT**GACGAC**GTACTCACTGTGATC),

$T(GAA)_2$ (5'-ACTGGCCGTCGT**AAGAAG**GTACTCACTGTGATC),

$T(GAA)_1$ (5'-ACTGGCCGTCGT**AAG**GTACTCACTGTGATC),

$T(AAA)_1$ (5'-ACTGGCCGTCGT**AAA**GTACTCACTGTGATC),

$T1(CAA)_1$ (5'-ACTGGCCGTCGT**AAC**GTACTCACTGTGATC),

$T(TAA)_1$ (5'-ACTGGCCGTCGT**AAT**GTACTCACTGTGATC),

$T2(CAA)_1$ (5'-ACTGGCCGTCGT**AAC**CTACTCACTGTGATC),

$T(CTT)_1$ (5'-ACTGGCCGTCGT**TTC**CTACTCACTGTGATC),

$T(CCC)_1$ (5'-ACTGGCCGTCGT**CCC**CTACTCACTGTGATC),

$T(CGG)_1$ (5'-ACTGGCCGTCGT**GGC**CTACTCACTGTGATC) were used as templates;

P1 (5'-GATCACAGTGAGTAC),

P2 (5'-GATCACAGTGAGTAG),

P3 (5´-GATCACAGTGAGTACCC) and

P4 (5´-GATCACAGTGAGTACCCC) were used as primers.

Oligonucleotide D contains a phosphate at 5'-end. DNA oligonucleotides used as primers (P1 and P2) were labelled at its 5'-end with [γ^{32}P-ATP] and T4 polynucleotide kinase. To construct the different gapped molecules used in the polymerization assays, P1 was simultaneously hybridized to

a downstream oligonucleotide D and one of the following template oligonucleotides: $T(GAC)_2$, $T(GTC)_2$, $T(AAG)_2$, $T(CTT)_2$, $T(CAG)_2$, $T(GAA)_2$, $T(GAA)_1$, $T(AAA)_1$, $T(CAA)_1$ or $T(TAA)_1$; P2 was simultaneously hybridized to D and one of the following template oligonucleotides: $T(CAA)_1$, $T(CTT)_1$, $T(CCC)_1$ or $T(CGG)_1$; P3 and P4 were hybridized to D and $T(CGG)_1$. For NHEJ assays, oligonucleotides D3 (5´-CCCTCCCTCCGCGGC), D3BB1 (5´-CCCTCCCTCCGCGGAC), D3BB2 (5´-CCCTCCCTCCGCGAGC), D3T (5´-CCCTCCCTCCGCGGT), D3TT (5´-CCCTCCCTCCGCGGTT) and D3G (5´-CCCTCCCTCCGCGGG) were used as labelled primers, hybridized to oligonucleotide 5´-GGGAGGGAGGC, while oligonucleotides D4 (5'-CGCGCACTCACGTCCCGGCC) or D4-AA (5'-5'-CGCGCACTCACGTCCCAACC) were hybridized with the 5'-phosphate-containing D1 (5'-GGGACGTGAGTGCGCG) to form a template/downstream substrate. Hybridizations were performed in the presence of 50 mM Tris-HCl pH 7.5 and 0.3 M NaCl. All the oligonucleotides described above were purified by electrophoresis in 8 M urea/20% polyacrylamide gels.

3 Biochemical assays

3.1 DNA polymerization assays

Different DNA substrates containing 5'-P labelled primers (described above) were incubated with the indicated amounts of either differents proteins indicated in each case. The reaction mixture, in 20 μl, contained 50 mM Tris-HCl pH 7.5, 1 mM DTT, 4% glycerol and 0.1 mg/ml BSA, in the presence of 4 nM of the indicated DNA polymerization substrate, 50 μM of the NTP/dNTP indicated in each case, and activating metal ions. After the incubation indicated in each case, reactions were stopped by adding gel loading buffer (95% (v/v) formamide, 10 mM EDTA, 0.1% (w/v) xylene cyanol and 0.1% (w/v) bromophenol blue). Samples were analyzed by 8 M urea/20% PAGE and autoradiography.

3.2 NHEJ assays

NHEJ polymerization assays were carried out essentially as described above for polymerization assays, but using independent DNA primer (labeled) and template (unlabeled) molecules. When indicated, we used variable concentrations of ddNTPs instead of dNTPs/NTPs to limit incorporation to a single nucleotide on the 3′ -end of the labeled oligonucleotide.

3.3 Evaluation of mutagenic DNA repair activity

Extracts from wild type C57BL6, KOμ, KOλ and Double KO mice were prepared essentially as previously described (Biade et al. 1998). Briefly, tissues were washed three times with ice-cold phosphate-buffered saline and resuspended in 1ml for 500μg tissue of Buffer I (10 mm Tris-Cl, pH 7.8, and 200 mm KCl). After the addition of an equal volume of Buffer II (10 mm Tris-Cl, pH 7.8, 200 mm KCl, 2 mm EDTA, 40% glycerol, 0.2% Nonidet P-40, 2 mm dithiothreitol, 0.5 mm phenylmethylsulfonyl fluoride, 10 µg/ml aprotinin, 5 µg/ml leupeptin, 1 µg/ml pepstatin), the suspension was rocked at 4 °C for 1 h and then centrifuged at 16,000 × g for 10 min. The supernatant was recovered and stored in small aliquots at –80 °C.

PAGE-purified oligonucleotides were 5′ end labeled with [γ-32P]ATP by polynucleotide kinase. The oligonucleotides used to generate the DNA substrates were the following: for gapped 8oxoG containing substrate, P15 (5′-CTGCAGCTGATGCGC-3′), T348G (5′- GTACCCGGGGATCC GTAC8GCGCATCAGCTGCAG-3′) and 5′ phosphate-containing D18 (5′-GTACGGATC

CCCGGGTAC-3′), where 8 indicates the presence of an 8oxoG moiety; for standard (gap-filling) polymerization assays T348G oligonucleotide was substituted for T34 (5′- GTACCCGGGG ATCCGTACGGCGCATCAGCTGCAG-3′). For *ex vivo* evaluation of extracts, appropriate template primer (T/P/D) substrates were used with the clarified brain extracts (wt vs KO).

For standard (gap-filling or bypass mutagenic repair) polymerization assays, the incubation mixture (20 µl) contained 50 mM Tris-HCl (pH 7.5), 1 mM MnCl2 (alternatively 10 mM MgCl2), 1 mM DTT, 4% glycerol, 0.1 mg/ml BSA, 5 nM gapped DNA, the indicated concentration of NTPs, and either wt or KO brain extracts (10 mg). After 30 min of incubation at 30°C, reactions were stopped by addition of loading buffer (10 mM EDTA, 95% [v/v] formamide, 0.03% [w/v] bromophenol blue, 0.3% [w/v] cyanol blue) and subjected to electrophoresis in 8 M urea-containing 20% polyacrylamide sequencing gels. After electrophoresis, the unextended, degraded or extended DNA primers were detected by autoradiography, and quantified.

4 3D-modeling

The different conformations of selected residues of Pol*µ* were analyzed by using the Swiss PDB-Viewer (http://www.expasy.ch/spdbv/) and MacPymol (The PyMOL Molecular Graphics System, Schrödinger, LLC, http://www.pymol.org/).

5 Mice

Mice were bred at Centro de Biología Molecular 'Severo Ochoa' (Madrid, Spain). Four or five mice were housed per cage with food and water *ad libitum*. Mice were maintained in a temperature-controlled environment on a 12 h light/dark cycle with lights onset at 7:30 AM. All experiments were performed in accordance with institutional guidelines approved by the ethical committee of Consejo Superior de Investigaciones Científicas (CSIC).

6 Generation and culture of MEFs

MEFs were generated at embryonic day 13.5 and cultured as previously described (Babu et al. 2003) Primary MEFs were frozen at passage 2 (P2) or P3 and used for experimentation between P4 and P6. At least three independently generated MEF lines per genotype were used.

7 Cell senescence analysis. SA-β-Gal staining

Cell senescence was assessed by using the Senescence ß-galactosidase kit from Cell Signaling according to manufacturer's protocol. Cells were incubated at 37ºC until ß-gal staining becomes visible, at 17h. Development of color was detected under light microscope. 2000 Cells in passage 5 were seeded and stained after 3 days. Staining was performed in p35-well plates after seeding 2000 cells and the SA-ß-Gal-positive cells were detected by phase contrast microscopy using a Zeiss Axiovert 200M fluorescence microscope (Zeiss). Quantification was performed by counting the positive cells present in 20 independent fields of view at 20 magnification, and images were captured and processed using Adobe Photoshop CS5.

The percentage of SA-ß-gal–positive cells was determined microscopically by counting the number of positive-staining cells among over 200 cells in total. Images were recorded using a microscope (BZ-9000; KEYENCE) using a 10× 0.45 NA Plan-Apochromat objective lens.

8 Colony Forming Assay

Cells were plated at a density 1 x 10^3cells per well in a 10-cm dish in DMEM medium for 24 hr. The next day cells were treated for 1h with 2,5 μM Etoposide. After treatment, cells were washed with PBS and reincubated for consecutive 14 days to allow colony formation. Colonies were stained using 0.25% crystal violet in 80% methanol for 30 min, washed with water, and counted.

9 Viability Assays

Cells were seeded at a density of 2*10^3 cells/well in 96-well dishes. The following day, cells were exposed to increasing dosages of different drugs as detailed. MTT assay was done using the CellTiter 96 Aqueous One Solution Proliferation Assay System (Promega). MTT was added to the culture wells, and the mixture was incubated at 37°C for 3 h. Absorbance was measured at 490 nm using a microplate reader and is directly proportional to the number of viable cells in the cultures. The relative toxicity was calculated by comparing with nontreated cells.

10 Indirect immunofluorescence

For immunofluorescence microscopy, cells cultured on coverslips were fixed in 4% formaldehyde and permeabilized by 0.1% Triton X-100 in two consecutive steps, each for 15 minutes at RT. After washing with PBS, cells were blocked for 30 minutes in 10% fetal calf serum. The following primary antibodies were used: rabbit polyclonal antibody against 53BP1 (53BP1 (H-300); Santa Cruz Biotechnology, 1:500).

Incubation with primary antibodies was performed for 60 minutes at RT and then cells were washed with PBS. Secondary antibodie Alexa Fluor® 488 goat anti-rabbit (Invitrogen, #A11034, 1:500) was then applied for 60 minutes at RT, followed by final wash in PBS. Coverslips were mounted in Vectashield Mounting Medium with DAPI (Vector Laboratories, # H-1200). Confocal images were acquired on LSM-510 (Carl Zeiss Microimaging Inc., Germany) equipped with Plan-Apochromat 63x/1.4 oil immersion objective, ZEN2009 software (Carl Zeiss Microimaging Inc., Germany) and with appropriate configurations for multiple color acquisition. For quantitative and comparative imaging, identical image acquisition parameters were used.

11 Flow Cytometry

Cells were plated 24 h prior to etoposide treatment at 7,5*10^5 cells/p100. At the indicated time points, adherent and non-adherent cells were collected. Cell cycle analysis was performed by propidium iodide staining. Briefly, adherent and non-adherent cells were collected at the indicated time points, washed with PBS, resuspended in 70% cold ethanol and incubated at 20 °C for at least 24 h. Cells were collected and incubated in the dark with RNase A (25 g/ml) and PI stain (1 g/ml) for 30 min at 37 °C followed by 1.5 h at 4 °C. Flow cytometric analysis was performed on a BD FACScan with gated events plotted against the FL2-area parameter. Paired Student's test was used to determine statistical significance.

12 DNA Extraction, RNA Extraction, and CAG PCR Amplification

Amplification of the CAG repeat from R6/1 and R6/2 mouse DNA and human DNA was performed with a FAM-labeled forward primer (ATGAAGGCCTTCGAGTCCCTCAAGTCCTTC) and reverse primer (GGCGGCTGAGGAAGCTGAGGA) in 20-ml reactions containing 0.2 mM dNTPs, 10% DMSO, and 1 unit of Taq DNA polymerase (Biotools). Cycling conditions were as follows: 90s at 94°C; (30s at 94°C-30s at 57,3°C-30s at 72°C)x 40 cycles; 600s at 72°C. *Hdh*Q150 DNA was amplified in 20 ml containing 0.1 mM dNTPs, 2 M Betaine (Sigma), Detloff buffer [15 mM Tris·HCl, pH 8.8/15 mM Tris·HCl, pH 9.0/16 mM $(NH_4)_2SO_4$/2.5 mM $MgCl_2$/0.15 mg/ml BSA/0.007% 2-mercaptoethanol], 10 ng/ml forward primer 40224FD (CCCATTCATTGCCTTGCTG), 10 ng/ml reverse primer 40225 (GCGGCTGAGGGGGTTGA), and 0.5 units of AmpliTaq DNA polymerase (Applied Biosystems). Cycling conditions were 5 min at 94°C, 29 times (30 s at 94°C, 30 s at 53°C, 3 min at 72°C), 5 min at 72°C.

13 Repeat Sizing by ABI 377

PCR amplification conditions were optimized to detect both small-pool and conventional PCR using the ABI377 sequencer (SI Fig. 9). A total of 2 ml of each FAM-tagged PCR product together with GeneScan2500 ROX internal size standard were denatured at 94°C for 5 min with 2 ml of HiDi formamide (Applied Biosystems). Denatured products were loaded onto a 4.25% acrylamide gel (AccuGel; National Diagnostics; 7 M urea; 12 cm) and run on ABI Prism 377 in TBE buffer for 1.5 h. The ABI Prism 377XL collection software operated the run module "GS run 12A-1200" with the following parameters: 3,000 V, 50 mA, 150 W, oven temperature 51°C. Data from the ABI377 were analyzed by using GeneScan 3.1.2 (Applied Biosystems) software.

14 Htt inclusions counting in mouse samples

In each experiment, all mice were processed in parallel and samples have been treated identically. Briefly, mice were sacrificed by CO_2, and brains were removed and halved sagittally immediately after decapitation. Left hemispheres were processed for histology, fixed with 4% paraformaldehyde (PFA) in Sorensen's phosphate buffer overnight at 4°C, and then were immersed in 30% sucrose in PBS for 48 h for cryoprotection. Next, samples were frozen in OCT (Optimal Cutting Temperature, Tissue-Tek) and stored at –80°C until use. Sagittal sections (30 μm) were cut on a CM 1950 Ag Protect freezing microtome (Leica) and placed and stored in a solution containing 30% glycerol and 30% ethyleneglycol in 0.02 m monobasic phosphate buffer at pH 7.2 at –20°C. To detect α-syn aggregates by immunohistochemistry or by immunofluorescence, a previous epitope unmasking step was performed as above described for the human tissue staining. Four regularly spaced sections of each mouse were immunostained for anti-N-terminal Htt (MAB5374, Millipore). Digital images of striatal Htt inclusions were captured with an Olympus Bx 51 microscope, Color View IIIu digital camera with a 40× objective lens with the help of the Olympus Soft Imaging System. The number and size of inclusions were determined using the ImageJ software with the *Analyze Particles* routine (size 2.89–14.45 μm^2, threshold 0–75, circularity 0.81–1.00). Data are represented as the mean ± SEM.

15 Behavioral tests

Body weight

Starting at 2.5 months, mice were weighed once a month. Results are represented as the mean ± SEM. Behavioral testing started at 2.5 months and finished at 8 months, when transgenic mice presented several difficulties to perform the tasks.

Rotarod

Motor coordination was tested on an accelerating rotarod apparatus (Ugo Basile). Initially, each mouse was trained for 2 days. In the first day, mice performed four trials (1 h intervals) at a fixed speed (4 rpm) for 60 s. In the second day, mice performed also four trials at a fixed speed at 8 rpm for 60 s. The third day, rotarod was set to accelerate from 4 to 40 rpm over 5 min and mice were tested four times (1 h intervals). During accelerating trials, the latency of each mouse to fall from the rotarod was measured. Results are represented as the mean ± SEM of the latencies to fall in the four trials and as the percentage of mice on a rod at the highest speeds.

16 Cellular NHEJ assays

Substrates for *in vitro* assays were labeled by amplification in the presence of αCy5-dCTP (GE Healthcare), and cartridge purified (Qiaquick PCR Purification, Qiagen). Junctions were characterized by amplification with primers specific for head to tail junctions (5' – CCTTGGAGAGTGCCAGAATC & 5' – CTGGAGAATGAATGCCAGTG), and digested with NsiI (3'G), AatII (3'GCAG), or AfeI (3'GCG) as diagnostic for synthesis and ligation. Digestion products were resolved on a 5% polyacrylamide gel then visualized using a Typhoon Imager and quantified using ImageQuant (GE Healthcare).

MEFs were cultured in DMEM media with 10% fetal calf serum. 20 ng of the purified, validated substrate were introduced into $2x10^5$ of these cells by electroporation (Neon, Life Technologies) using a 10-µL chamber and one 1530 V, 20 ms pulse (HCT116) or three 1500 V, 10 ms pulses (NHM), then incubated in 300 µL of the appropriate DMEM without antibiotic at 37°C for 1 hour.

Electroporations were performed in triplicate, then repeated in triplicate for each substrate and cell line pair. Cells were then washed with phosphate buffered saline (PBS) before harvesting of total cellular DNA (QIAmp, Qiagen).

17 Statistical analysis

Results are reported as mean ± SD. Data were normalized versus control. Three independent experiments were analyzed. All values are expressed as mean ± SD. Statistical analysis were performed with Student's T-test for unpaired samples and normally distributed data sets. Statistically significant differences were considered at $P < 0.05$. (Statview, SAS Institute).

RESULTS

1

DNA expansions generated by human Polμ on iterative sequences

Among other the properties that characterize Polμ's activity, its large versatility resides in the capacity to induce/accept template distortions, bridge DNA ends with minimal or null complementary, or perform DNA synthesis despite the presence of mismatched nucleotides near the primer terminus (Duvauchelle et al. 2002). Consequently, the basis for Polμ's high misincorporation rate resides in its non-conventional interactions with DNA and nucleotide substrates, and in its ability to create or accept distortions and realignments of both primer and template strands, which are largely dependent on sequence context {Ruiz, 2004 #98;Zhang, 2001 #9}. To further understanding of these mechanisms, we decided to study Polμ in sequences contexts allowing different distortions.

1.1 Polμ's most extreme mutator behavior is triggered by a "slippage" mechanism

The 'slippage' mechanism was described initially for Polß on a template/primer (Kunkel 1985). This mechanism has been shown to be the cause of terminal transferase additions by Polμ in the context of heavily damaged DNA, such as substrates containing AAF adducts or abasic sites (Covo et al. 2004; Duvauchelle et al. 2002). Analysis of different DNA sequence contexts showed that Polμ displays the most extreme mutator behavior when is triggered by to a "slippage" mechanism [(Ruiz et al. 2004); Fig. 8].

When the first template nucleotide is complementary to the end of the primer, the propensity of Polμ to dislocate the template strand is such that it preferably incorporates the nucleotide complementary to the n+2 position of the template in each case (X in the scheme)(Fig. 8A). This n+2 position would then become the n+1, and therefore it directs the incorporation of the complementary dNTP, if the 3´-primer terminus realigns to perfectly match with the former n+1 position of the template. As shown, both type of initial insertions: directly opposite the n+1 templating base, or cpying the n+2 (by slippage-mediated dislocation), can be alternatively detected on this type of substrate, but the insertion produced by dislocation is even more efficient (Fig. 8A).

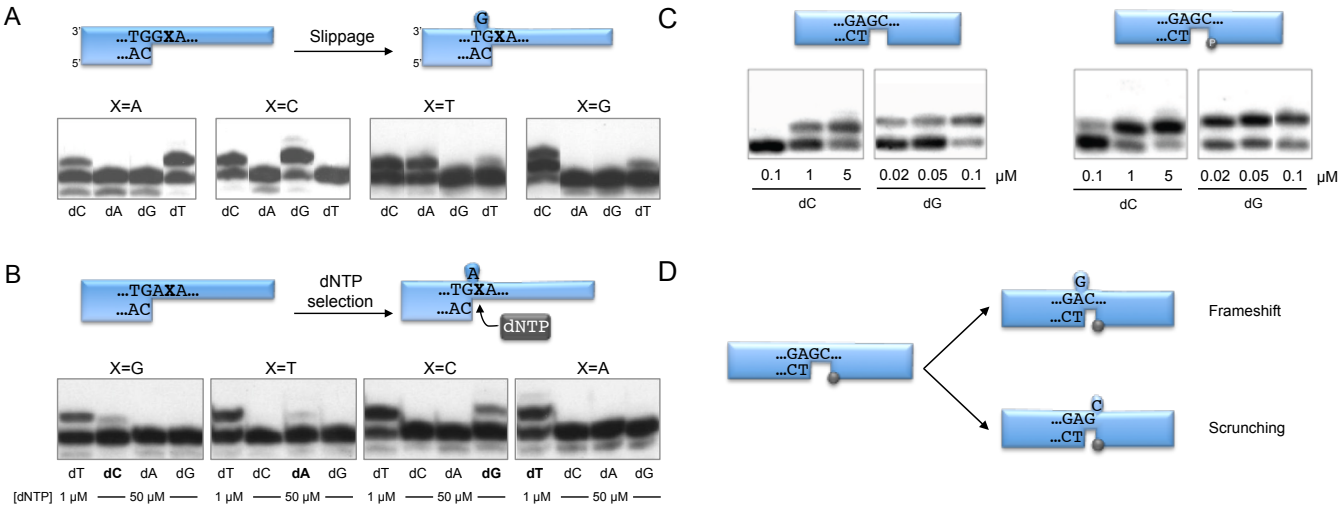

Figure 8. Mechanisms of Polμ-mediated dislocation: A) Slippage-mediated dislocation. **B)** dNTPmediated selection dislocation. **C)** Increased efficiency of dislocation by Polμ in gapped substrates. **D)** Scheme of the two possible outcomes when filling a 2nt-gap by human Polμ: 1) a dNTP selection-mediated distortion, leading to a -1 frameshift (the first base of the gap is not copied); 2) correct copying of the first templating base, via "scrunching" (Garcia-Diaz et al. 2008)

In order to observe Polμ-mediated dislocation, it is not strictly necessary that the n and n +1 bases are identical, as it can be observed in Fig. 8B (where the n (G) and n +1 (A) bases of the template strand are different). Template instruction by the n+2 is changed to each of the four bases to provide all possible template options. This direction by the n+2 base (X) would only occur if the

template "A" in position n+1 could be flipped out, being relocated outside of the enzyme active site without blocking its ability to polymerize.

Thus, an incoming nucleotide complementary to the X position (n+2) of the template would be responsible for stabilizing the dislocation of the "A". As shown in Fig 1.1B, although the major incorporation corresponds to the insertion of dT (complementary to the n+1 position of the template) there is also a minor insertion of each of the nucleotides complementary to the X position. That indicates that Polμ is able to achieve “dNTP-selection mediated” dislocation, although not as efficiently as in the case of “slippage-mediated” dislocation. The efficiency of the “dNTP selection-mediated” dislocation performed by Polμ on a template-primer substrate, can sharply increase to be comparable or exceed the “correct” dNTP entry in some sequence contexts, and especially when the substrate is a small gap (Fig 8C). In this case, dG is preferentially inserted as a result of “dNTP selection-mediated” dislocation (see scheme in Fig. 8D), at the various range of nucleotide concentrations used. From this result we can conclude that the “dNTP selection-mediated” dislocation capacity of Polμ is strongly stimulated in the presence of a gap, which emphasizes the importance of a stable binary complex (heterodimer formed of DNA polymerase-DNA) for this reaction to occur.

1.2 Pol*μ*, but neither Polλ nor Polß, produces large sequence expansions when a specific repeated trinucleotide sequence is used as a template

Pol*μ* can act as a mutator polymerase, based on its ability to realign and dislocate DNA chains during polymerization, whereas Polλ and Polß, belonging to the same family as Pol*μ*, are not so versatile and promiscuous in the use of DNA substrates (Picher et al. 2006). All three polymerases have a marked preference for 5’-P (phosphate) gapped molecules, as the 8 kDa domain strongly interacts with this group at the 5’ end of the downstream chain (Garcia-Diaz et al. 2002; Martin et al. 2012; Sawaya et al. 1997), improving binding stability.

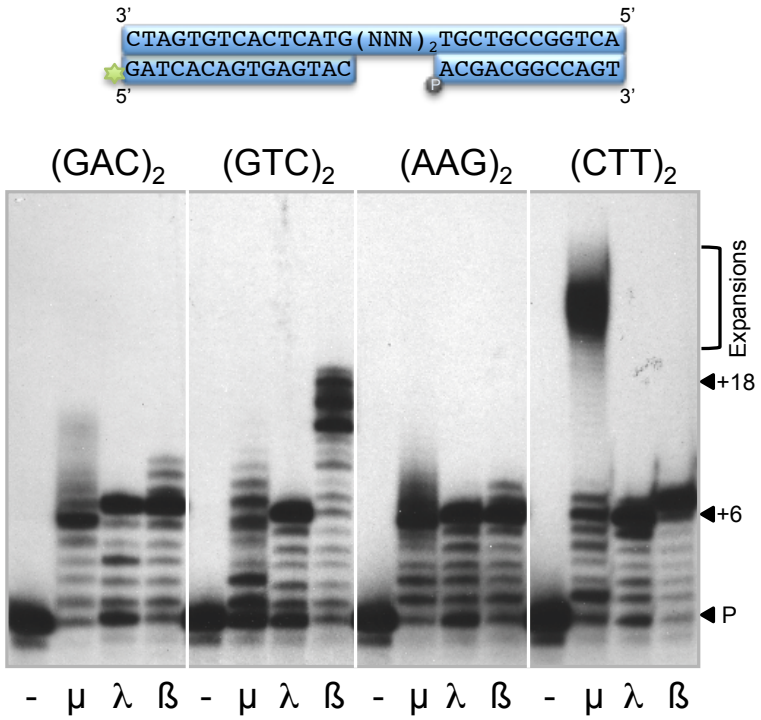

Figure 9. Pol*μ* generates a large sequence expansion on a DNA gap with a specific trinucleotide sequence. In the scheme, the template sequence indicated (NNN) corresponds to the trinucleotides shown below. Subindex “2” indicates that each trinucleotide sequence is twice repeated at the gap. The dNTPs provided in each case were those complementary to the gap sequence. P indicates the unextended primer; +6 the elongated product upon complete gap-filling; +18 the fully elongated product after gap-filling and strand-displacement; the products of nucleotide expansion are indicated with a bracket.

We addressed if any of these DNA polymerases could generate triplet repeat expansions in the context of a gap. According to the substrate preferences of these polymerases, four different DNA substrates containing a 6 nt gap were designed, with different trinucleotide sequences as templates, each one repeated twice (see scheme in Figure 9). Expansion of triplet repetitions of the sequence 3'-GAC (or its complementary chain 3'-GTC) are associated to Huntington's disease; triplet repeat expansions of 3'-AAG (or its complementary sequence 3'-CTT) are related to Friedrich's ataxia. Polymerization reactions were assayed on these molecules, in the presence of Polμ, Polλ or Polß, and the complementary dNTPs needed in each case (Figure 9). In general, Polλ and Polß filled the gap and then polymerization stopped (+6 product). In the case of 3'-$(GTC)_2$, Polß displayed a significant strand-displacement capacity and efficiently continued adding nucleotides after filling the gap (+18 product). This imprecise gap filling by Polß has been already described (Singhal and Wilson 1993). Interestingly, Polμ was eventually able to continue polymerization, producing extra additions that could be also originated via strand-displacement. However, this behavior is very remarkable in the case of 3'-$(CTT)_2$, where Polμ fills the gap and then efficiently generates a very large DNA expansion as a final product. The main difference between this sequence and the others is the presence of a dinucleotide (TT) in the template strand at the end of the gap.

1.3 Polμ requires a dinucleotide at the end of the template sequence to produce large sequence expansions

Taking into account the dislocation capacity of Polμ, strongly driven by the presence of dinucleotides in the template strand, we wanted to confirm if the presence of a repeated nucleotide at the end of the gap determines the capability of Polμ to produce sequence expansions. For this, two new DNA substrates containing 6 nt gaps were chosen: the first, with the template sequence 3'-$(CAG)_2$, with no repeated nucleotides, and the second 3'-$(GAA)_2$, which maintains the presence of a duplicated nucleotide at the end of the gap (Fig. 10).

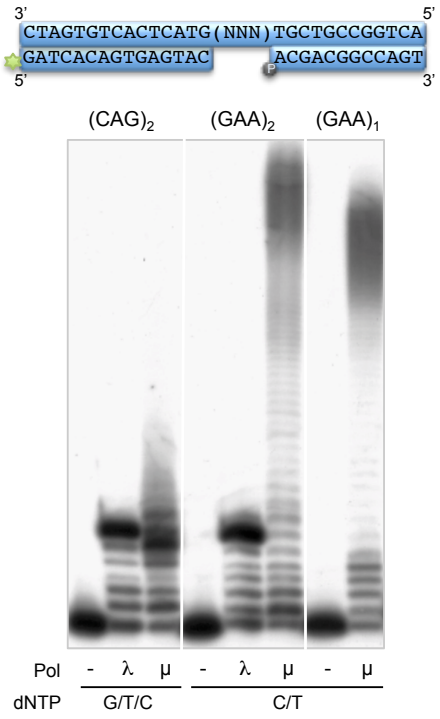

We compared the behaviour of Polμ and Polλ on these substrates, providing the complementary nucleotides needed in each case. As shown in Fig. 10, in both cases Polλ filled the 6 nt gap and then polymerization stopped. Conversely, Polμ was able to continue polymerization beyond the expected +6 product in both cases, producing a large sequence expansion only in the case of confronting a repeated nucleotide (AA) at the end of the gap. Thus, this iteration is a relevant requirement for Polμ in order to produce promiscuous elongation. Next we addressed if the repetition of the trinucleotide was specifically needed for Polμ to produce the expansion. For that, Polμ was assayed on a DNA substrate having only one repetition of the triplet sequence, forming a 3 nt gap containing the sequence 3'-GAA, that maintains the requirement of a repeated nucleotide at the end of the gap. As shown in Fig. 10, when complementary nucleotides (dC and dT) were provided, Polμ generated again a large sequence expansion, demonstrating that the dinucleotide is required only once at the end of the template strand.

Figure 10. A repeated nucleotide at the end of a gap is required to generate large sequence expansions. In the scheme, the template sequence indicated (NNN) corresponds to the trinucleotides shown below, that could be present twice (subindex 2) or only once (subindex 1). dNTPs provided in each case were the complementary to the gap sequence.

1.4 An initial dislocation and remaining distortion are necessary for the generation of large sequence expansions by Pol*μ*

By using additional sequence contexts, Pol*μ* was confirmed to be able to produce large sequence expansions of the four different duplicated nucleotides (AA, TT, CC and GG) at the end of a 3 nt gap (Fig. 11).

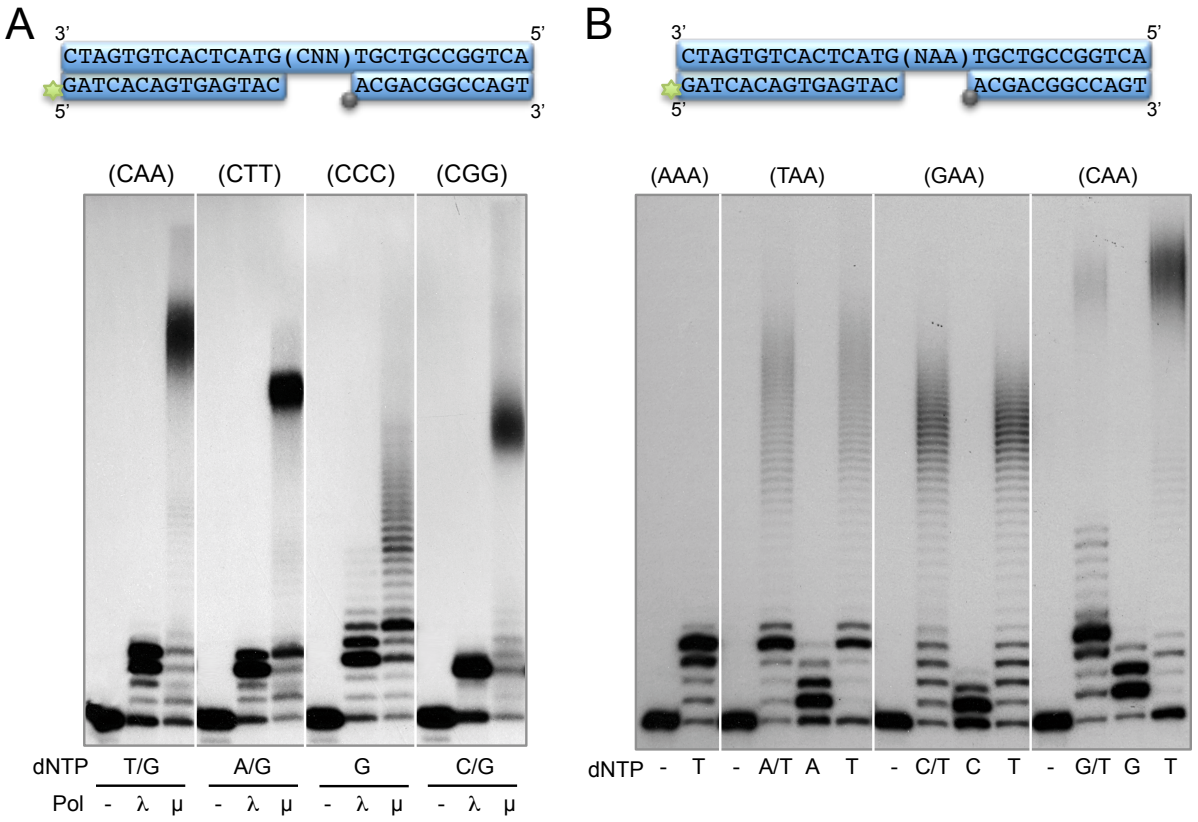

Figure 11. A distortion upstream to the dinucleotide is a prerequisite for the formation of Pol*μ*-mediated sequence expansions during gap-filling. A) In the scheme, the template sequence indicated (CNN) corresponds to the four trinucleotides shown below. The first base at the trinucleotide is always dC, followed by the four different homo-dinucleotides. **B)** Importance of the first nucleotide of the triplet (NAA) for the efficiency of expansion by Polμ. The gap sequence used and the different combinations of nucleotides provided, were as indicated. dNTPs provided in each case were the complementary to the gap sequence.

Polλ was used as negative control of expansion also in this experiment. Interestingly, in the 3'-CCC gapped substrate Pol*μ* had a different behaviour than on the other 3 DNA substrates (Fig. 11A) : no large sequence expansion was produced, but only a few more additions were observed once the gap had been filled. Strikingly, the behaviour appears to be the opposite in the case of Polλ, which produced some significant expansion only when copying the sequence 3'-CCC, perhaps the most prone to facilitate slippage after gap-filling. Thus, the modest outcome of the reaction on the 3'-CCC substrate indicates a new specific feature needed for the generation of large expansions by Pol*μ*: the nucleotide at the first (n+1) template position must differ from that forming the repetition in order to obtain the maximal sequence expansion. This demand at the trinucleotide sequence suggests that the expansion reaction begins with an initial dislocation reaction, a very particular mechanism described for Pol*μ* (Brook et al. 2009; Ruiz et al. 2004), producing a -1 frameshift during the initial step of the gap-filling reaction: Pol*μ*'s propensity to dislocate the template strand is such that it preferentially inserts the nucleotide complementary to the n+2 position of the template, both in an open template/primer and in a 2 nt gap (Fig. 8), either in the conditions that favor a mechanism of primer slippage (Fig. 8A) or when this is not possible due to the sequence context (Fig. 8B). This

second mechanism, “dNTP selection-mediated”, is not as efficient as the “slippage-mediated” alternative, but is considerably improved when the substrate is a small 5’-P-containing gap (Fig. 8C).

To further understand the requirements for the special mechanism of dinucleotide expansion by Pol*μ*, we evaluated both the impact of the sequence at the first position of the gap, and also the necessity of providing either the two nucleotides complementary to the sequence of the gap, or only the one complementary to the dinucleotide (the only one needed if dislocation occurs). We used four different 3 nt gapped DNA substrates (Fig. 11), with the same terminal repetition (AA), but different nucleotide at the n+1 position of the gap. As shown in Fig. 1.4B, a large expansion is obtained in the case of the 3’-GAA substrate, and no difference is obtained when providing either dC+dT or only dT, indicating that in most of the cases the first templating base (dG) is not copied. Such a preferential dislocation is compatible with a slippage-mediated mechanism, since the 3’-terminus of the primer strand (dC) could be realigned and matched to the first templating base (dG) [(Streisinger et al. 1966); see also Fig. 8A]. Moreover, large expansions on the gap sequences 3’-TAA and 3’-CAA are also obtained by providing only dTTP. In these two cases, the dTTP insertion event triggering expansion would be compatible with a dNTP-selection-mediated dislocation [(Ruiz et al. 2004); see Fig. 8B]. This mechanism dominates insertion in the 3’-TAA gap, as the addition of dATP+dTTP has minimal, if any, effect on expansion. Conversely, expansions on the 3’-CAA gap are significantly inhibited by the simultaneous addition of dGTP and dTTP. These results point to the efficiency of dislocation as an important factor determining the expansion capability, which could be also affected by an unbalanced concentration of the deoxynucleotide precursors.

In agreement with our previous observations using the 3’-CCC substrate (Fig. 11A), Pol*μ* did not produce a significant expansion on the 3’-AAA substrate. Assuming that an initial dislocation event can also occur, an important difference in these two cases is that, after complete gap filling, the nascent chain could be completely realigned, producing a perfectly matched +3 product. In this case, expansion seems to be precluded, as evidenced by the minimum extension of the primer over the size of the gap. Therefore, an initial dislocation of the template only triggers dinucleotide expansion if the distortion remains after gap-filling.

1.5 Origin of the distortion: polymerase-mediated?

Further analysis showed that the necessary distortion that allows generation of the observed sequence expansions might be present in the substrate prior to the arrival of the polymerase, triggering dinucleotide expansions even at single nicks in DNA (Fig. 12). The importance of an initial dislocation was analyzed in DNA substrates (progressively short gaps) with different primers As shown in Fig. 12, by providing only dCTP, Polμ was able to produce expansion on the DNA1, DNA5 and DNA6 substrates, confirming that the mechanism that produces these expansions is triggered by the presence of a pre-existing distortion upstream to the polymerization site.

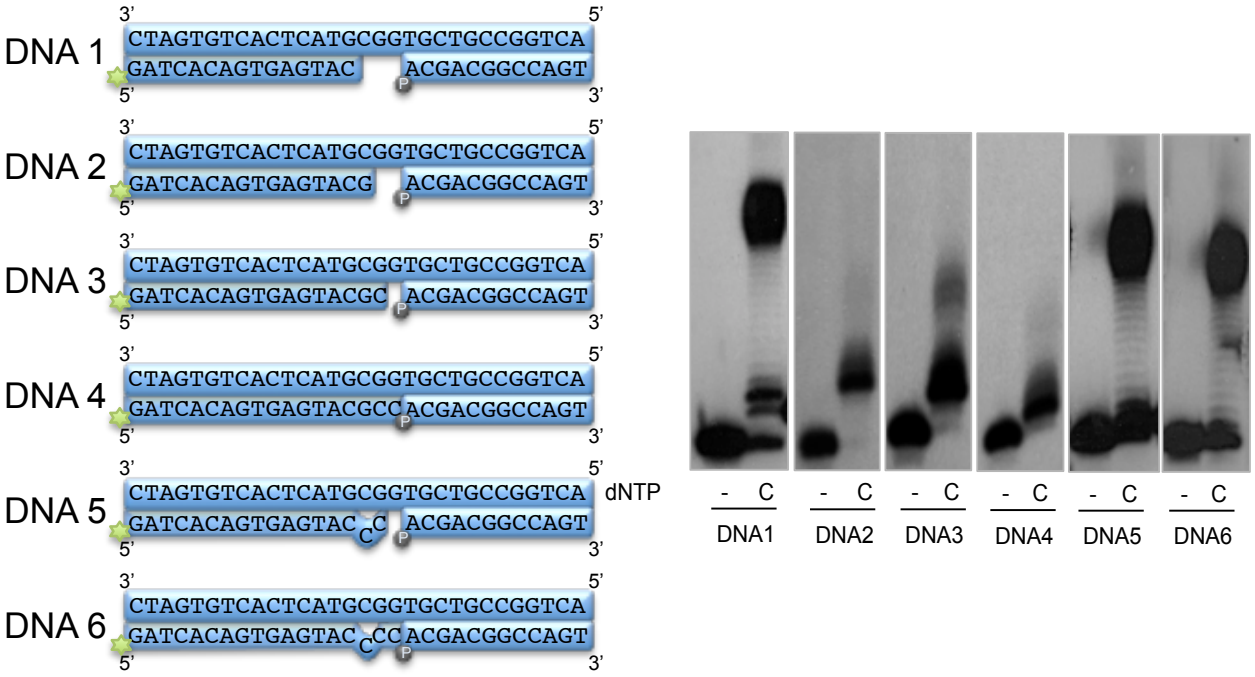

Figure 12. Origin of the distortion: polymerase-mediated? The importance of an initial dislocation was analyzed in DNA substrates (progressively short gaps) with different primers that produce: a fully matched primer preceding a 3, 2 or 1 nt gap (DNA1, DNA2, DNA3) or a nick (DNA4), a 1 nt gap with a mismatch at the -1 position (DNA5), or a nicked substrate with a mismatch at the -3 position (DNA6). DNA1 contains the templating sequence 3'-CGG as a positive control of expansion.

As it will be evaluated later, this is particularly relevant considering the *in vivo* situations where Pol*μ* deals with substrates containing distortions and/or misalignments, caused by microhomology search during the bridging of two DNA ends in NHEJ reactions. The presence of a 5'P group at the downstream strand of the gap is also a pre-requisite for the generation of these nucleotide expansions, as shown in Fig 1.6 this observation was expected since the 5'-P is a main anchor point for Pol*μ* on the DNA substrate (Martin et al. 2012).

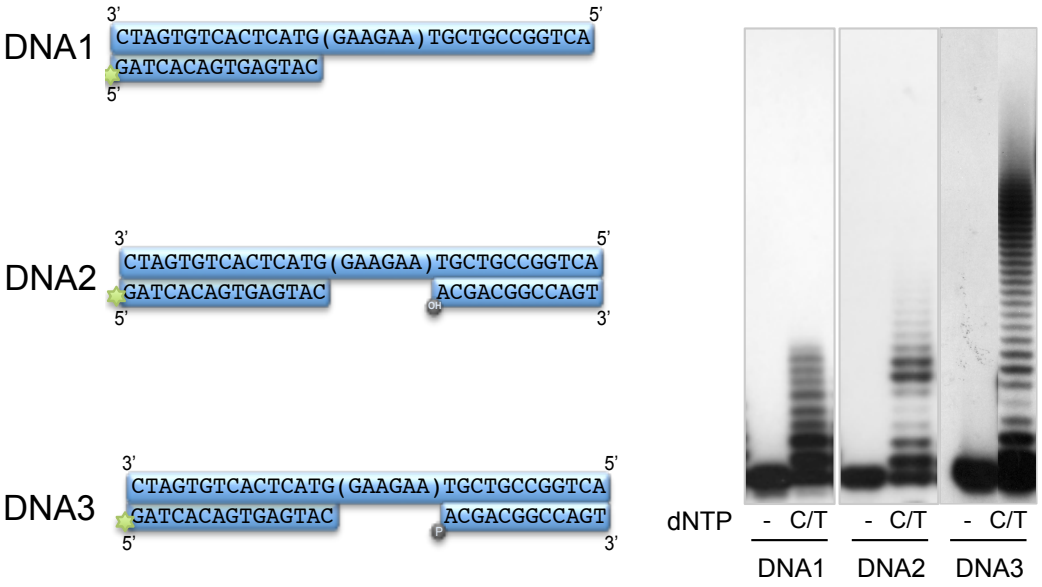

Figure 13. Importance of the 5'P group. Polμ-driven nucleotide expansion depends on the presence of the downstream oligo at the 3' end of the gap, containing a 5' phosphate group. The schemes correspond to the different substrates used (DNA1: template/primer; DNA2: gap lacking 5'P; DNA3: gap bearing 5'P group).

1.6 Specific residues regulating the expansion of repeated sequences

Polμ is an exceptional enzyme since it is the only DNA polymerase able to display template-independent (terminal transferase) and template-dependent activities (Dominguez et al. 2000; Ruiz et al. 2001). Recent structure-function studies have shed light on the molecular basis for the terminal transferase activity: on the one hand, Pol*μ* contains a flexible piece, Loop 1, which is able to undergo conformational changes, acting as a pseudo-template that allows incorporation of nucleotides in the absence of template information (Juarez et al. 2006), or during NHEJ of some incompatible ends (Nick McElhinny et al. 2005b). Moreover, the crystal structure of Polμ in ternary complex with gap DNA and deoxynucleotide (Moon et al. 2007) allowed to infer that a specific histidine residue (His329 in Polμ and His342 in TdT; absent in Polß and Polλ) could play an important role to overcome the rate-limiting step of untemplated polymerization, allowing terminal transferase activity to occur. In fact, this residue, involved in the proper positioning of the primer terminus and the incoming nucleotide (Figure 13A), was shown to be critical during template-independent polymerization but also in template-directed reactions associated to NHEJ of short incompatible ends (Andrade et al. 2009; Moon et al. 2007). Furthermore Arg387, is a specific DNA binding ligand (Figure 14.A) that limits untemplated nucleotide additions and is thus responsible for the lower terminal transferase activity of Polμ in comparison to TdT (Andrade et al. 2009).

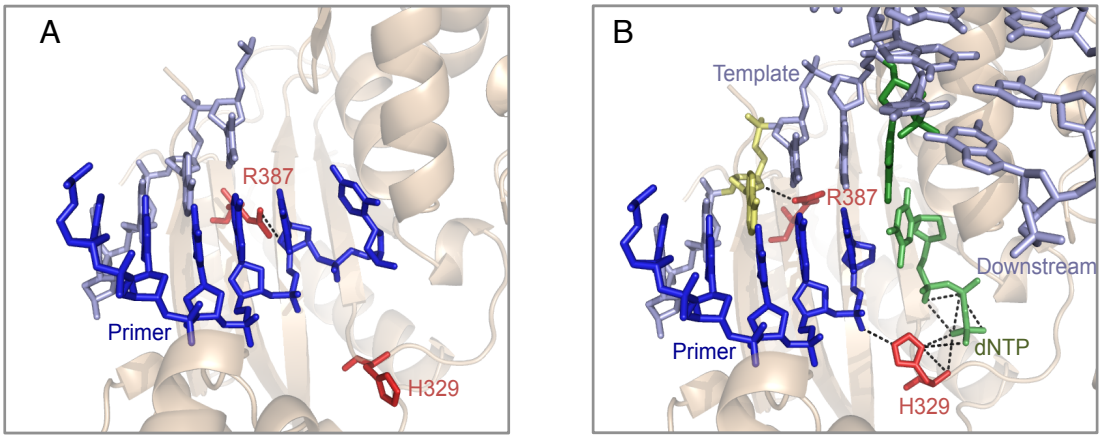

Figure 14. His^{329} allows while Arg^{387} limits sequence expansions by Pol*μ*. A) Top: Model of Pol*μ* bound to a template/primer substrate in which the 3'-protruding primer terminus is in an unproductive position, occupying the incoming dNTP site. Residue Arg^{387}, in a conformation modeled to match that of the lysine present in TdT in a similar structure, is contacting the primer impeding its backwards translocation. His^{329}, modeled in the conformation observed for the same residue in the crystal of TdT bound to a ssDNA primer, is not making any contacts with the DNA substrate. **B)** Crystal structure of Pol*μ* bound to a gapped DNA substrate and incoming dNTP. His^{329} has rotated and is contacting both incoming dNTP and primer terminus, helping to reposition the latter. Arg^{387} is now contacting the template strand (n-3 position; indicated in yellow), having allowed the movement backwards of the primer. DNA substrates are indicated in dark (primer strand) and light (template and downstream strand) blue. Incoming dNTP is indicated in green.

To study the relevance of both residues in the expansion of repeated sequences we used two mutants: H329G (with a strongly reduced terminal transferase activity) and R387K (displaying an augmented terminal transferase activity). The selected mutants, obtained and purified as described (Andrade et al. 2009), were tested on the set of gapped DNA substrates that maintain the same repetition (AA) at the 5' end, but differ in the nucleotide at the n+1 position in the gap. As shown in Fig. 15 the wild-type Pol*μ* produced and expansion pattern similar to that described before (Fig 11B). Strikingly, mutant H329G was only able to fill the different gaps, displaying very minor or even undetectable levels of sequence expansions on these substrates. Mutant R387K, on the other hand, produced a level of expansions similar in most cases to that of the wild type enzyme (Fig 15), but, remarkably, was also able to produce a significant expansion in the case of the 3'-AAA substrate. This was striking as the latter substrate does not allow formation of the distortion that was an obligatory requirement for producing expansions by the wild-type enzyme. These results support our

initial hypothesis that Arg387 has a constitutive role in preventing slippage of the primer in each round of the catalytic cycle, through a direct contact between this residue and the -2 position of the primer strand that can be observed in the ternary complex of Pol*μ* (Fig 14B). Mutation of this arginine to lysine favors expansion in the absence of distortions through a mechanism that facilitates the backwards translocation of the primer strand. In the case of distortion-mediated expansions, where the primer strand is not properly oriented, Arg387 cannot exert its "braking" role. Mutation of arginine to lysine in this context does not increase the sequence expansions any further since the control mechanism is already compromised.

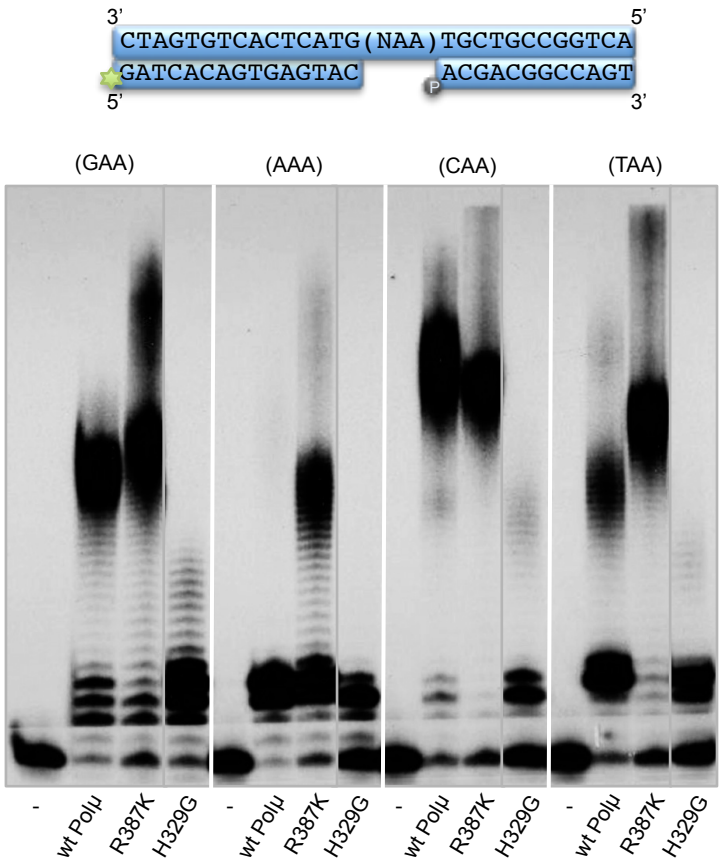

Figure 15. His^{329} allows while Arg^{387} limits sequence expansions by Pol*μ*. In the scheme, the template sequence indicated (NAA) corresponds to the four trinucleotides shown below. The two last bases always form the dinucleotide AA, preceded by any of the four different nucleotides.

1.7 Impact of the sequence expansions during end-joining reactions

As noted before, Pol*μ* could generate dinucleotide expansions as a byproduct of its physiological role of repairing double strand breaks (DSBs) by the NHEJ pathway. We wanted to check whether the sequence expansion capacity exhibited by Pol*μ* in the context of DNA gapped substrates is also demonstrated during NHEJ reactions that include the formation of short gaps, and if the requirements detected during gap-filling (i.e. the formation of a distortion upstream of the polymerization point, and the presence of a dinucleotide in the template strand) also need to be met during end-joining of two DNA ends. For this we used a tailored set of 3'-protruding NHEJ substrates whose protrusions provide, once bridged by the polymerase, a microhomology of 3 base-pairs, the flipping-out of a nucleotide at the -1 position of the primer strand, and the formation of two 1 nt gaps at both sides of the connection (see scheme on Fig. 16).

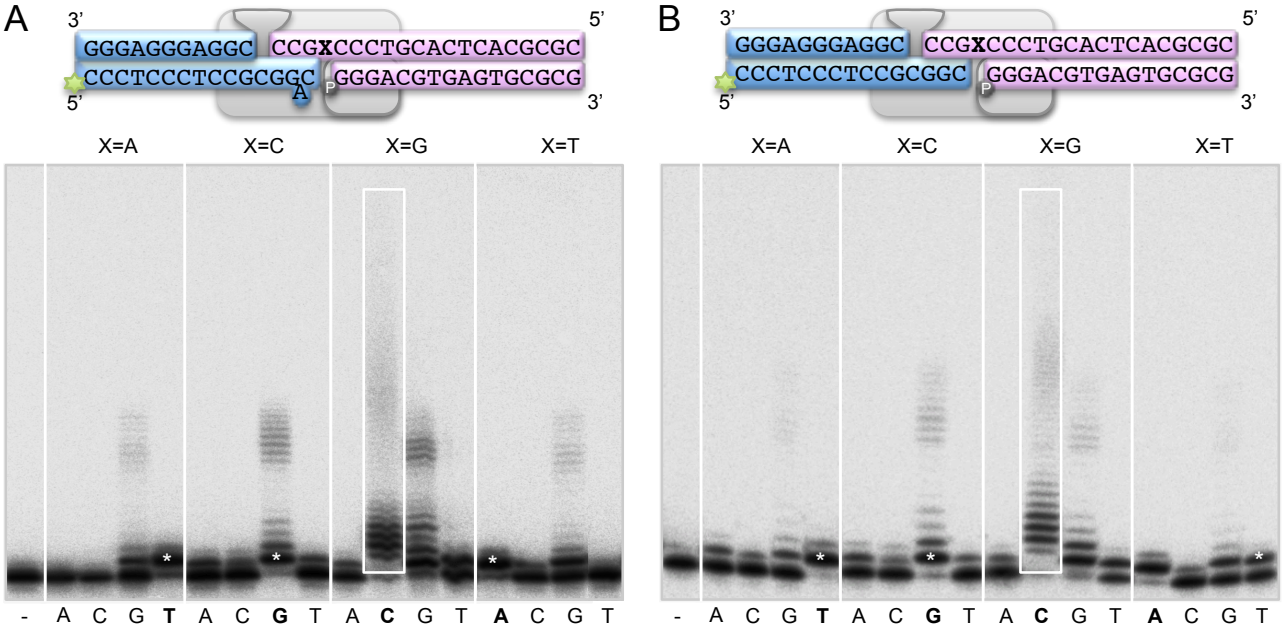

Figure 16. Impact of the generation of sequence expansions during NHEJ repair reactions by Pol*μ*. A) The scheme corresponds to the end-joining substrates used, whose 3'-protrusions can be connected by three bases pairs but leaving a distortion (1 flipped-out base) close to the 3'-primer terminus. Such a connection leaves two different 1nt-gaps. Gap-filling of one of them (that flanked by a 5'-P) is evaluated as a function of each possible templating base (X). Thus, the 5'-labelled substrate (dark gray) will be tested as primer, whereas the cold substrate (light gray;in which the X in the scheme is changed to A, C, G or T) is providing the template for the connection. **B)** Polymerization reactions performed as in A, but using end-joining substrates used whose 3'-protrusions can be connected by three bases pairs with no distortion.

Radioactive labeling of one of the 3'-protruding strands allows detection of nucleotide incorporation on this end, using the template information provided in trans by the other 3'-protrusion, that contains a 5'-P group and will thus be used as a template/downstream structure (through binding of the phosphate by the 8 kDa domain of Pol*μ*). In order to evaluate if the reaction is trans-directed, the templating base (X) on this second DNA substrate was changed to A, C, G or T (Figure 16). Our results showed that Po*μ* is able to perform an efficient and mostly template-directed trans-polymerization on this kind of NHEJ substrates, since the polymerase incorporated preferentially the nucleotide complementary to the templating base (white asterisks and box in Figure 16). As expected, when the templating base is a G and thus the template strand contains a dinucleotide (GG), large sequence expansions were produced when providing the nucleotide (dCTP) complementary to the dinucleotide. The reiterative additions of dGTP that are also catalyzed by Pol*μ*

in every case can be considered pure terminal transferase incorporations, since control experiments in which the template-providing end is not present, also showed this outcome (Fig. 17). This is in accordance with the preference for nucleotide incorporation displayed by Pol*μ* during untemplated additions (Juarez et al. 2006).

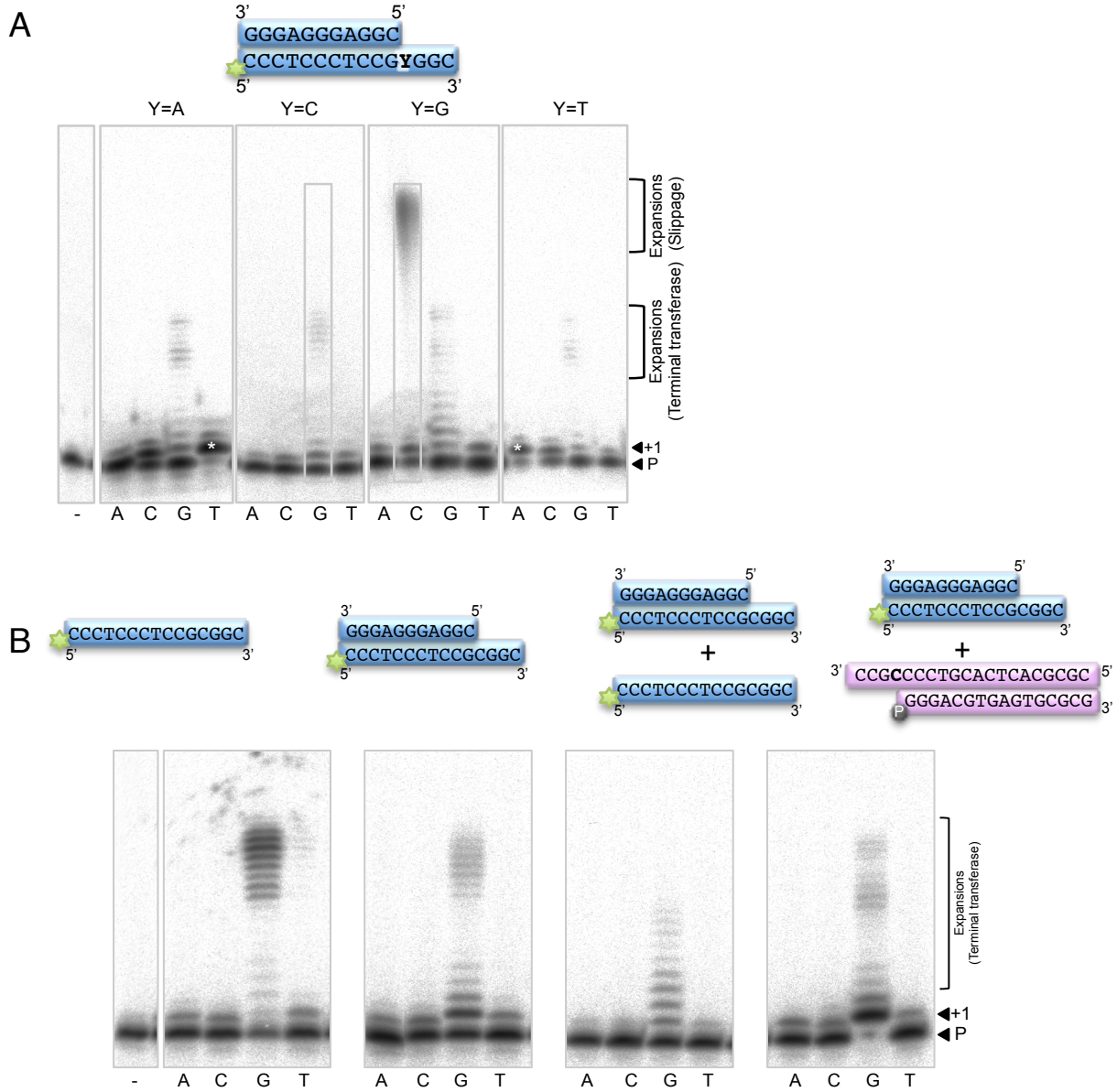

Figure 17. Sequence expansions versus terminal transferase additions during NHEJ. A) The reiterative addition of dGTP catalyzed by Polμ in the studied sequence contexts (see Fig. 16) is due to pure terminal transferase activity, since control experiments in which the template-providing end is not present, also showed this outcome (second panel, Y=C, and also other sequence contexts such as Y=A and Y=T). We can also clearly differentiate between the terminal transferase additions obtained in each case with dGTP and the template directed sequence expansions, which are slippage-mediated and thus only occur when the template contains a homo-dinucleotide (third panel, Y=G). **B)** To help differentiate between pure terminal transferase additions and templated reiterative incorporations we used a new set of substrates: a labeled single-stranded heteropolymeric substrate, a labeled double-stranded 3'-protruding substrate, this same dsDNA together with the cold versions of the ssDNA and the original bipartite NHEJ substrate. Reaction on the ssDNA substrate resulted in the most efficient generation of ladder products. This outcome is greatly inhibited by the presence of a hybridized strand and further by the presence of cold ssDNA, suggesting that these products are the result of pure terminal transferase additions. On the other hand, the strongest +1 reaction was observed in the last case, indicating that this reaction is preferentially template directed.

Strikingly, in the context of NHEJ we were able to observe the formation of large sequence expansions even in the absence of a provided distortion upstream to the polymerization site (Fig. 16B), thus limiting the requirements of this reaction only to the presence of a dinucleotide, a prerequisite that still needs to be met in this context. The amount of nucleotide that Pol*μ* requires to produce these expansions is low (20 *μ*M), indicating that this process is highly efficient (Fig. 17). Again, dGTP is being inserted as a result of pure terminal transferase additions, as demonstrated by a control experiment, in which the template-providing end is not present (Fig. 17). We also detected expansion during NHEJ when the dinucleotide was formed by a pair of adenines (Fig. 18), indicating that this mechanism is independent of the sequence context. Taken together, our results indicate that if the sequence context is favorable to the expansions (i.e., iteration of nucleotides at the template strand), the polymerase itself may generate the required upstream distortion by adjusting the bridging of the two ends, a scenario that emphasizes the importance of the mutagenic potential of Pol*μ* during the NHEJ pathway, specifically regarding nucleotide expansions.

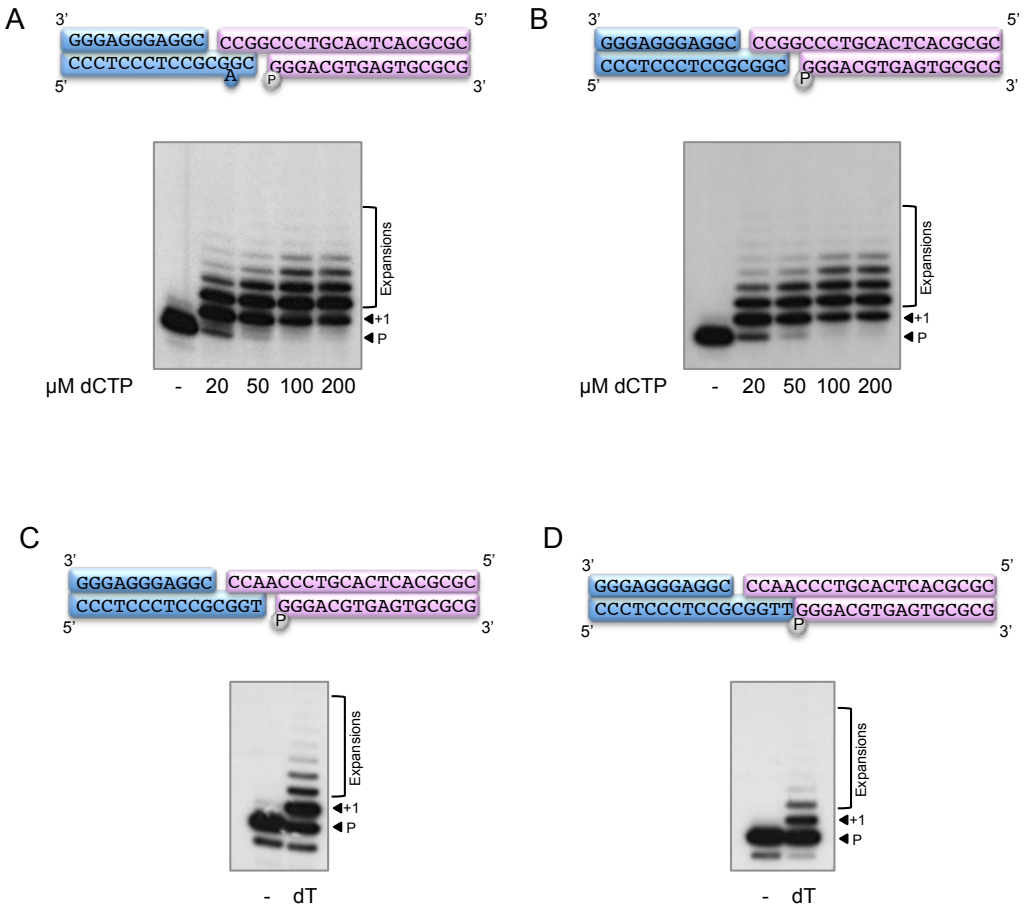

Figure 18. Sequence expansions catalyzed by Polμ during NHEJ. A&B) The amount of nucleotide required by Polμ to produce nucleotide expansions during NHEJ is very low (20 μM), indicating that this process is highly efficient. Polymerization reactions were performed in the presence of the indicated range of concentrations of dCTP. **C&D)** Nucleotide expansions occurring during NHEJ were also generated when the template dinucleotide closer to the 5´P was formed by a pair of adenines, either forming a 1 nt gap, or even forming a nick neighbour to the 5´P. Polymerization reactions were performed in the presence of 100 μM dTTP, and with the following substrates: the labelled substrate (dark grey) is formed by hybridization of oligonucleotides D3+T and D1.

2

Analysis of genetic instability in Mouse Embryonic Cells (MEFs) deficient in Polλ and Polμ

Over the last 15 years, the Blanco laboratory has been focused in the study of mammalian DNA polymerases Pol*μ* and Polλ in the repair of DSB via NHEJ, since they were identified in our lab at 1999. Since then, we have obtained viable single and double knock-out (KO) models for these DNA polymerases. As it was already described in Gloria Terrado's PhD Thesis (2010), by retrocrossing these single models, we have recently obtained a mouse model deficient in both polymerases for a further analysis of their role in maintaining genome integrity.

As a first approach to study the potential role of these two enzymes in DNA repair and tolerance to oxidative damage, we obtained the corresponding mouse embryonic fibroblasts (MEFs) from the KO animals, deficient in ether Polλ, Pol*μ* or in both DNA polymerases (Double KO, DK).

Whereas several studies have deciphered some interesting phenotypes of the inidividual KO models for these polymerases (Bertocci et al. 2006; Lucas et al. 2009b), this thesis is now focused in the study of the double knockout (DK) model, which hasn't been described yet.

2.1 DK MEFs entry earlier in senescence than wt MEFs

As it was previously described, MEFs deficient in Ku86, a NHEJ factor, present diminished proliferative capability (Espejel and Blasco 2002; Vogel et al. 1999). Moreover, Pol*μ* Knockout MEFs entried earlier in senescence than wt cells (Lucas et al. 2009a). We were interested in checking if this phenotype was maintained in the DK model, or increased.

When cultured in a 3T3 protocol (Todaro and Green 1963) MEFs behave in 3 distinct phases: 1) Exponential growing; 2) Senescence and 3) Immortalization. There are many molecular mechanisms described that are involved in MEFs' senescence and immortalization (Ben-Porath and Weinberg 2005; Campisi et al. 2001; Irani et al. 1997; Parrinello et al. 2003; Sharpless and DePinho 2004; Sherr and DePinho 2000; Woo and Poon 2004). Most of them remark that, in the case of MEF culture, senescence is related to an increase in oxidative damage and the general DSB repair operating in these cells.

We used the 3T3 protocol in early passage MEFs to check whether the absence of both Pols in DK MEFs led to a higher senescence than wt MEFs. As we can see in Fig. 19, the capability to duplicate in DK cells sharply diminished after passage 3 compared to wt, indicating an earlier entry of senescence in these cells, slightly larger than the one described previously for Pol*μ* in Beatriz Escudero's PhD Thesis (2010), and Polλ (E. K. Braithwaite et al. 2005a). We used the single model KO as an internal control in the 3T3 assay (data not shown).

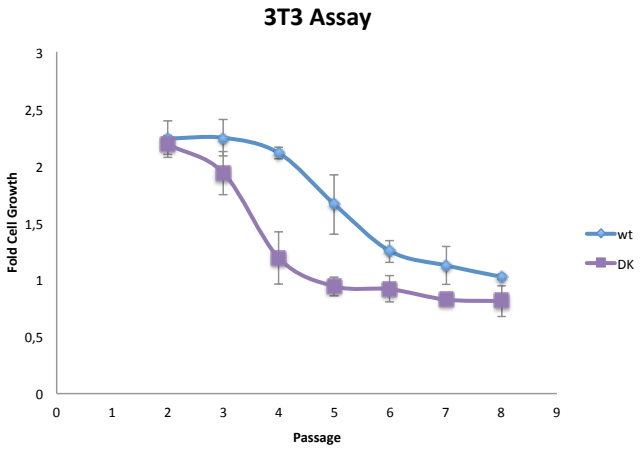

Figure 19. DK MEFs entry earlier in senescence. 3T3 assay in primary MEFs from wt and DK mice. Each point represents mean value of 3 independent experiments.

2.2 DK MEFs present higher sensitivity to Gamma Irradiation

In general, cells deficient in DNA repair factors are sensitive to genotoxic agents. Among them, gamma irradiation is one of the most common agents used in the study of genetic instability.

Gamma irradiation is frequently used to generate randomly induced DSBs (Natarajan 1993), reviewed by (Pfeiffer et al. 2000). It was previously known that mice lacking NHEJ factors and KO*μ* mouse present hypersensitivity to gamma radiation (Bassing and Alt 2004; Lucas et al. 2009a; Meek et al. 2004). To further understanding the phenotype of the DK MEFs, we decided to check how gamma irradiation affects to its proliferation and survival. For that, we irradiated wt and KO MEFs with 5 and 10 Greys (Gy). After 3 days, we tested cell survival by counting cells using a hemocytometer.

As shown in Fig. 20, in the case of the single KO MEFs (KOλ and KO*μ*) we observed a slightly higher sensitivity than wt using in 5 Gy dose, and a similar survival percentage to wt using 10 Gy (quite severe to all MEFs types, including wt). It was very remarkable that at both irradiation doses (5 and 10 Gy), DK MEFs were 3 times more sensitive to gamma radiation than wt cells, indicating that the absence of the two polymerases has an impact in DSB repair.

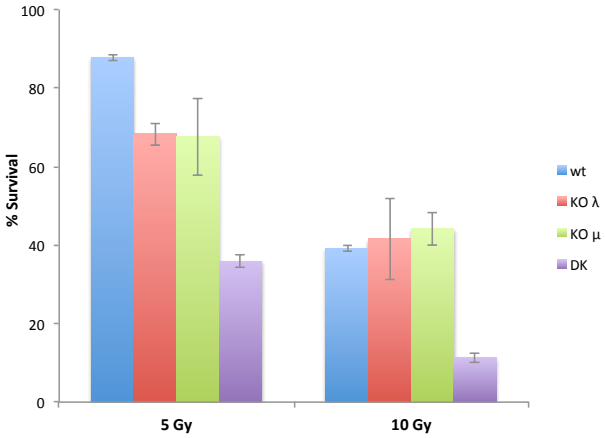

Figure 20. DK MEFs present higher sensitivity to Gamma irradiation. Effect of different doses of gamma irradiation (5, 10 Greys) on MEFs. MEFS were irradiated at different doses and counted for survival after 72h recovery. The data shown are mean ± SD of 3 independent experiments with MEFs in passage 3-5. Error bars show SD.

2.3 Impact of different DNA damage agents in cell viability

In general, cells deficient in DNA repair factors are sensitive to genotoxic agents. Some of these genotoxic agents can be classified as oxidative damage agents or chemotherapeutical agents. The mechanism by which each agent affects DNA is different, but they all have major impact in DNA integrity. Taking this into consideration, we thought that it would be interesting to evaluate the sensitivity of KOλ, KO*μ* and DK MEFs to different drugs using the MTT-sensitivity assay (described in materials and methods).

2.3.1 Oxidative agents: H_2O_2, TBH

During metabolism, reactive oxygen species (ROS) cause oxidative DNA damage. This represents a significant contribution to genomic instability, carcinogenesis or cellular ageing. ROS introduces DNA base or sugar damage that normally leads to single-strand breaks (SSB), but also at a lower frequency than double-strand breaks (DSB) (Lindahl et al. 1993). Considering this, we used

the MTT survival assay to examine the effect of H_2O_2 in KO MEFs (Fig. 21). Briefly, we treated the cells during 1h with the drug concentration indicated; washed and let them recover from the damage for 48h.

In the case of H_2O_2, we couldn't observe big differences in the survival of wt and KOμ MEFs, indicating that the drug dose was insufficient to affect the control. Interestingly, in the case of the higher dose (50 μM), we observed that KOλ and DK MEFs sensitivity was affected, reducing viability to about 70%. With this result, we confirmed previous data that described KOλ MEFs were sensitive to this drug (E. K. Braithwaite et al. 2005b), and DK MEFs corroborated that the lack of Polλ affected the survival of these MEFs in the presence of this kind of damage.

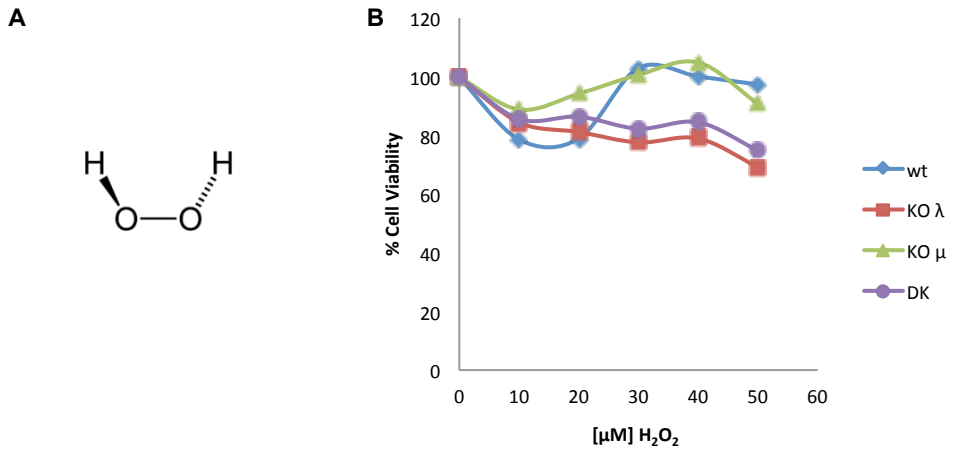

Figure 21. Cell viability in presence of H_2O_2. A) Molecular structure of H_2O_2. **B)** Dose-response curves for cell viability of wt, KOλ, KOμ and DK MEFs. Cells were exposed to H_2O_2 at the indicated concentrations for 1h, and survival was measured by the MTT assay after 48 h. The data shown are mean ± SD of 3 independent experiments with MEFs in passage 3-5. Error bars show SD.

Considering that H_2O_2 didn't affect wt and KOμ MEFs and to confirm if there was an effect due to oxidative damage in KOμ MEFs, we decided to try TBH, which is a stable H_2O_2 derivative that also generates ROS. As we can see in Fig. 22, the doses of TBH used were enough to compromise the survival of the wild-type MEFs, reducing the viability to about 60%, and indicating that the drug was functional.

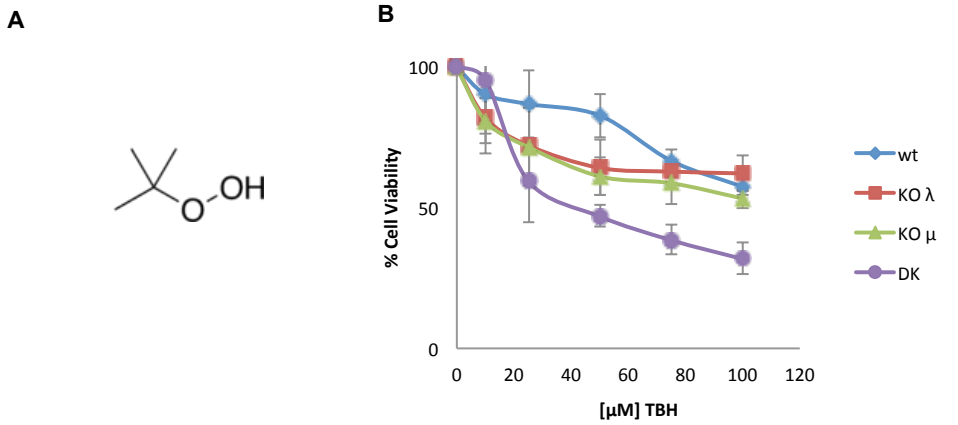

Figure 22. Cell viability in presence of TBH. A) Molecular structure of TBH. **B)** Dose-response curves for cell viability of wt, KOλ, KOμ and DK MEFs. Cells were exposed to TBH at the indicated concentrations for 1h, washed and survival was measured by the MTT assay after 48h. Data shown are mean ± SD of 3 independent experiments with MEFs in passage 3-5. Error bars show SD.

On one hand, we could see that the single KO MEFs behaved very similar, although with a slightly higher sensitivity to low and medium doses (25, 50 μM) of TBH compared to wt; at higher doses (75, 100 μM), this difference disappeared. On the other hand, DK cells were extremely sensitive to this agent even when the dose was low (20 μM), indicating that Polλ and Polμ might participate in the repair of the lesions caused by oxidative damage induced by TBH, causing cell death when both DNA polymerases are absent in the cell.

2.3.2 Chemotherapeutical agents: Cytarabine (AraC), Fludarabine, Cisplatin, Curcumin, Etoposide

The most commonly used chemotherapeutic agents include alkylating agents, nucleotide analogs, and topoisomerase inhibitors, among others. The main goal of these compounds consists in impairing cancer growth and progression by different mechanisms: from intercalation between base pairs of DNA/RNA strand, alkylation of DNA, to suppression of proper coiling and uncoiling of DNA (Esteva et al. 2001).

2.3.2.1 Cytarabine (AraC)

Cytarabine (or AraC) is a nucleoside analog of cytosine that presents arabinose instead of ribose or desoxirrobose (Fig. 23A). This drug has been successfully used in antitumor therapy in myelogenous leukemia (Estey et al. 1987; Keating et al. 1982; Mastrianni et al. 1992).

AraC acts as a DNA replication and repair resynthesis inhibitor, and it has been used extensively in the study of DNA repair. It was previously shown that most PolXs were able to insert AraC in DNA, being Polμ and Polλ more efficient than Polß in this insertion step (Gloria Terrados, PhD thesis). Therefore, we decided to test this compound in vivo, and if it affects viability of the different MEF strains.

As shown in Fig. 22B, addition of AraC to the WT MEFs had a double effect, considering the doses. At low dosis (x-10 μM), AraC progressively affected cell viability, that was reduced up to 60%; at higher doses (up to 100 μM), there was no further reduction in viability. When this compound was added to the single KO MEFs, we didn't find any remarkable difference in sensitivity at any dosis tested. Both KOλ and KOμ behaved similar to wt, indicating that the lack of one of these

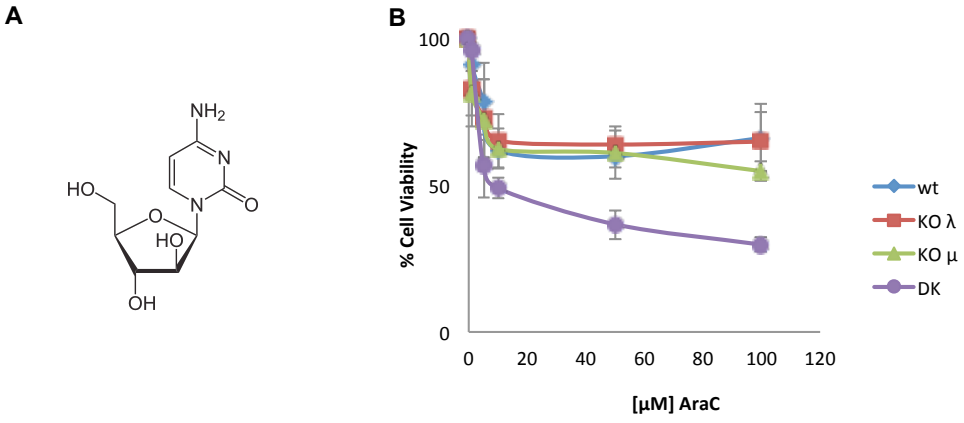

Figure 23. DK MEFs present higher sensitivity to AraC. A) Molecular structure of AraC. **B)** Dose-response curves for cell viability of wt, KOλ, KOμ and DK MEFs. Cells were exposed to AraC at the indicated concentrations for 72h, and survival was measured by the MTT assay after 24h. The data shown are mean ± SD of 3 independent experiments with MEFs in passage 3-5. Error bars show SD.

polymerases didn't affect to the direct survival. In contrast, cell viability of the DK MEFs fell more drastically, even at the higher dosis tested (100 μM). The repair of the damage provoked by the incorporation of AraC is sharply affected in DK MEFs.

2.3.2.2 Curcumin

Curcumin is an active ingredient in powder isolated from *Curcuma longa*. Curcumin has potent anti-inflammatory, anti-bacterial and anti-cancer effects (Lu et al. 2009). Curcumin was found to produce oxidative stress and DNA damage at high doses (Cao et al. 2006). Moreover, curcumin treatment was shown to decrease expression levels of many DNA damage response genes involved in NHEJ, including ATM, ATR, BRCA1 or DNA-PK PK (Lu et al. 2009){, #0}. These findings suggested that both direct and indirect effects explain a deficit in the DNA damage response, and ultimately the curcumin-induced growth inhibition. Therefore, and considering the mild effects observed with other compounds on the single-KO MEFs, we decided to test how this compound affects the viability of MEFs that simoultaneously lack the two DNA polymerases Polλ and Polμ.

We treated the DK MEFs with increasing doses of Curcumin for 48h (Fig. 24), and checked sensitivity with MTT-assay. We observed that the lowest dose of curcumin used (10 μM) strongly affected cell viability of the DK MEFs compared to wt, presenting a survival rate of 40% against 90% in wt. This difference was maintained at 20 μM curcumin (10% vs. 50%), but vanished at higher doses (30 and 40 μM), perhaps indicating a general toxicity of these relatively high doses.

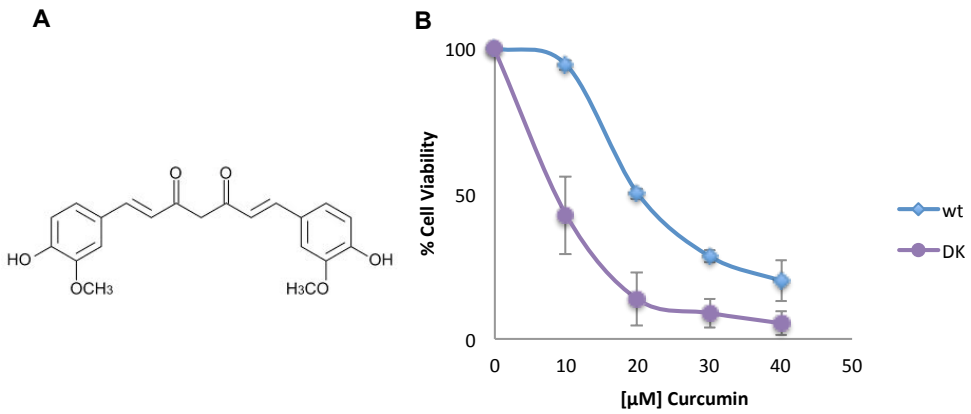

Figure 24. Cell viability in presence of Curcumin. A) Molecular structure of Curcumin. **B)** Dose-response curves for cell viability of wt, KOλ, KOμ and DK MEFs. Cells were exposed to Curcumin at the indicated concentrations for 48h, and survival was measured by the MTT assay after 24 h. The data shown are mean ± SD of 3 independent experiments with MEFs in passage 3-5. Error bars show SD.

2.3.2.3 Fludarabine

Fludarabine (F-ara-ATP) is a purine nucleoside analogue used for the treatment of blood system cancers such as lymphomas and leukemia (Catapano et al. 1991). It becomes incorporated into DNA or RNA, thus blocking further nuclei acid synthesis. Besides, fludarabine directly inhibits ribonucleotide reductase, and is also able to inhibit both DNA ligase and DNA primase. However, *in vitro* studies have shown that the loss of cell viability correlates directly with the level of incorporation of the analog into cellular DNA (Rai et al. 2000).

We tested this drug in our MEFs, administrating different doses during 72h. After this time, we drug sensitivity linked to cell survival was analyzed with the MTT-assay (Fig. 25). We observed that single KO and DK MEFs present similar sensitivity at very low dose (0,2 ng/ml), being always more severe than that shown by wt MEFs (55% cell viability in wt *vs* 30% in the rest). When increasing the

dose, DK MEFs maintained severe sensitivity but single models, especially KO*μ*, presented a milder effect. We could conclude that fludarabine affected DNA integrity more intensively in DK MEFs.

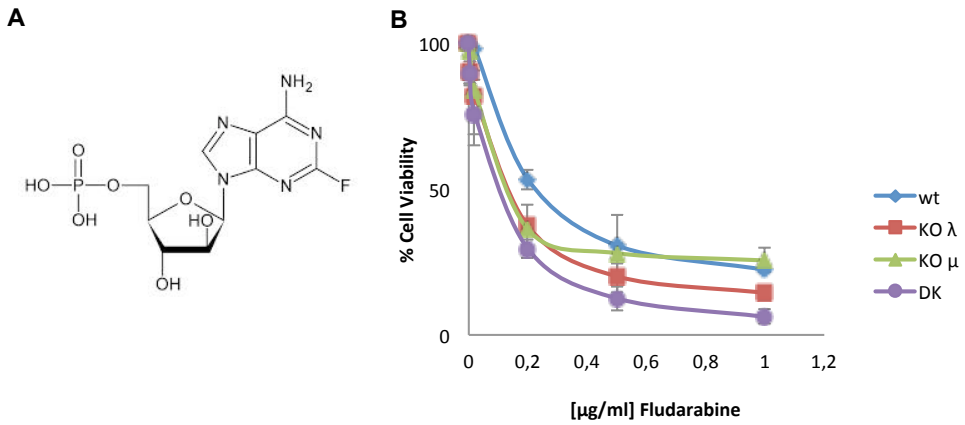

Figure 25. Cell viability in presence of Fludarabine. A) Molecular structure of Fludarabine. **B)** Dose-response curves for cell viability of wt, KOλ, KO*μ* and DK MEFs. Cells were exposed to Fludarabine at the indicated concentrations for 72h, and survival was measured by the MTT assay after 24 h. The data shown are mean ± SD of 3 independent experiments with MEFs in passage 3-5. Error bars show SD.

2.3.2.4 Cisplatin

Cisplatin is a widely used anti-cancer drug. Cisplatin binds to DNA, produces intrastrand and interstrand crosslinks, which induce structural distortions in DNA. These distortions produced by the DNA adducts have a cytotoxic effect by inhibiting DNA replication and transcription (Rosenberg 1985). Considering this, we decided to check if the sensitivity to thid drug is modified in MEFs that lack one or both DNA polymerases Polλ and Pol*μ*.

Again, cell viability was determined by the MTT-assay after 72h of treatment (Fig 26). Interestingly, KOλ and KO*μ* MEFs presented a higher sensitivity to low doses of cisplatin compared to wt, which was maintained up to the highest dose. DK MEFs viability was sharply reduced even in the lower dose. DK MEFs viability did not show a synergistic effect, and paralelled the profile of KO*μ*, with the exception of a slightly higher inhibition observed at the lowest dose. It is important consider that Pol*μ* has been involved in the bypass of cisplatin adducts (Havener et al. 2003), which might explain why KO*μ* and DK present similar viability.

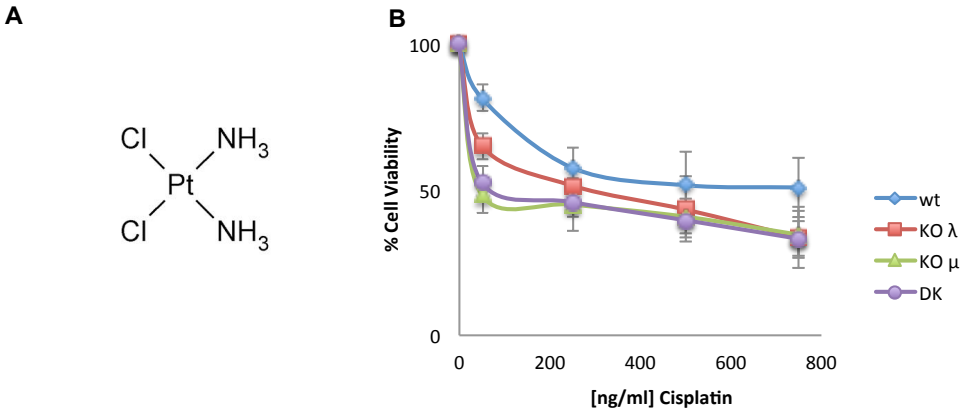

Figure 26. Cell viability in presence of Cisplatin. A) Molecular structure of Cisplatin. **B)** Dose-response curves for cell viability of wt, KOλ, KO*μ* and DK MEFs. Cells were exposed to Cisplatin at the indicated concentrations for 72h, and survival was measured by the MTT assay after 24 h. The data shown are mean ± SD of 3 independent experiments with MEFs in passage 3-5. Error bars show SD.

2.4 Use of Etoposide to decipher DK MEFs deficiency in NHEJ

DNA Topoisomerases class II (topoII) are proteins that cleave and re-ligate the DNA double helix to relieve topological constraints during DNA replication. TopoII is a homo-dimeric enzyme where each subunit cleaves one strand of the DNA double helix creating a transient DSB to allow the passage of an intact DNA strand through it. There are some chemotherapeutic drugs that target topoII to compromise DNA replication. One of these drugs is etoposide. Etoposide inhibits the action of topoII, that can not complete the reaction; instead, the enzyme remains covalently bound to the 5′-end of the DNA, as a frozen intermediate. Etoposide is an antitumor drug that has been widely used to couple DNA damage to cell cycle arrest and apoptosis (Shimazaki et al. 2012).

Taking into account all the data available describing etoposide, widely used to induce DSB associated to replication forks, we decided to test sensitivity to this drug when either one or both DNA polymerases, Polλ and Polμ, were absent in the cell, and therefore NHEJ is severely compromised as a potential mechanism to fix etoposide-induced DSBs.

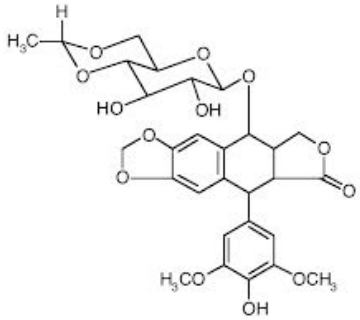

Figure 27. Molecular structure of Etoposide.

2.4.1 Etoposide provokes major senescence in DK MEFs

To measure the effects of etoposide on cell senescence in DK MEFs, we used the senescence-associated β-galactosidase (SA-β-gal) staining. As shown Fig. 28, we used wt and DK MEFs in passage 5, administrating 2,5 μM etoposide during 24h. MEFs corresponding to an early passage (5), already shown senescence-like phenotype (Fig. 28, pictures on the left) as we could see in 3T3 assay (Fig. 19). This phenotype exhibited typical enlarged and flattened senescence morphology, even when no etoposide was administered to MEFs. We observed that DK MEFs showed 3 times more ß-gal staining in both situations compared to wt, either without etoposide or after treatment with 2,5 μM etoposide. Interestingly, we observed that DK MEFs present more ß-gal associated senescence with no etoposide dose than wt MEFs with etoposide. We could conclude that DK MEFs enter in senescence earlier than wt MEFs, which may indicate a strong defect in DNA repair in the absence of these two DNA polymerases.

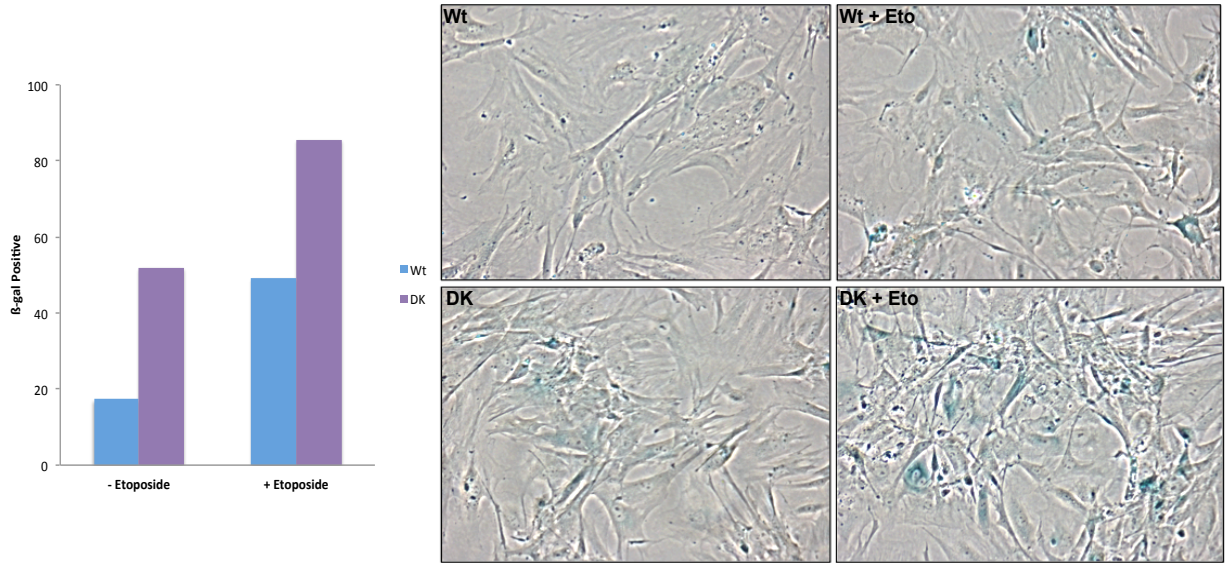

Figure 28. Effect of etoposide on wt and DK MEFs. MEFs senescence was measured by the senescence-associated β-galactosidase (SA-β-Gal) activity assay. MEFs were cultured with etoposide 2,5 μM for 48h. Representative images of SA-β-Gal staining: wt, wt + Etoposide, DK and DK + Etoposide.

2.4.2 Clonogenic assay

The clonogenic assay enables a reliable assessment of the differences in cell survival between control untreated cells and cells that have undergone treatment. It is commonly used for determining the effects of cytotoxic agents (Rafehi et al. 2011). We evaluated wt and DK MEFs ability to form colonies after different doses of etoposide. After 14 days, we fixed, stained and counted the colonies formed (Fig. 29). We observed that wt MEFs were able to form colonies more efficiently than DK MEFs at every dose of etoposide. In the case of 2,5, 5 μM and 10 μM, the survival rate is almost half in DK compared to wt. This result confirmed that it is necessary the lack of these two DNA polymerases to produce an effect in the DSB repair.

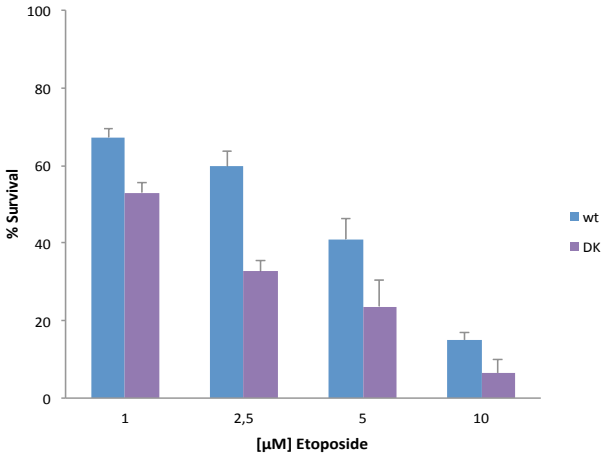

Figure 29. The inhibitory effects of etoposide on cell proliferation and colony formation in wt and DK MEFs. For colony-forming assay, the clonogenic assay was done as described in Materials and Methods. *Columns,* mean of three determinations; *bars,* SD. Results shown are representative of three independent experiments with MEFs in passage 3-5.

2.4.3 DK MEFs present a persistent 53BP1 foci formation in time

53BP1 is phosphorylated by ATM and forms nuclear foci that colocalize with Y-H2AX at sites of DBSs. In contrast, Y-H2AX accumulation alone occurs in the absence of DSBs such as sites of UV-damage or in senescent cells (Goodarzi and Jeggo 2009). Interestingly, etoposide-induced DSBs are repaired more rapidly than ROS or IR-induced DSBs consistent with the notion that directly ligatable DNA ends are repaired more rapidly than 'dirty' DNA ends (Goodarzi and Jeggo 2009).

We tested the kinetics of 53BP1 foci formation after administrating 2,5 μM etoposide to WT versus DK MEFs, that directly correlates with the kinetics of etoposide-induced DSB repair. After 30 min of etoposide treatment, the ability of WT and DK MEFs to repair etoposide-induced DSBs (measured by the presence of p53BP1 foci) was tested at the indicated times (Fig. 2.5.3). We observed that DK MEFs present an acute damage right after the removal of etoposide (Fig. 2.5.3A, time 0), compared to wt and single KO. The presence of more than 5 foci per cell indicates severe DNA damage that should be solved within time. After removal of the drug, wt and single KO MEFs diminished the number of cells presenting more than 5 foci per cell (about 20% *ad initio*) as recovery time increased, indicating that DNA damage is being repaired. In the case of DK MEFs, we observed that the damage (about 40% of cells showing more than 5 foci) persisted for longer, indicating that DSB repair is dramatically delayed.

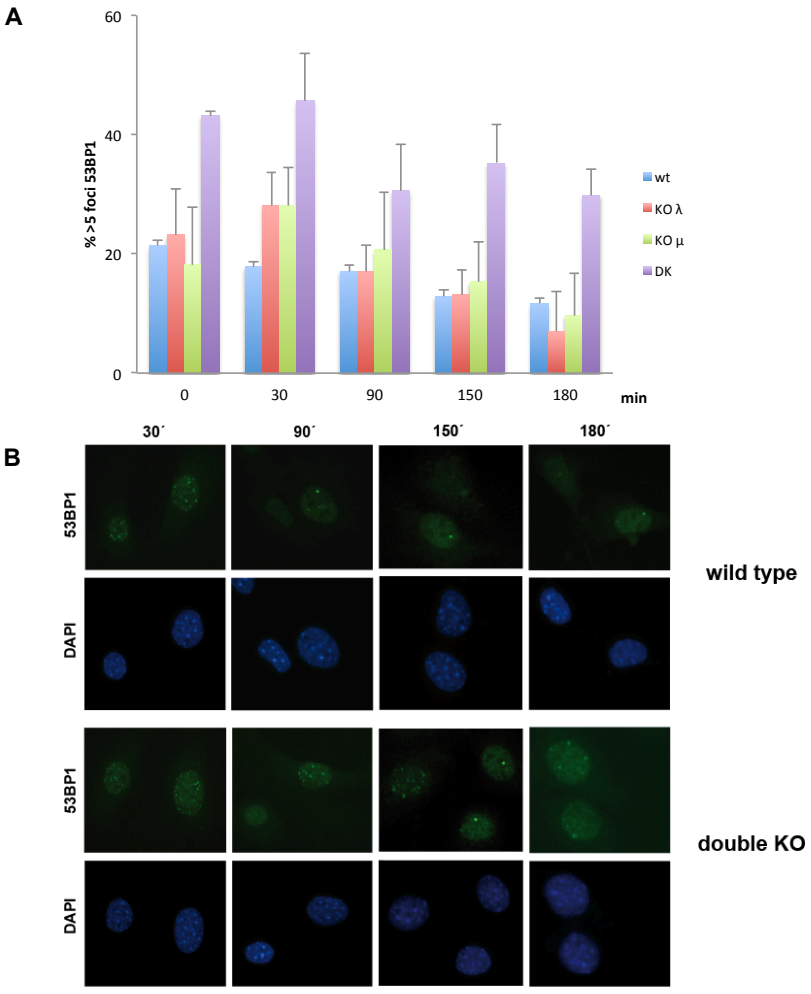

Figure 30. 53BP1 foci formation remains in time in DK MEFS. A) Percentage of nuclei exhibiting >5 53BP1 foci in MEFs in passage 3-5 at different recovery time after etoposide removal. Error bars indicate SD. Results shown are representative of three independent experiments with MEFs in passage 3-5. **B)** Representative images of 53BP1 foci and DAPI of the indicated genotypes at different recovery time after etoposide removal.

2.4.4 Etoposide drastically affects the cell cycle in DK MEFs

DSB repair is tightly regulated during the cell cycle. In G1 phase, NHEJ is the prominent pathway for DSB repair because of the absence of a sister chromatid. In late S and G2 phases, even though NHEJ remains functional, there is an increase in the repair of DSB by HR (Mao et al. 2008; Natarajan et al. 2008; Takata et al. 1998);(Takashima et al. 2009). However, NHEJ is active during all stages of cell cycle, but its efficiency is the highest during G2/M. Although HR is active primarily in the S-phase, has lower activity in G2/M. HR and NHEJ are regulated independently, since inactivation of one mechanism is not counter-balanced by increasing the other. Taken this together, we evaluated if the cell cycle is altered in DK MEFs treated with etoposide (reported to induce damage in all phases of the cell cycle).

We administrated a 3 μM dose of etoposide during 1 h to an asynchronous culture of WT or DK MEFs. If there was a deficiency in NHEJ, we would expect to see an increase in G2/M phase due to the cell cycle arrest at that point.

First, we harvested wt and DK MEFs at different recovery times after drug treatment, 4 (Fig. 31A). After 4h recovery, the wt MEFs treated and non-treated presented similar patterns in the cell cycle distribution, indicating that wt MEFs were normally able to recover from the drug treatment. However, in the presence of etoposide almost 70% DK MEFs were arrested in G2/M(Fig. 31B).

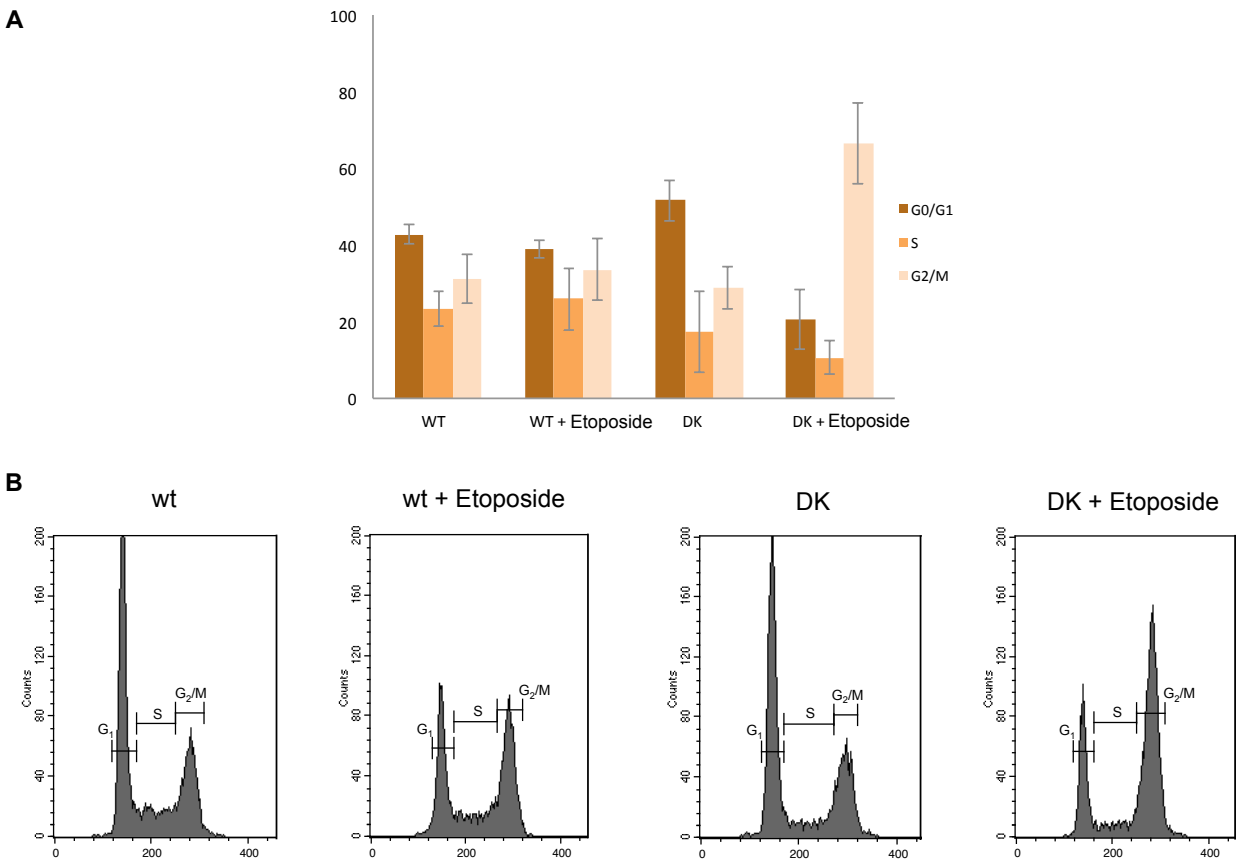

Figure 31. Etoposide affects the cell cycle in DK MEFs. A) Graphic cell cycle distribution of wt and DK MEFs in an asynchronous culture in basal conditions or after etoposide treatment. On the left, bars represent wt and DK genotypes at 4h recovery; on the right, at 24h recovery. Error bars indicate SD Results shown are representative of three independent experiments. **B)** Representative cell cycle distributions of wt and DK MEFs at 4h recovery after etoposide treatment.

Despite the single KO MEFs presented similar behavior pattern than wt MEFs in most of the MTT-sensitivity, clonogenic and 53BP1 foci assays, we decided to test whether etoposide affected their cell cycle distribution after 4h recovery (Fig. 32).

In the case of KOλ, we observed a slight accumulation in G2/M when compared to non-treated cells (40% *vs*. 25%). This delay in G2/M was larger in KO*μ* (45% *vs*. 25%), but not as significant compared to wt (70% *vs*. 30%). The absence of one of these DNA polymerases mildly affected cell cycle regulation in the case of damage. However, when both DNA polymerases are lacking and there is DNA damage, cell cycle was drastically affected provoking major arrest in G2/M. That could trigger the G2/M checkpoint, to limit the proliferation of chromosomally unstable cells (Lobrich and Jeggo 2007).

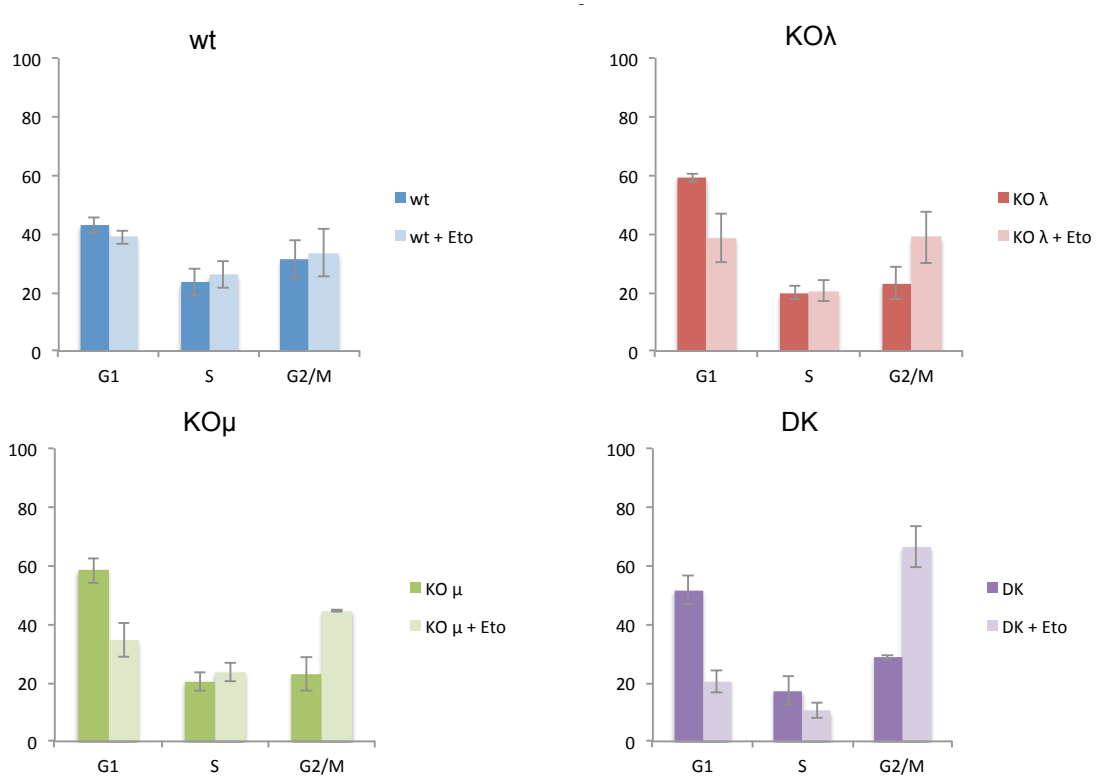

Figure 32 Cell cycle distribution of MEFs. Graphic cell cycle distribution of wt, KO, KO*μ* and DK MEFs in an asynchronous culture in basal conditions or after etoposide treatment. On the left, bars represent wt and DK genotypes at 4h recovery; on the right, at 24h recovery. Error bars indicate SD Results shown are representative of three independent experiments.

3

Using murine models for in vivo *analysis of Polλ and Polμ in repair and tolerance of oxidative damage*

3.1 Generation and use of murine deficient in DNA polymerases Polλ and/or Polμ

The functional importance of Polλ and Polμ has been previously studied in a cellular context. As described in chapter 2, we have analyzed the genetic instability occurring in MEFs lacking one (KOλ; KO*μ*) or two (DK) of the NHEJ DNA polymerases (Polλ and Polμ), specially focusing on DK MEFs. These MEFs were derived from animal models of single and double deficiency previously generated in our laboratory (Gloria Terrados 2010, PhD Thesis). In order to continue with the characterization of these mouse colonies, we analyzed the lifespan and survival of each colony (Fig. 33).

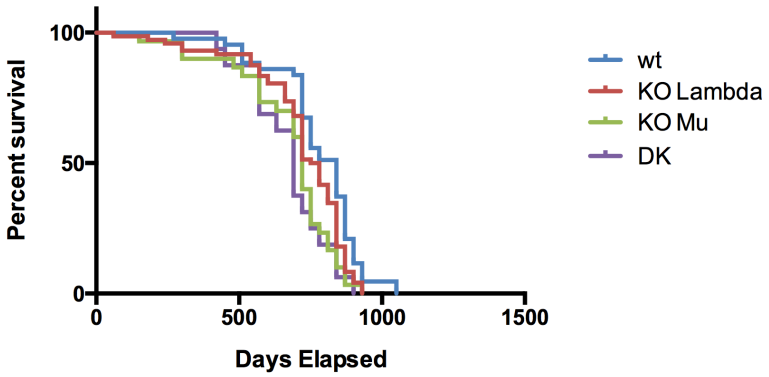

Figure 33. Kaplan-Meier analysis of overall survival in mice colonies

We observed that the absence of these two polymerases doesn't affect the survival of the DK model. However, the number of pups per litter is smaller in DK colony than in single KO models. That explains in part the difficulty to generate and establish this double KO model. Each colony is in C57BL6 pure genetic background.

In table 3 we show a general description of the different colonies. The different parameters studied, as length, weight, sex, etc…were similar among the four colonies.

	wt	KOλ	KO*μ*	DK
Pups per litter	7	7	8	5±2
% Male/Female	50,7/49,3	49,9/50,1	51,2/48,8	58/42
Length	8,7 cm	9,1 cm	9,0 cm	9,7 cm
Weight	30,8 ± 1,6 g	32,7 ± 3,7 g	34,0 ± 5,7 g	35,0 ± 1,0 g

Table 3. Comparative study of C57BL6 colonies, lacking Polλ and/or Polμ

3.2 NHEJ activity and oxidative damage tolerance analysis in crude extracts

As shown in Chapter 2, after obtaining satisfying results in the study of the genetic instability of MEFs in culture, we performed an enzymatic analysis of crude extracts of different tissues derived from these models.

As a first approach, we obtained crude extracts from testis, a tissue expressing huge levels of Polλ (Garcia-Diaz et al. 2000). After obtaining the crude extract, we analyzed the activity of these extracts to fill the gap in a NHEJ context created by a 4-base pairs connection (Fig. 34). We firstly analyzed template-dependent activity in wt testis to demonstrate the occurrence of a *bona fide* NHEJ reaction. We used a set of 4 molecules in which the templating base (position X in figure 34) was any

of the four possible options. The results showed a preferential insertion of the complementary deoxynucleotide (directed by the base at the X position in each case), supporting that the extracts can perform an orthodox NHEJ reaction.

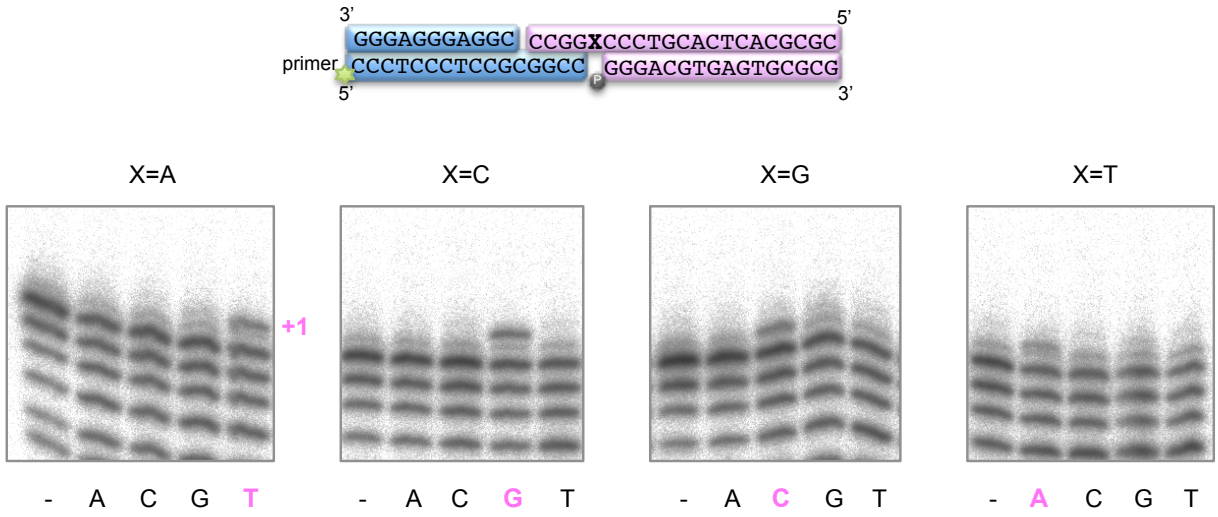

Figure 34. Crude extracts from wt testis can perform accurate NHEJ. NHEJ reactions were carried out as described in Materials and Methods, using the four DNA substrates (a scheme is shown) differing in the templating base (X), with 10 μg of wt testis crude extracts, and the indicated deoxynucleotide (xx μM). After 1h of reaction at 30ºC, extension of the labelled primer was evaluated by denaturing electrophoresis and autoradiography. The grey ball indicates the presence of a 5'-P group in one of the recessive strands, which orients gap-filling. In pink, the correct nucleotide to be inserted, to generate a +1-extended primer

Secondly, we wanted to check whether this activity was affected in the extracts obtained from the single KO models and the DK. Thus, we first tested the NHEJ activity of these extracts, having C as the templating base (Fig 35A). We first analyzed the ability to fill the gap and ligate the final product (these other NHEJ proteins, as ligases, are presumed to be present in the extract). For this, we independently provided each one of the 4 different deoxynucleotides to each crude extract. As we could observe, the four extracts were able to fill properly the gap (+1 band) only when provided with the complementary base (dG) to the template (dC). Interestingly, all extracts also presented additional extension products (up to +4) that can be explained by insertion of three additional dG units directed by the next templating bases CCC. For that reaction to occur some strand-displacement must be generated to allow template dictation when extending the +1 product (see the scheme at Fig. 35). Besides, the four extracts produced a full-length (+33) product, indicating that there was also a ligated product in the reaction. Strikingly, the KOλ extracts produced an accumulation of the +4 product and a small amount of a further +5 product: that could indicate a defective coordination of strand-displacement polymerization, with FEN-1 processing of the displaced strand and final ligation, in the absence of Polλ.

We also tested the influence of providing dideoxinucleotides to the same type of reaction, to limit the activity to a single nucleotide extension (Fig. 35B). In this case, the four extracts were able to insert the correct incoming nucleotide (ddGTP), but we didn't find any relevant difference between them. It is quite possible that this NHEJ reaction, based on a complementarity of 4 base pairs is not requiring specialized NHEJ DNA polymerases as Polλ and Polμ, but it uses the housekeeping family member, Polß. To elaborate more this data, we decided to use a different type of substrate.

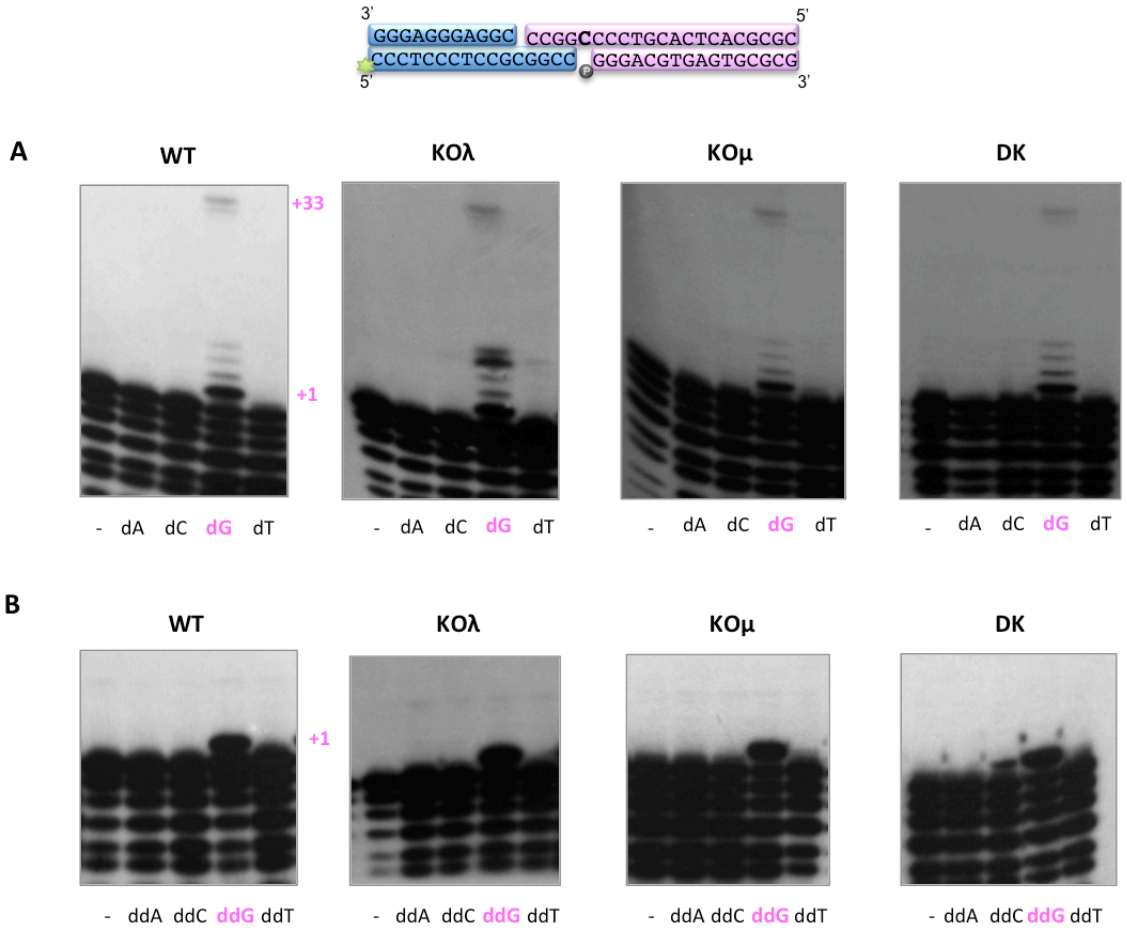

Figure 35. NHEJ template dependent activity is not affected in crude extracts. NHEJ reactions were performed as described in Materials and Methods, using the DNA substrates (two DNA ends; one of them labeled) shown in the scheme, with 10 μg of wt testis crude extracts, and xx μM of each independent dNTP or ddNTP. After 1h of reaction at 30ºC, extension of the labeled primer strand (blue) was detected by electrophoresis and autoradiography. The green star indicates the 5´-P labeling of the 3´-protruding strand of one of the two DNA end substrates (boxed in blue).The grey ball indicates the presence of a 5'-P group in the downstream strand of the substrate. In pink, the correct nucleotide to be inserted. **A) Use of deoxynucleotides.** Crude extracts from different mice colonies are shown at the top. **B) Use of dideoxynucleotides.** Crude extracts from different mice colonies are shown at the top.

3.3 Evaluation of 8oxoG tolerance activity in testis extracts

In post-mitotic organs like testis, repair of deleterious oxidative DNA damage associated with 8-oxo-guanine (8oxoG) generation is a substantial need. Base excision repair is the main mechanism eliminating 8oxoG from DNA, but several other mechanism have been proposed, as the tolerance/repair alternative (Kirouac and Ling 2011; Maga et al. 2007). 8oxoG behaves as a pre-mutagenic lesion; when used as template by a replicative polymerase activity, 8oxoG dictates not only the insertion of a correct dCTP residue (when 8oxoG is in *anti*-orientation) (Fig. 36A), but also has the potential to direct misinsertion of dATP (when 8oxoG adopts a *syn*-orientation), thereby forming an 8oxoG:dAMP mismatch.

Currently, it is well documented the importance of Polλ in 8oxoG tolerance, specifically during the correction of 8oxoG:dAMP mispairs started by the MutYH glycosilase (Amoroso et al. 2008; Locatelli et al. 2010; Maga et al. 2008; Markkanen et al. 2012a; van Loon and Hubscher 2009). As noted before and due to the high expression of Polλ in testis, we decided to test the translesion activity of testis extracts to bypass the oxidative lesion 8oxoG.

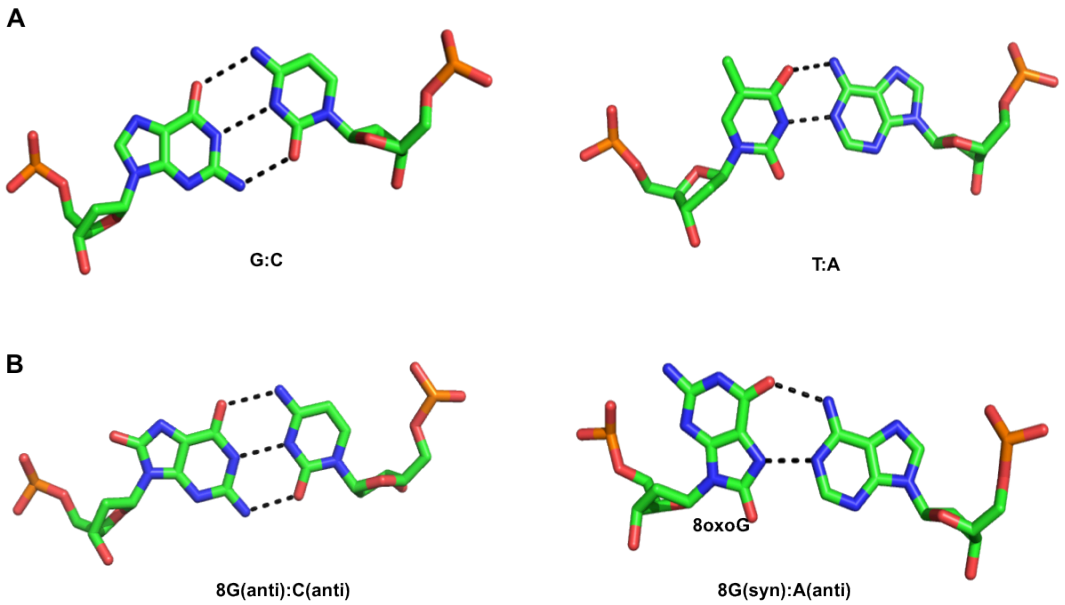

Figure 36. Representation of the possible matching in the modified based 8oxodG. A) Watson and Crick's normal pairing between dG and dC bases PDB id 1U48) and dT and dA (PDB id 178D). Hydrogen bonds are represented with dotted lines. **B)** 8oxodG:dC pairing (PDB id 1U48) and 8oxodG:dA pairing (PDB id 178D). Hydrogen bonds are represented with dotted lines. Adapted from Ana Gómez (PhD thesis; 2013).

As shown in Fig 37A, we firstly tested the four testis extracts in a one-gap filling context containing G as template base, and a 5' phosphate. As already described (Martin et al. 2013), Pol*μ* is able to insert ribonucleotides in addition to deoxynucleotides. Thus we independently provided the four nucleotide substrates, two of them non-complementary to the template G (rA and dA), and other two complementary (rC and dC). The wt extract preferentially inserted the correct dC, but also some rC. insertion of rCTP was likely Pol*μ*-dependednt, as this activity remains using the KOλ extract but disappears when using KO*μ* or DK extracts. Moreover, we observed that there was a ligated product (+34) present when providing rA, dA and rC. This ligated product evidences the activity of ligases present in the extract,taht are frequetly activated by adenine nucleotides..

In Fig 37B, we analyzed the ability of these extracts to bypass the mutagenic lesion produced by the presence of 8oxoG in the template (see scheme in the upper part) in a gap-filling context. Interestingly, all the extracts were able to tolerate the damage and insert dA or dC, as it was described in vitro (Picher et al. 2007). The insertion of dA was weaker in Pol*μ* and DK, indicating that Pol*μ* preferentially makes the error-prone bypass of 8oxoG lesions. Again, rC insertion was only present when Pol*μ* was in the extract (wt and KOλ samples). The mutagenic full-length bypass product was stronger when providing rA in all the extracts, but interestingly, it was significantly dedreased in the Pol*μ* and DK.

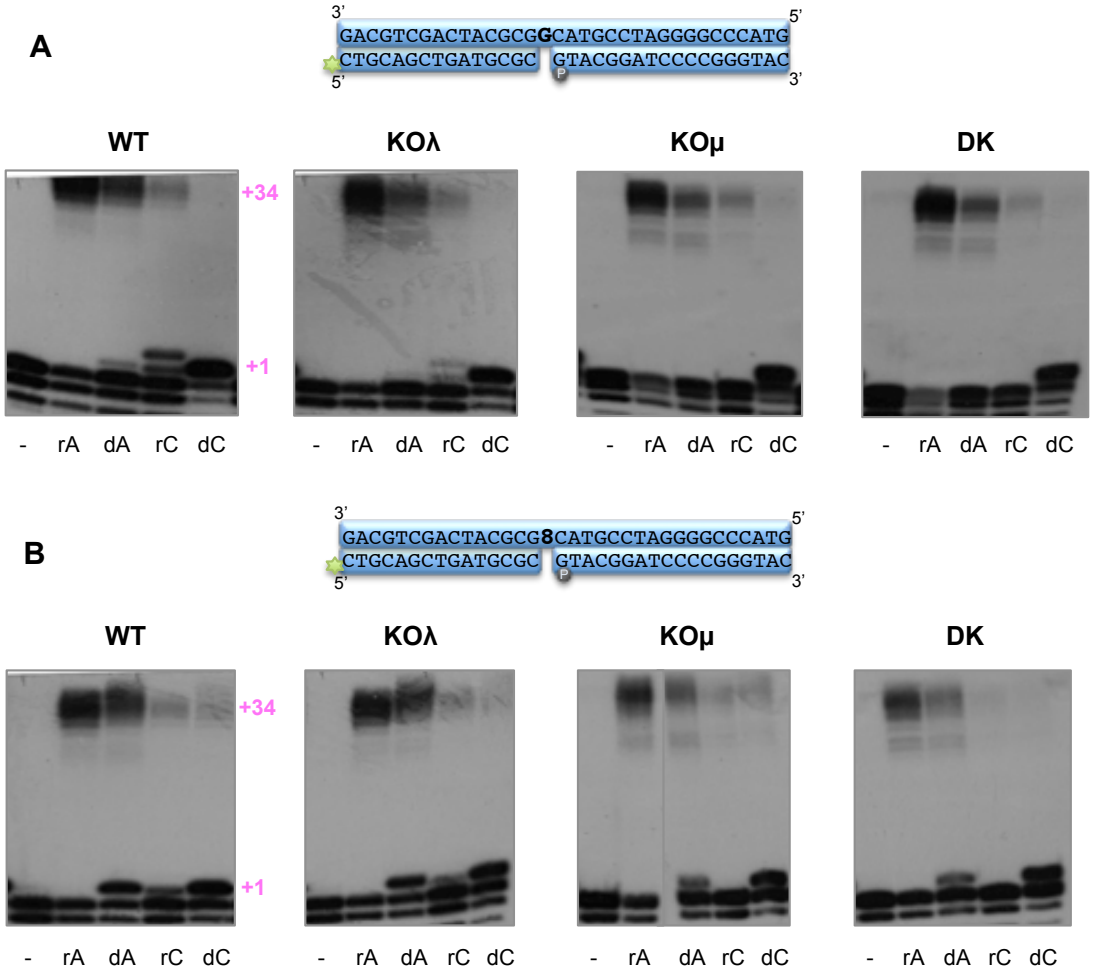

Figure 37. Translesion of 8oxoG as template during gap-filling by testis crude extracts. Reactions were performed as described in Materials and Methods, using the DNA substrate shown in the scheme, 10 μg of wt testis crude extracts, and 100 μM of the indicated ribo or deoxynucleotide. After 1h of reaction at 30ºC, the gap filling and fully repaired/ligated products were detected by denaturing gel electrophoresis and autoradiography. The grey ball indicates the presence of a 5'-P group in the downstream strand of the substrate. **A) Control g**ap-filling assay using crude extracts corresponding to WT or different KO colonies. Crude extracts from different mice colonies are shown at the top. **B)** Gap-filling assay using crude extracts corresponding to WT or different KO colonies, and a gap containing an 8oxoG as the templating base.

It is known that Polμ is highly expressed in the spleen (Dominguez et al. 2000), so we thought it would be interesting to measure the lesion bypass/repair potential of crude extracts derived from this tissue. Unfortunately, spleen contains high concentration of different nucleases, and we couldn't make a proper evaluation of repair and tolerance of oxidative damage because the substrate to evaluate was extensively degraded by nucleases (data not shown).

3.4 Evaluation of 8oxoG tolerance activity in brain extracts

3.4.1 KOμ mice brain shows a molecular profile compatible with a delayed aging phenotype

These results were obtained in collaborationwith Dr. Antonio Bernad Laboratory (CNIC, Madrid, Spain). This group had shown that Polμ$^{-/-}$ mouse presents impaired DSB repair which in turn causes a significant alteration in hematopoietic homeostasis (Lucas et al. 2009a), more recently, they have shown that Polμ deficiency increases resistance to oxidative damage and delays liver aging (Escudero et al. 2014). Although Polμ is expressed in the central nervous system (Dominguez et al. 2000), its specific function in it remains to be determined. Considering this, we analyzed the gap-

filling activity, as an indication of the repair potential, of brain extracts from wt versus KOμ, in old mice (21-23 months). Figure 38 shows that the control gap-filling activity (a gapped DNA with no lesion; scheme in the upper part) rendered very similar results with both extracts, as indicated by the formation of new band (16mer) when using ddCTP and several variations of divalent activator metal.

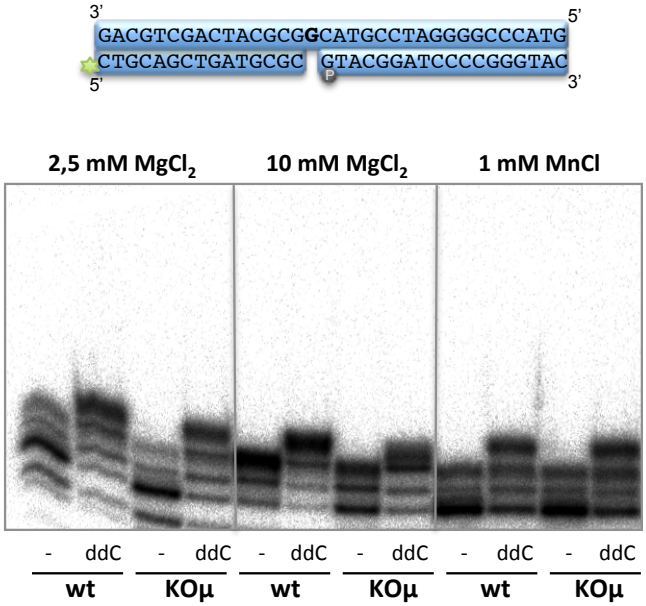

Figure 38. Evaluation of gap filling activity in brain (wild-type vs. Pol$\mu^{-/-}$) extracts using the indicated labeled-template primer (upper part). After incubation (30′–1 h, 30°C) with the clarified extracts (10 μg), with the addition of the indicated concentration of ddCTP, products were recovered and resolved in 20% PAGE / 8M urea. As an additional variable, we tested different combinations of divalent activation cation. The different products are indicated. The original labeled primer appears partially intact (15mer) or degraded by endogenous nucleases, meanwhile extended primers appear at position (16mer).

This evaluation of wild-type versus Polμ brain extracts from old (21–23 months) mice demonstrated a similar overall gap-filling activity in both samples (Fig. 36), in agreement with a greater contribution of other repair polymerases from family X, such as Polβ and Polλ, but – strikingly – Pol$\mu^{-/-}$ extracts presented a significant reduction in mutagenic 8oxoG bypass activity (Fig. 37). When the 1nt-gapped DNA substrate contained an 8oxoG residue as template, the two extracts produced a similar level of the immediate insertion step of the short-patch reactions (16mer; indicated by a white asterisk in Fig. 39A), using either dA or dC; however, a significant difference was demonstrated for the generation of the full-length (34mer) "repaired/ligated" product (also indicated by a white asterisk in Figure 39A). That full-length bypass product (in which 8oxoG was tolerated as template) was especially prominent when dATP (error-prone reaction) was provided in comparison with dCTP (error-free reaction), and was mostly Polμ-dependent (Fig. 39 and 40).

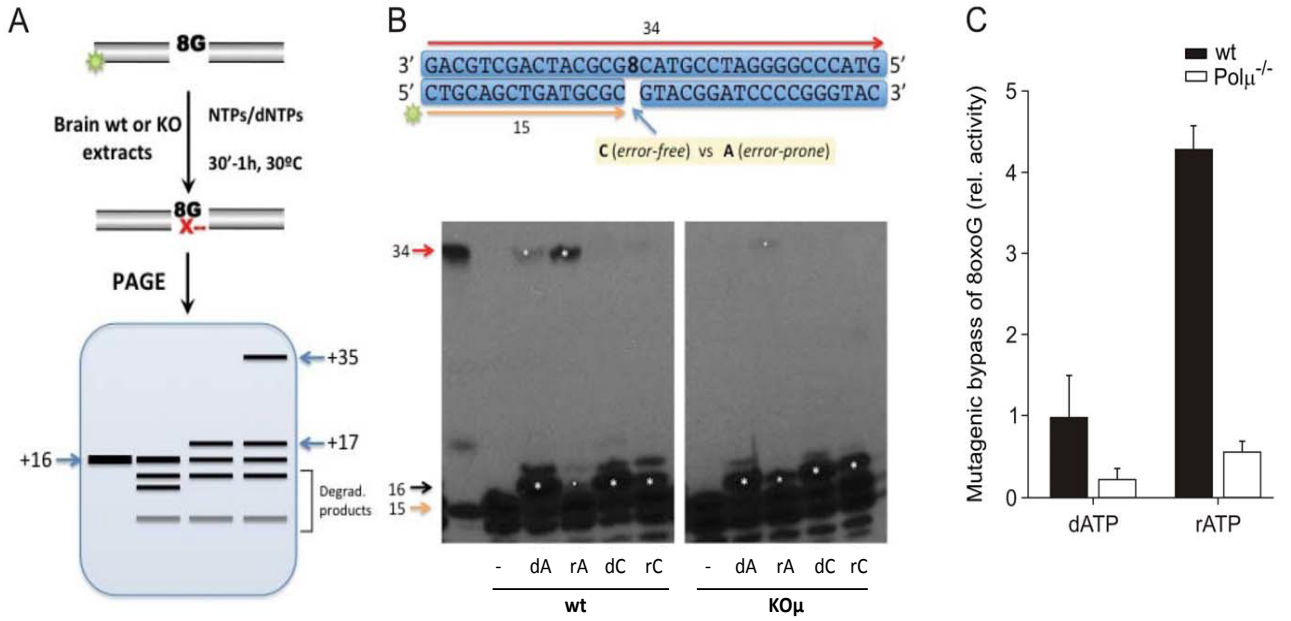

Figure 39. Evaluation of 8oxoG bypass repair activity (tolerance) in brain (wt vs. Pol$\mu^{-/-}$) extracts, using the indicated labeled-template primer. The scheme **(A)** illustrates the mobility of the different expected products: the original labeled primer (+15) could appear intact or degraded by endogenous nucleases (degraded products); extended primers appear at positions (+16 or +17) if no ligation with the 5′-flank of the gap has occurred (short-patch repair), and at full-length repaired (or mutated) product (+34) if ligation did occur. **B)** After incubation with the clarified extracts (10μg), with the addition of the indicated nucleotides (50μM) and 1 mM $MnCl_2$, products were resolved in 20% PAGE. **C)** Densitometric analysis of full-length repaired (+34) product was carried out, for the reaction using dATP or rATP, and represented relative to the activity yield by wild-type brain extracts using dATP.

By providing either dGTP or dTTP (Fig. 40B), Polμ-dependent mutagenic bypass of 8oxoG (in which 8oxoG was tolerated as template) was also observed, but at a lower level than that obtained with dATP, mimicking the substrate preference observed with purified human Polμ (Fig. 38D). Polμ has an unusually low discrimination between dNTPs and rNTPs, leading to the proposal that the use of ribonucleotide substrates could be advantageous for DNA repair, especially in non-dividing cells where the dNTPs pool could be greatly reduced (Ruiz et al. 2003; McElhinny et al. 2003). Interestingly, when 8oxoG tolerance was evaluated in wild-type versus Polμ–/– brain extracts using ribonucleotides (rATP versus rCTP), the 34-mer full-length bypass product was preferentially obtained with rATP (mutagenic), and the reaction was about 4-fold more efficient than that with dATP (Fig. 40B,C). As shown with deoxynucleotides, the mutagenic (rATP) bypass product was considerably reduced in Polμ–/– brain samples (about 7-fold lower). By providing either rGTP or UTP, Polμ-dependent mutagenic bypass of 8oxoG was also observed (Fig. 40C), but at a lower level than that obtained with rATP, again mimicking the substrate preference observed with purified human Polμ (Fig. 40E).

These combined data imply that brains from old wild-type animals have a significant mutagenic bypass activity in templates harboring 8oxoG lesions, as the most representative oxidative damage, and that this mutagenic potential is significantly reduced in the absence of Polμ. This revealed global reduction in mutagenic bypass of modeled 8oxoG lesions and can be considered a relevant difference that could have a direct or indirect impact in brain physiology.

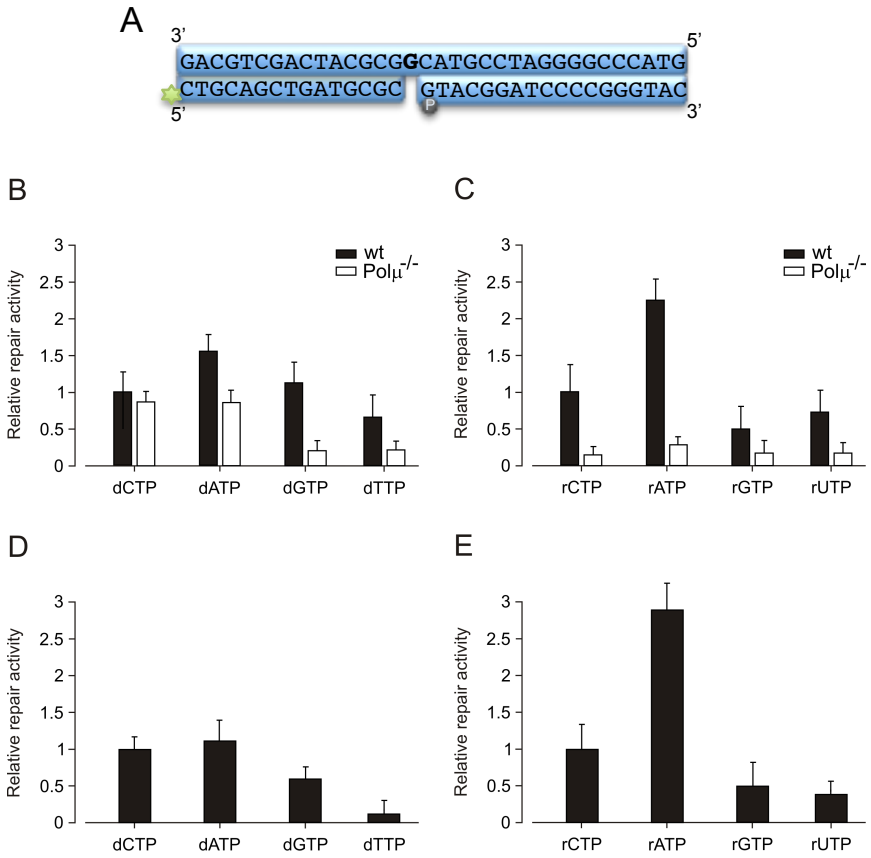

Figure 40. Comparative evaluation of DNA repair activity in brain extracts. (B, C). Evaluation of the "repair" activity on the above indicated **(A)** template primer in brain (wild-type vs. Pol$\mu^{-/-}$) extracts, using dNTPs **(B)** or rNTPs **(C)**. The graphics show a quantification of the generation of the full-length (+34) "repaired" product (also indicated by an asterisk in Fig. 37). The figure also shows the preference of immediate insertion (+16) in the template primer used **(A)** of purified hPolμ enzyme (25 nM), using dNTPs **(D)** or rNTPs **(E)**, and identical reaction conditions to **(B, C)**. That profile found is quite similar with the revealed in the wild-type brain extracts **(B, C)**.

4

Effect of DNA Polymerase λ knockout on CAG somatic expansion in a Huntington´s disease model

In order to widely approach and understand the role of Polλ and Pol*μ* in DNA repair, we have studied single and double deficient models of Polλ and Pol*μ* in collaboration with other groups. One of these collaborations, included in this PhD work, is the study of Polλ and its possible role in Huntington's disease.

Huntington's disease (HD) is an autosomal dominant progressive and fatal inherited neurodegenerative disorder caused by a polyglutamine repeat expansion (CAG) in the coding region of the Huntingtin (HTT) gene. Huntington's disease (HD) is the most common of a group of inherited devastating neurological disorders, including myotonic dystrophy (DM1) and several spinocerebellar ataxias (SCAs)(Lopez Castel et al. 2010), caused by CAG triplet-repeat expansions encoding expanded polyglutamine (polyQ) sequences which in turn confer toxicity to their mutated protein products.

The length of the polyglutamine tract in the N-terminal region of the huntingtin protein determines the age of onset of HD as well as the disease severity. Normal individuals present the range of 6-35 repeats in the HTT gene, whereas affected individuals have between 36-250 CAG repeats. HD is characterized by many symptoms: cognitive and memory impairment, dementia, changed personality and behavior, weight loss, and prominent choreic motor abnormalities(Jonson et al. 2013; Ortega et al. 2007).

Previous studies reported intergenerational instability, since CAG repeats tend to be unstable on paternal transmission (Kovtun et al. 2000). Furthermore, somatic instability is also apparent and appears most pronounced in the Central Nervous System. Hence, somatic repeat instability was postulated to contribute to polyQ toxicity. Patterns of CAG repeat distributions are remarkably reproducible between individuals, implying that the mutation behaves in a predetermined manner (Gonitel et al. 2008; Mangiarini et al. 1997). In addition, since neurons are postmitotic, somatic expansion is believed to occur during DNA repair, triggered by oxidative damage.

Many studies support the idea of the contribution of DNA repair and replication processes to the instability of the size of CAG repeats.

Several DNA repair mechanisms have been proposed to be involved in trinucleotide repeat (TNR) somatic expansion such as Mismatch Repair (MMR) and Base Excision Repair (BER)(Mason et al. 2014). However, the precise mechanism of somatic expansion has not been yet elucidated. Many proteins that participate in MMR have been involved in HD, demonstrating that contractions and expansions are suppressed in the absence of MMR. This suggests a possible role of MMR to promote CAG/CTG repeat expansion {, }

DNA Polß has been also involved in TNR, as it can generate the expansions through a slippage mechanism (Petruska et al. 1998). Besides, it has been described that these kind of expansions occur at regions able to form non canonical DNA structures (hairpins, slipped-DNAs, triplexes, R-loops) that are usually repaired during replication or recombination (Bacolla and Wells 2004; McMurray 1999; Wells et al. 2005). These unsolved structures are considered one of the main reasons for the expansions to occur.

Moreover, oxidative damage has been related to aging (Cardozo-Pelaez et al. 1999), and also to repeat expansions in the brain (Kovtun et al. 2007). The BER enzyme OGG1, a glycosidase involved in the removal of one of the most common DNA oxidative damages, 8oxoG, was recently linked to somatic CAG/CTG repeat expansion, creating ssDNA breaks. Polß participates in BER through its dRP lyase activity; however, it is known that oxidative damage can produce oxidized dRP residue that Polß was not able to properly removed (Matsumoto et al. 1994).This oxidized dRP residues can

be eliminated by FEN1 during in long-patch BER. The lack of coordination between Polß and FEN1 provokes triplet expansion (Liu et al. 2009).

Polλ has been implicated in gap filling during BER and during repair of DSB in DNA by NHEJ. It shows dRP lyase activity and a high frame shift infidelity. In addition, Polλ has been identified to play an important role in repair of oxidative damage, especially in the correction of the pair 8oxoG:A to 8oxoGC (van Loon and Hubscher 2009). As mentioned before, MEFs deficient in Polλ entry prematurely in senescence when cultured in oxidative stress conditions, 20% O_2 (Bertocci et al. 2003).

Given the susceptibility to oxidation of CAG repeats and the implication of Polλ in BER, we reasoned that, in the context of HD, this DNA polymerase might be implicated in the promotion of CAG repeat expansion in somatic cells. Thus, we decided to take advantage of mouse genetics to explore this.

4.1 Murine model generation

Following up the work done in our laboratory and presented in Gloria Terrados PhD Thesis (2010), we establish a collaboration with Professor JJ Lucas (CBMSO, Madrid), whose lab has a wide expertise in HD disease and neurodegenerative disorders.

To decipher at which extent Polλ might contribute to CAG repeat expansion *in vivo*, we first generated Polλ knockout mice by gene targeting, which were viable and fertile, as it was described in Chapter 3. Then, we combined the R6/1 N-mutant Htt (N-mutHtt) mice with the Pol λ knockout mice.

R6/1 is one of the 6 transgenic mouse lines generated to be used use as a chronic disease model, each one representing a different range in the severity of the disease. R6/1 contains ≈ 1 kb of human HD promoter region followed by exon 1 of the Htt gene with 115 CAG repeats (Mangiarini et al. 1996).

In order to obtain the murine model to study, we designed the breeding protocol as shown in Fig. 41A. Firstly, R6/1 males were crossed with KO λ females. After genotyping the F1, R6/1 λ+/- males from this F1 generation were selected to cross with λ+/- female. This way, in a F2 generation we obtained all the possible genotypes: mice with no Htt (wt) that can be homozygous ($\lambda^{+/+}$), heterozygous ($\lambda^{+/-}$) or knockout ($\lambda^{-/-}$) for Polλ; and R6/1 transgenic mice with Htt that can be homozygous ($\lambda^{+/+}$), heterozygous ($\lambda^{+/-}$) or knockout ($\lambda^{-/-}$) for Polλ. Overall, the 6 genotypes maintained a Mendelian segregation (Fig. 27C). These mice were bred up to 5-8 months for a further study, as described below.

A

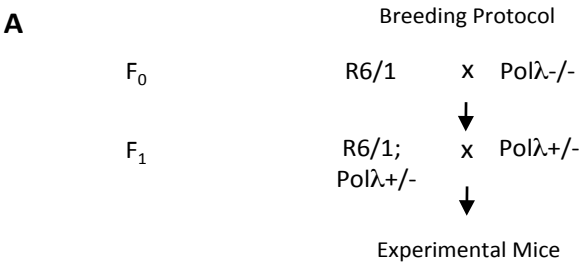

B

F_2	Wt	Polλ+/-	Polλ-/-	R6/1	R6/1; Polλ+/-	R6/1; Polλ-/-
number	12	46	21	21	48	23

C

	Frequencies					
observed	7.02%	26.90%	12.28%	12.28%	28.07%	13.45%
expected	12.50%	25.00%	12.50%	12.50%	25.00%	12.50%

Figure 41. R6/1 mice in DNA Polλ background. A) Schematic representation of the breeding protocol to obtain R6/1 mice with decreased Polλ dosage. **B)** Number of experimental mice obtained for the whole study. C) Frequencies of the observed and the expected number of animals per each genotype is shown. A normal Mendelian segregation among the six possible genotypes was confirmed by χ^2 analysis (*P*=0.692).

4.2 Lower CAG repeat somatic expansion and even contraction in R6/1 mice lacking Polλ

After 40 weeks, mice were sacrificed to obtain DNA from different tissues. The tissues obtained from the Central Nervous System were: striatum, cortex, olfactory bulb and cerebellum. Besides, peripheral tissues were also extracted: liver, heart, kidney, spleen and tail. DNA was extracted from each sample and analyzed for somatic expansions by sequencing the CAG repeats with DNA Analyzer 3730.

HD displays significant non-random somatic mosaicism, both in humans and mice. Moreover, age correlates with somatic instability. Interestingly, two brain structures are especially sensitive to display the largest range of CAG repeats, striatum and cortex, whereas cerebellum harbors smaller CAG repeats (Ishiguro et al. 2001). This highly tissue-specific mosaicism is also present in peripheral organs, with liver and kidney as the organs that present the largest CAG repeats, and therefore, higher mosaicism.

In the R6/1 mice, it was described a multimodal distribution of the CAG repeats. Repeat instability was assayed by high-resolution capillary gel electrophoresis where repeat length distribution present a typical 'hedgehog' pattern (Mangiarini et al. 1997) (Fig. 42A).

Tail has been previously described to be relatively stable towards expansions (Mangiarini et al. 1997). Accordingly, in the case of the tail from 3 week-old mice (Fig. 42A), there is only one peak (named as 'conservative component') of the same size in both mice, R6/1 with Polλ expressed (in blue) and R6/1 KOλ, where Polλ's expression was deleted (in red). Tail shows a constant pattern in both genotypes (125 CAG repeats).

Nevertheless, we can observe an apparent mosaicism in the other tissues shown, analyzed at 8 months. Liver, described before as a peripheral tissue with pronounced instability, exhibits two peaks in R6/1 mice, the conservative component, of the same size as tail, and a 'radical component' at 170 CAG repeats (second peak on the right). However, R6/1; Polλ-/-mice do not show this radical

component. Even more, R6/1 Polλ$^{-/-}$ mice display a left radical component (below 150 CAG repeats) that is absent in R6/1 mice.

Regarding brain tissues, somatic instability is also evident. R6/1 Polλ$^{-/-}$ striatum only presents the conservative component, but at lower intensity. In the case of cortex, radical component is decreased in R6/1 Polλ$^{-/-}$mice, but it is possible to observe a left radical component in one of the knockout mice analyzed (red dashed line), as seen in liver. Both olfactory bulb and liver present a displaced conservative component in R6/1 mice, while R6/1 Polλ$^{-/-}$ mice exhibit tail pattern.

We analyzed the mean CAG expansion area obtained in the peak size distribution (Fig. 42B). We observed that the area remains diminished in R6/1 Polλ$^{-/-}$ compared to R6/1 mice, and it is remarkably lower in the analysis of striatum, one of the major tissues affected by mosaicism and expansion. These findings allowed us to consider a possible involvement of Polλ in the somatic expansions that produce HD.

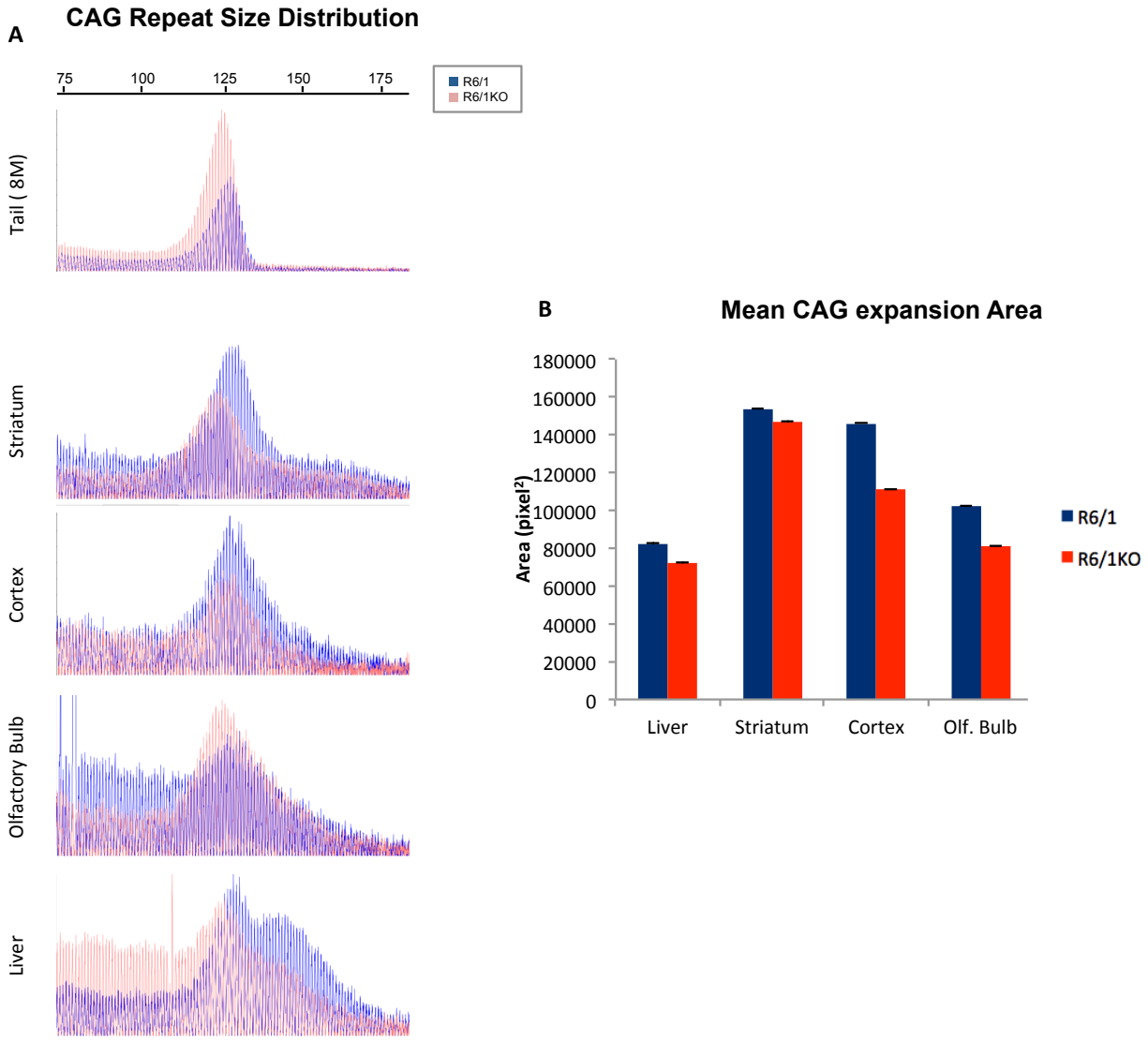

Figure 42. Analysis of somatic instability in the F2 progeny. Representative GeneMapper profiles of *HTT* CAG repeat size distributions in the tail, striatum, cortex, olfactory bulb and liver. Panels in **A** and **B** show representing tissues from R6/1 (blue) and R6/1: Polλ$^{-/-}$ (red) mice. Panel A shows 3-weeks tail traces, where there is one peak representing a conservative component of the same size in both genotypes (150 CAG repeats). Tissue analysis of the same mice at 8 months of age reveals an apparent mosaicism. *X* axis, CAG repeat length as indicated; *Y* axis, allele abundance. B) Quantification of CAG instability index reveals a statistically significant decrease in somatic *HTT* CAG instability in the striatum and liver of R6/1 Polλ$^{-/-}$; Bar graphs represent mean ±SD;.

4.3 Decreased size of huntingtin inclusions in R6/1 mice lacking Polλ

It has been described that deletion of genes involved in MMR was enough to delay the accumulation or accessibility of mutant huntingtin in the nuclei of striatal neurons (Dragileva et al. 2009; Kovalenko et al. 2012). This characteristic also works as a sensitive marker of the ongoing pathogenic process in HD mice.

To determine whether the lack of Polλ also modified this phenotype, we quantified nuclear huntingtin in striatum and prefrontal cortex in 8-month-old R6/1; Polλ$^{-/-}$ animals (Fig. 43). In striatum (Fig. 43A), the number of nuclear huntingtin aggregates, with a diameter higher than 4 μm, showed no differences among genotypes (center). However, the inclusion area measurement was significantly reduced in R6/1; Polλ$^{-/-}$ in both tissues (right). However, the number of aggregates and the inclusion area measurement did not show any differences in the case of prefrontal cortex (Fig. 43B). The absence of Polλ resulted in a fall in CAG expansion in striatum, and besides, it also had an impact in the area of huntingtin aggregates in this tissue. Considering this, we demonstrated a connection between the size of expansions, huntingtin aggregates and lack of Polλ.

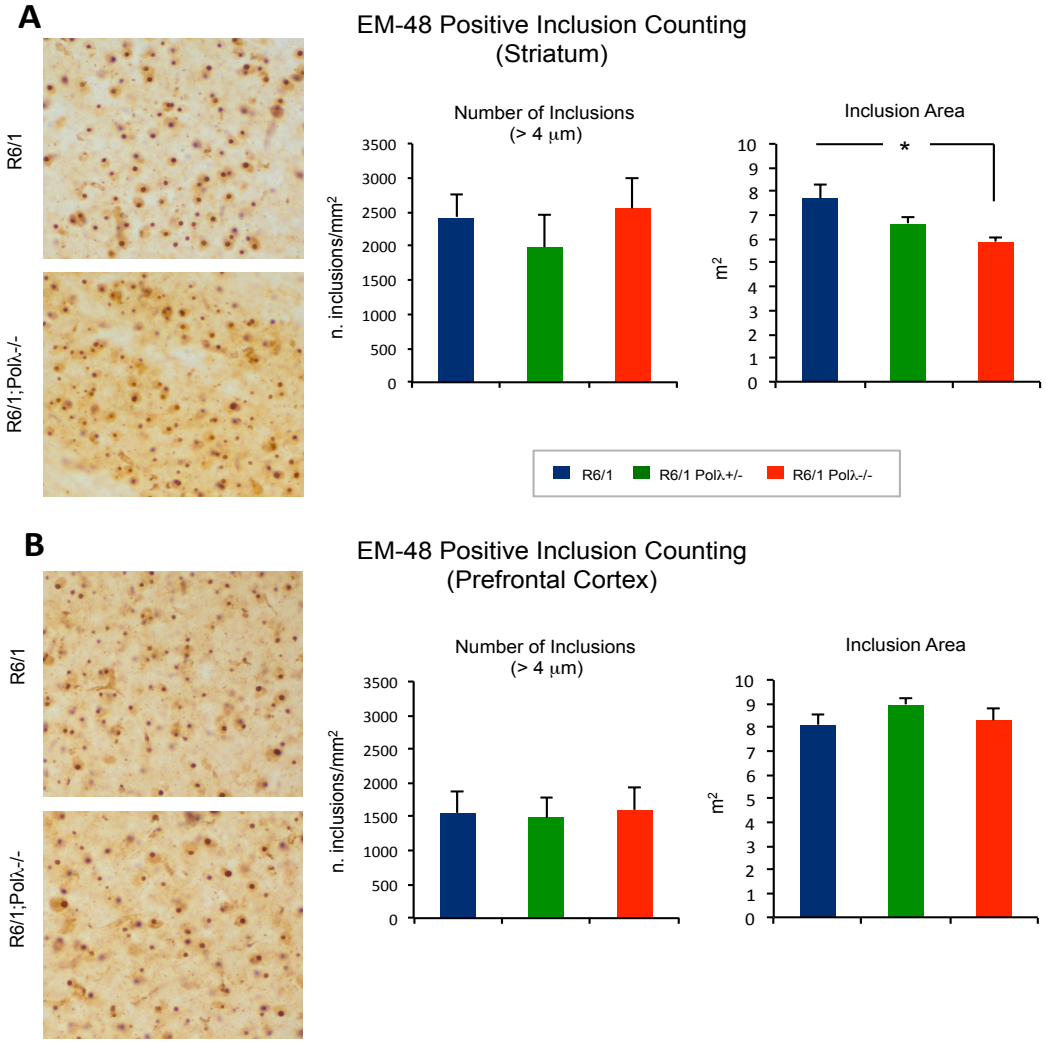

Figure 43. Huntingtin (N-mutHtt) immunodetection in brain sections from 8-month-old R6/1 mice with different Polλ dosage. A and **B,** *N-mutHtt immunohistochemistry on brain sections from 8-month-old R6/1 mice with different Polλ dosage.* **A)** Left: representative images of the striatum. Center: Counting of aggregates, with diameter higher than 4 μm, show no differences among genotypes. Right: Inclusion area measurement show a significant decrease area in R6/1; Polλ$^{-/-}$ mice. **B**) Left: representative images of the Prefrontal cortex. Counting of aggregates (center) and Inclusion area measurement (right) At least four animals per genotype were analyzed. Data are presented as the mean+SEM. ∗P , 0.05.

4.4 Attenuated somatic expansion in R6/1; Polλ -/- mice does not affect HD phenotypes like body weight loss or motor impairment

HD phenotypes are well described by body weight loss or motor impairment. In order to test whether the lack of Polλ combined with R6/1 mice had major impact in these parameters, mice body weight was monitored at 4 and 6 months of age (Fig. 44). We observed that R6/1 mice were not able to progressively gain weight as seen in wt mice after 6 months. However, there was no difference in weight gain or loss among R6/1 genotypes.

There are many different tests available to measure motor impairment in HD disease. One of the most common and widely used is Rotarod, which basically consists of an apparatus set to accelerate from 4 to 40 rpm along a 5-min period and mice were tested in four trials with 1 h inter-trial periods. Again, mice were examined at the age of 4 and 6 months. As expected, N-mutHtt-expressing (R6/1) mice showed a deficit in this motor coordination task (**B**, **D**).

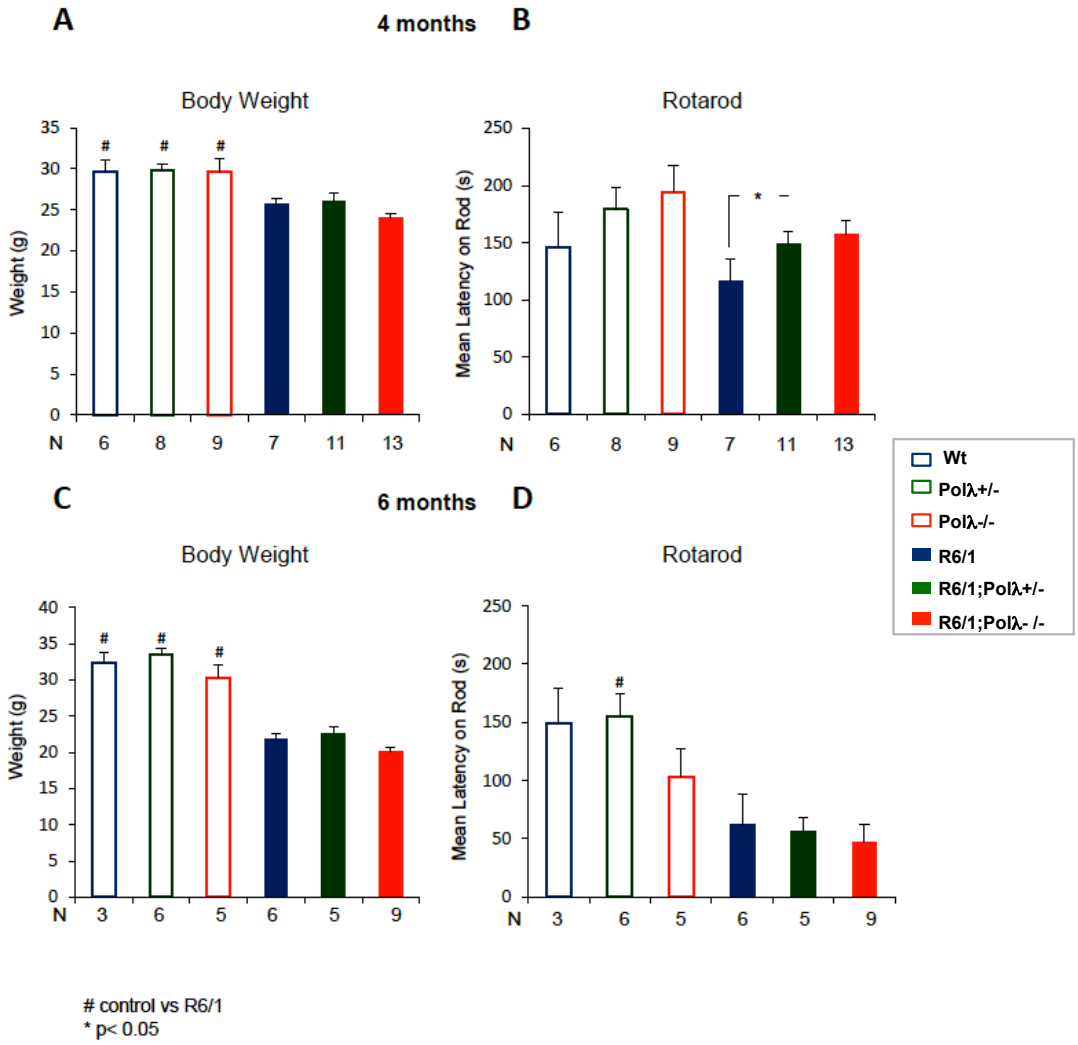

Figure 44. Global indicators of the potential effect of polλ gene dosage on polyQ-induced disease *in vivo*. Body weight was monitored at 4 and 6 months of age (**A** and **C**). Motor phenotype of R6/1 mice was assessed by means of Rotarod (**B** and **D**), a common test widely used to examine HD mouse model. Mice were examined at the age of 4 and 6 months. Data are presented as the mean+SEM. $^{\#}$ P<0.05, control vs. R6/1mice; * P<0.05, among N-mutHtt-expressing mice

Interestingly, at 4 months R6/1; Polλ+/+ mice showed worse motor impairment than R6/1; Polλ-/-. This difference disappeared when comparing Rotarod results at 6 months. Giving that R6/1; Polλ-/- mice showed delayed motor impairment and minor area inclusion in huntingtin aggregates compared to R6/1; Polλ+/+, we decided to study whether these changes had any effect on the lifespan of these mice.

4.5 Average survival

Despite the R6/1; Polλ$^{-/-}$ mice did not show a significant motor impairment or body weight, we also consider the impact of this genotype lacking Polλ on lifespan. As shown in Fig. 45A, the Kaplan-Meier cumulative survival didn't appear to change significantly among the different genotypes. Indeed, the average survival shown in Fig 31B exhibits very similar average survival in all the genotypes. Thus, the lack of Polλ doesn't seem to affect R6/1 lifespan.

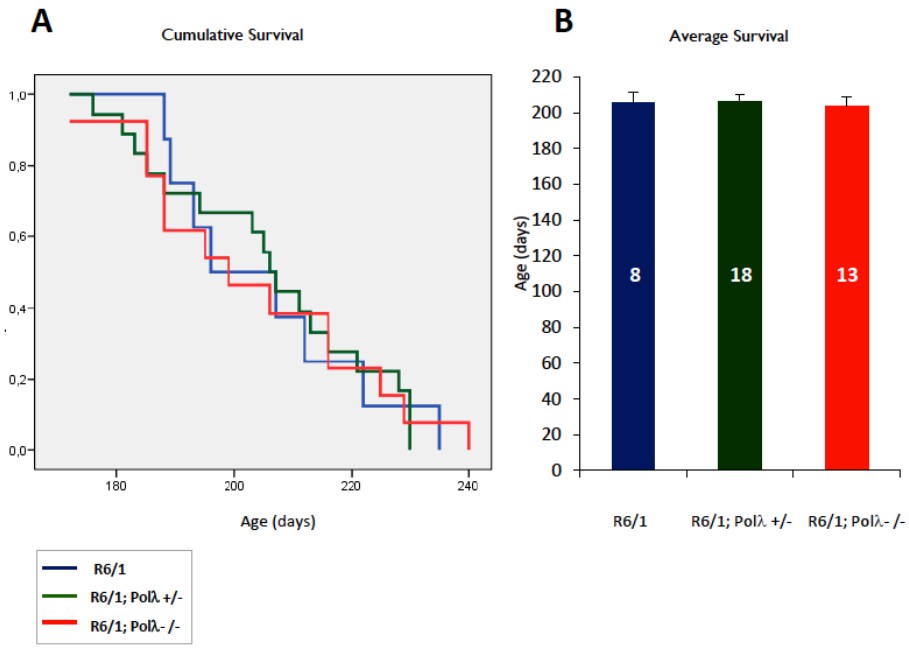

Figure 45. Lifespan is not affected in R6/1;Polλ-/- mice. A) Cumulative survival curve (Kaplan-Meier survival plot) of mice. **B)** Average survival. The numbers in each bar reflects the number of mice represented in each sample.

4.6 F3 progeny analysis

CAG repeats tend to expand when transmitted from a male parent to offspring in both mice and humans, and contract when transmitted from a female (Kovtun et al. 2001; Mangiarini et al. 1997). As shown in section 4.2 from this chapter, F2 progeny of R6/1; Polλ$^{-/-}$ mice showed less somatic expansions than the parental R6/1 mice. To decipher Polλ's possible role in germline expansion, we examined whether germline expansion was affected. It was defined as the increase in repeat length between generations in tail samples taken at age of 2-3 weeks.

We analyzed germline expansion from R6/1 male parents up to three generations (F3)(Fig. 46A). In F0 and F1, the peaks were the same as they were littermates. 166 is the number of basal expansions in F0, corresponding to the state of R6/1 mouse at the moment we started the experiment. The repeated tract expands from male parents to offspring in R6/1; Polλ$^{+/+}$ and it

increases in F3 as a result of a germline expansion. However, in R6/1; Polλ$^{-/-}$ mice the repeat tract was more stable, with a tendency towards contraction when transferred to offspring.

In Fig. 46B we represented the mean of the expansions through the three generations and their correspondent genotype. It is very remarkable that R6/1;Polλ$^{-/-}$ in F3 showed less expansion than their progenitor in F0 compared with control mice, in this case R6/1;Polλ$^{+/+}$. These results indicate that Polλ contributes to germline TNR expansion in male R6/1 mice, maintaining the contractions.

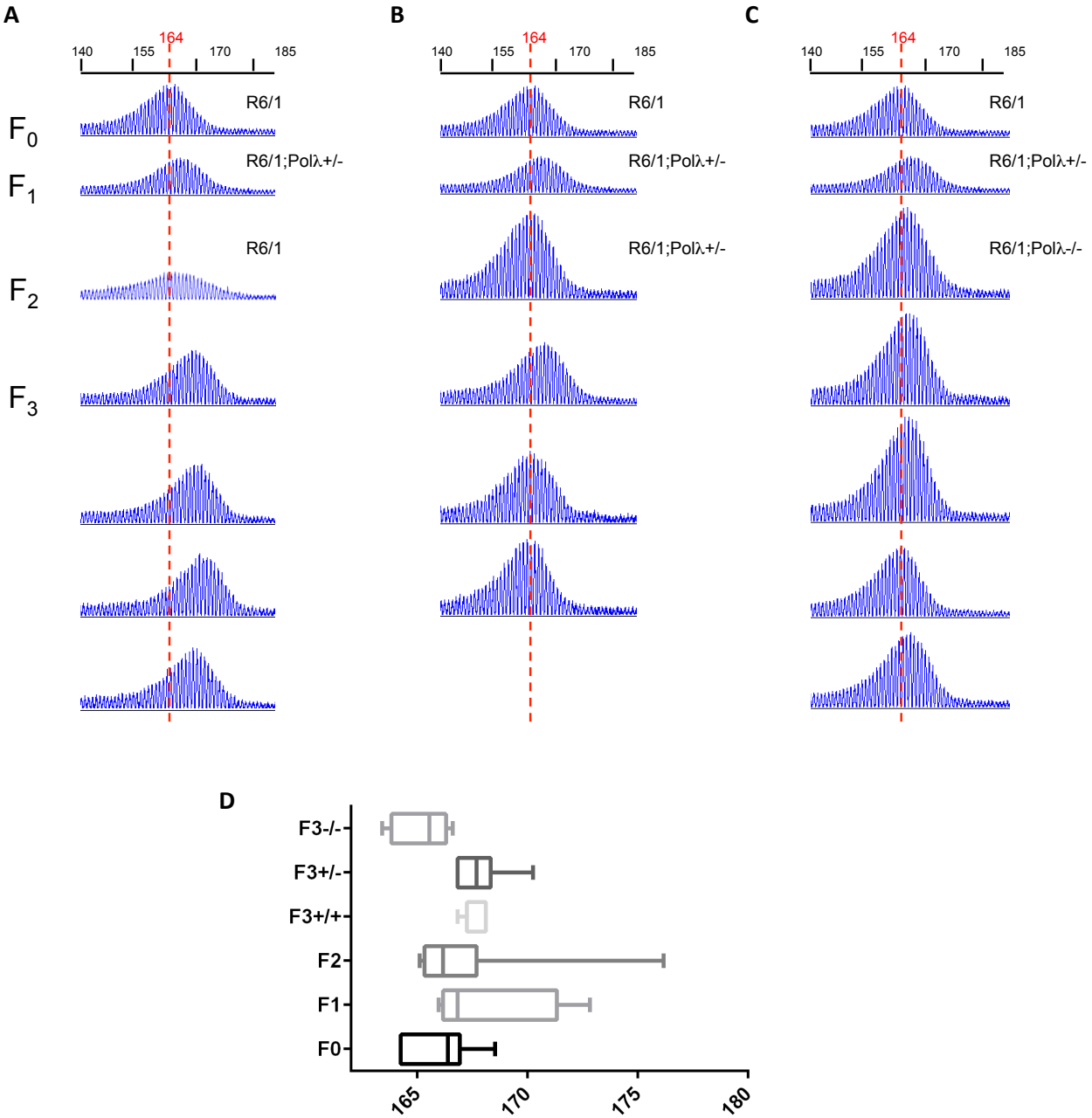

Figure 46. F3 Progeny TNR expansion analysis. (A, B, C) GeneMapper plots showing the distribution of CAG repeat fragment lengths present in each generation. Red dashed line shows the initial number of repeats in F0 (164). **A)** Corresponds to R6/1;Polλ$^{+/+}$ **B)** to R6/1 Polλ$^{+/-}$ and **C**) to R6/1 Polλ$^{-/-}$ D) Mean of expansion repeat in the three generations. *X* axis corresponds to number of repeat, *Y* axis represents the offspring generation.

5

Distribution of labour between Polλ and Polμ during NHEJ in vivo

5.1 Interchanging Nail and Loop1 motifs between Polλ and Pol*μ*: Use of chimeras in the study of NHEJ specificity

Polλ and Pol*μ* have complementary, non-redundant roles in NHEJ due to their different degree of sequence complementarity that they are able to use for gap-filling DNA synthesis in NHEJ (Ramsden and Asagoshi 2012). The capacity of a DNA repair polymerase to operate on a NHEJ intermediate may thus depend on its ability to interact with other NHEJ factors (e.g., via BRCT domains), as well as on complementarity of DNA ends.

Comparing the aminoacid sequences and crystal structures of Polλ and Pol*μ* (Fig. 47), we found two domains that differ among them, which could explain their characteristic substrate specificity in NHEJ reactions. Thus, a segment named 'Loop1' is specifically present in Pol*μ* and TdT, and has an important role during NHEJ and terminal transferase activity in Pol*μ* (Juarez et al. 2006; Nick McElhinny et al. 2005b). On the other hand, Polλ presents a small region named 'nail' in the thumb subdomain that interacts with the template strand. This small domain, absent in Pol*μ*, is related to Polλ's ability to count and copy correctly the bases of the template strand. Moreover, it could be also involved in the capacity of this protein to accept DNA distortions (Garcia-Diaz et al. 2006). Besides, these polymerases have both a BRCT domain, but it is quite different among them (23% sequence identity), suggesting that this domain may also play a polymerase-specific role.

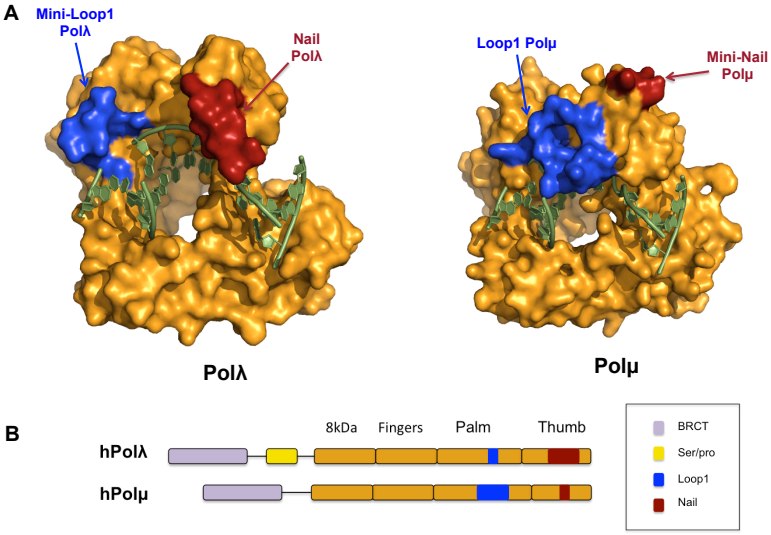

Figure 47. A) Cartoon representation of Polλ (left: PDB id 1XSN) and Pol*μ*'s modeled over Tdt structure (PDB id 1JMS). In both cartoons Loop1 is shown in blue and Nail is shown in red. **B)** Structural organization of Polλ and Pol*μ*. Polß catalytic core, containing the subdomains *8kDa, Finger, Palm* and *Thumb,* is shown in orange. Additional domains are shown: *BRCT* in mauve, and *Ser/Pro* in yellow.

Thus, to further understand the structural and functional differences between human Polλ and Pol*μ* that allow them to be complementary in their role in DSB repair via NHEJ, we have developed various chimeras, single and double.

In the single ones, the Polλ mini Loop1 and large Nail regions have been replaced with Pol*μ*'s correspondent regions: Polλ's Loop1 was replaced by Pol*μ*'s Loop, conforming Polλ(Loop1*μ*) chimera; and Polλ's Nail (27 aminoacids) replaced by Pol*μ*'s (17 aminoacids), conforming Polλ(Nail*μ*) chimera. In addition, to obtain the double chimera, we have replaced both regions in Polλ polymerase, introducing the corresponding Loop1 and Nail regions of Pol*μ*, conforming Polλ (Loop1*μ*+Nail*μ*) (Fig. 48).

These chimeric proteins have been purified and characterized biochemically in our laboratory (Ana Gómez Bedoya, PhD Thesis, 2013). As demonstrated, they are enzymatically active, have polymerization activity and the ability of recognizing the phosphate group in a 5' gapped-substrate, a very specific property of most PolX DNA polymerases. Interestingly, preliminary results showed that these chimeras present a deficient activity in NHEJ reactions carried out in the absence of additional NHEJ factors. In the light of such promising results, we analyzed the behavior of these chimeras during NHEJ both *in vivo* and *in vivo*.

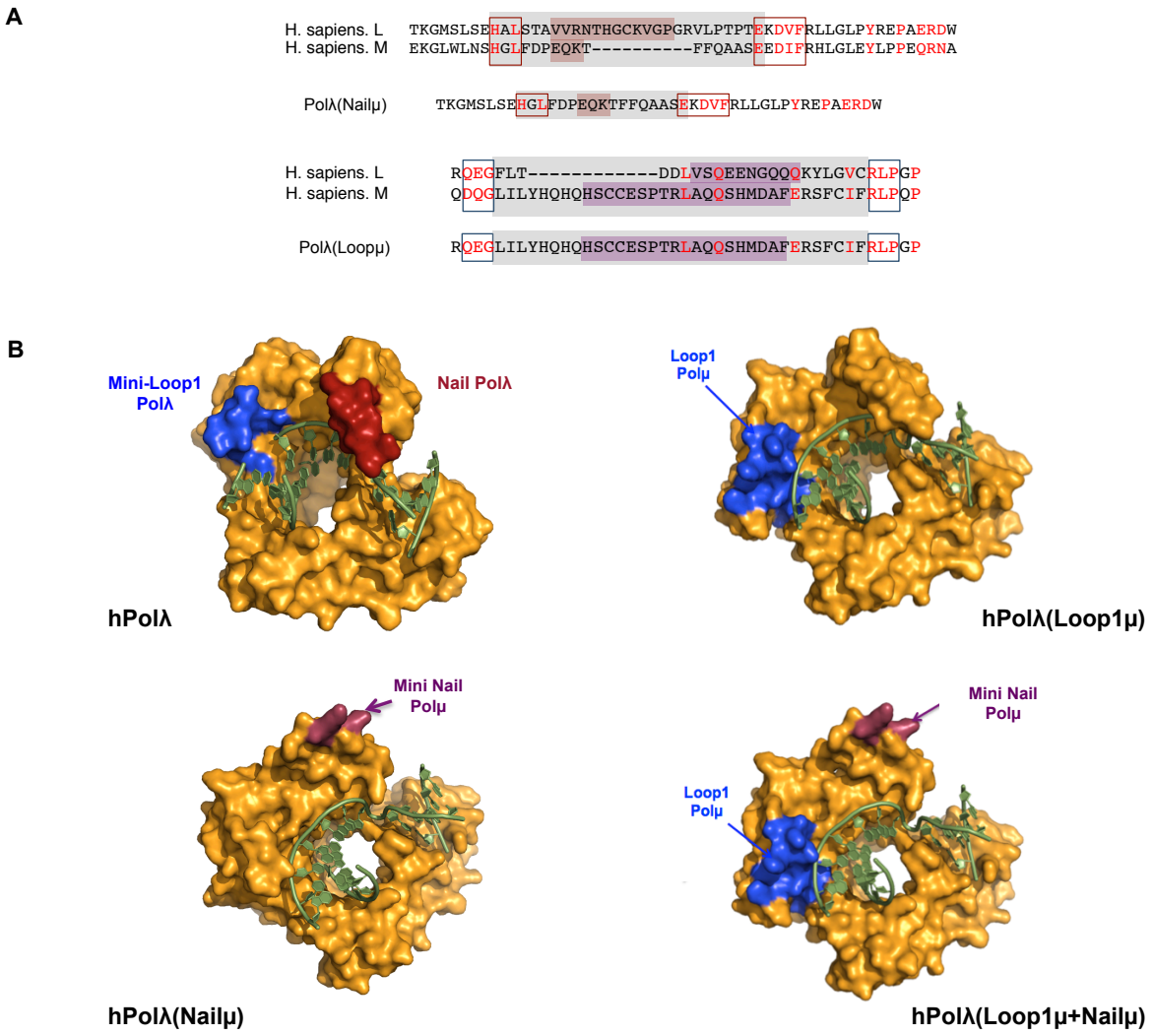

Figure 48. A) Amino acid sequence alignment of human Polλ and Pol*μ*. In the upper alignment, Nail region is marked with a red box whereas the grey box indicates the region switched. The sequence of the chimeric protein obtained is shown. In the bottom alignment, Loop region is marked with a mauve box whereas the grey box indicates the region switched. The sequence of the chimeric protein is shown. **B)** Cartoon representation of Polλ and the three chimeras (modeled over Polλ's structure). In all cartoons Loop1 region is shown in blue and nail region is shown in red.

5.2 *In vivo* analysis of NHEJ using extrachromosomal DNA substrates

The laboratory of Prof. Dale A. Ramsden, at the University of North Carolina (Chapel Hill, NC, USA) has developed an elegant and efficient methodology to measure the activity of specialized DNA polymerases on (systematically varied) NHEJ substrates *in vivo* (see scheme in Fig. 49). Briefly, we introduced both extrachromosomal DNA substrates and the protein to be analyzed into cells by electroporation, incubated the cells at optimal temperature during an hour and then harvested them one hour later. We evaluated how these substrates were joined by NHEJ, the recovered DNA was specifically amplified by PCR, and digested with specific restriction enzymes that recognize their target sequence if the different polymerases perform NHEJ. If the proteins were able to fill correctly the gaps formed after bridging the two DNA ends, the restriction enzymes would recognize their target sequence and digest the DNA fragment. If not, the DNA would remain intact.

In principle, we used three specific substrates that emulate different NHEJ sequence contexts, with different overhang polarity, different degrees of sequence complementarity and gap size. As shown in table 4, previous results obtained in Ramsden's laboratory deciphered the preference of each PolX for its cognate substrate, in agreement with the previous data obtained for each polymerase *in vitro*. These sequences were: 3'(GCGA)-protruding, creating a 2 nt gap if connecting 2 base pairs; 3'(GCG)-protruding creating a 1 nt gap if connecting two base pairs; and 3('G)-protruding, with no complementary sequence.

Substrate	Polarity	Gapsize	Aligned?	Polμ	Polλ	Other Pols?
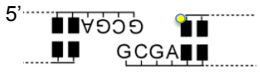	3'	2	Yes	-	+++	-
	3'	1	Yes	++	+++	-
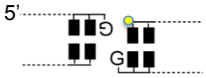	3'	1	No	+++	-	-

Table 4. Preference of each polymerase for each cognate substrate. Scheme of the substrates used to analyze Polλ and Pol*μ* polymerization activity *in vivo*. Polarity indicates overhang orientation. Gap size indicates the number of nt to be polymerized after substrates aligned and joined. Pol*μ* and Polλ columns indicate the preference of each polymerase for each substrate.

Taking this into consideration, we decided to evaluate the activity of the chimeras *in vivo* on these 3 substrates in the absence of both endogenous polymerases using our double-KO MEFs context. Bothe when using the control MEF line (wild-type), and the MEF line deficient in both DNA polymerases (DK), the transfections were efficient and did not compromise cell integrity.

In a first experiment, we could evaluate the NHEJ accuracy of these mutants *versus* the wild-type DNA polymerases. When the digested DNA was run in an acrylamide gel, it produced two bands: the bottom one corresponds to the accurate filling of the gap by the polymerases and cut by the restriction enzyme, and the upper one corresponds to the ligated fragment or non-accurate gap-filled fragment.

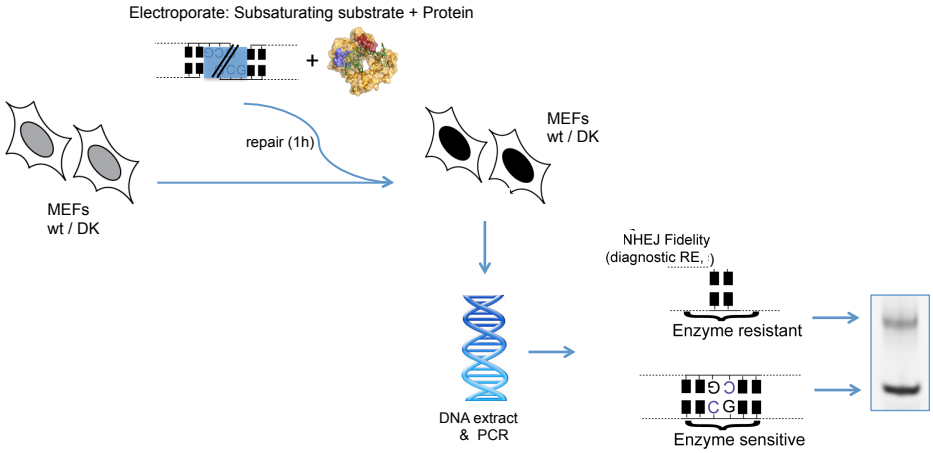

Figure 49. In vivo analysis of extrachromosomal NHEJ substrates. Scheme of the methodology used to analyze different NHEJ in a cellular context. Substrates and protein of interest (chimeras in this case), are electroporated into wt/DK immortalized MEFs. Cells were recovered one hour after electroporation, and whole DNA recovered with low throughput automation (Qiacube). Recovered DNA was specifically amplified and subsequently digested with specific restriction enzymes that recognize the sequence reconstituted after a faithful gap-filling-mediated end joining. If thepolymerases were able to fill the gaps correctly, restriction enzyme is able to cut this sequence. If not, DNA would remain intact.

5.3 DNA polymerization activity of chimeras on different NHEJ substrates

5.3.1 3'GCGA-overhangs (partially complementary substrate)

In the case of this substrate, if the NHEJ machinery is able to bring together two molecules, the partial complementarity of these 3´overhanging ends would lead to the formation of two 2-nt gaps, which are the preferred substrates for PolX activity. Indeed, as described in a submitted work (Pryor et al. 2014), these situation is very specific for Polλ. This substrate allowed us to evaluate the activity of the chimeras and see if the interchanged regions affected the protein's properties *in vivo* as it was described *in vitro*.

As shown Fig. 50B, measurement of the ratio between non-accurate (upper band) and accurate gap filling synthesis (lower band) showed a clear defect in the activity of these chimeras compared to Polλ wt protein, especially in the case of the double chimera, Polλ (Loop1μ+Nailμ).

As a positive control of the correct NHEJ reaction we used wild type MEFs electroporated only with DNA substrates (no protein) (Figure 50, second line on the left). In such conditions, a highly accurate end joining was observed. In contrast, DK MEFs (lacking both Polλ and Polμ), with no protein transfected by electroporation (third lane on the left) were not able to perform an accurate end joining reaction. The different chimeras were analyzed in the context of DK MEFs in order to obtain a neat result from the transfected protein activity itself.

Notably, Polλ wt (fourth lane on the left) showed a very similar activity compared to wt MEFs. That indicates that, in a DK MEFs background, the ability to join and accurately fill the gap of this NHEJ specific substrate is cognate to Polλ. Interestingly, both Polλ(Loop1μ) and Polλ(Loop1μ+Nailμ) lost the ability to efficiently repair this substrate even in saturating conditions (Fig. 50C). In addition, Polλ(Nailμ) was less active too, but this difference was reduced when using saturating amounts of enzyme (10 ng). In conclusion, by using a very specific substrate for Polλ as 3'GCGA, we observed that all the chimeras were less active than wild-type Polλ.

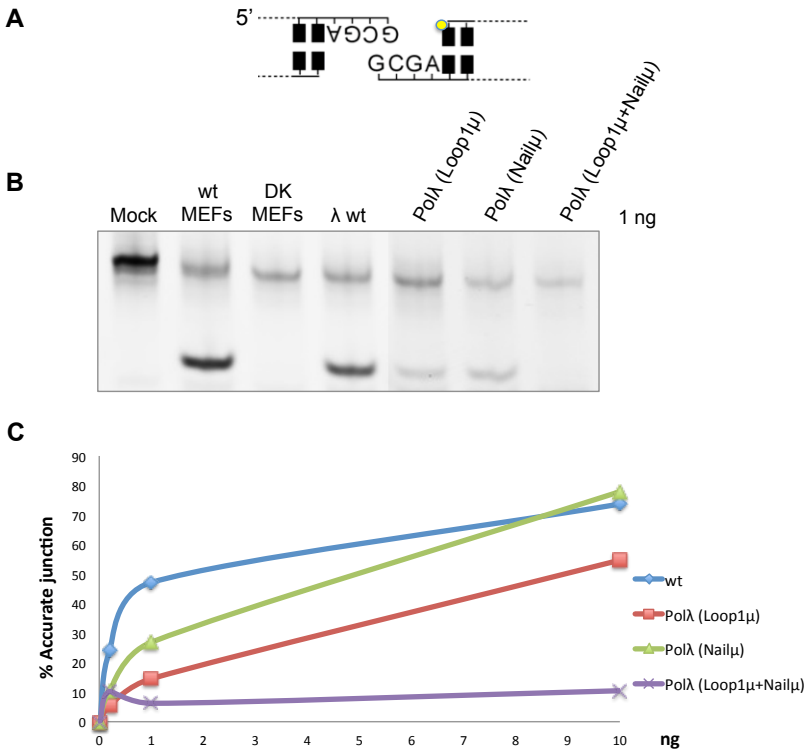

Figure 50. 3'GCGA-overhangs (partially complementary substrate). A) Schematic representation of the substrate analyzed. Yellow dot indicates the presence of a downstream 5' phosphate. **B)** Polλ chimeras show deficient activity in a Polλ specific sequence context. From left to right: Mock as a negative control, represents the pool of 3 independent electroporation experiments with wt MEFs, but lacking the restriction enzyme digestion step of the PCR fragment obtained; wt MEFs with no protein transfected; DK MEFs with no protein transfected. Polλ wt, Polλ(Nail*μ*), Polλ(Loop1*μ*) and Polλ(Loop1*μ*+Nail*μ*) were electroporated (1 ng in each case). **C)** Titration of the NHEJ accuracy in this substrate. Graph represents quantification of the assays shown in B), with different amounts of protein transfected.

5.3.2 3'GCG-overhangs (partially complementary substrate)

When we used the 3´GCG-overhangs substrate (Fig. 51), NHEJ of two molecules can be stabilized by a 2-nt base pairing between overhanging ends. In such situation, two 1-nt gaps are generated, which can be specifically filled by a NHEJ DNA polymerase. When we used these substrates, Polλ showed a higher efficiency than Pol*μ* (data not shown). Interestingly, the behavior of the chimeras was similar to the experiment with the 3'GCAC-overhang substrate. Polλ(Loop1*μ*) and Polλ(Loop1*μ*+Nail*μ*) were unable to fill the 1-nucleotide gap as accurately as Polλ wt protein. On the other hand, Polλ(Nail*μ*) reatined a significant activity even at non-saturating conditions.

We can conclude that the Nail region of Polλ is partially dispensable for filling-in the 1 nucleotide gap in this context. Conversely, the small Loop1 of Polλ cannot be interchanged by that of Pol*μ*, either alone or in combination with Pol*μ*´s Nail.

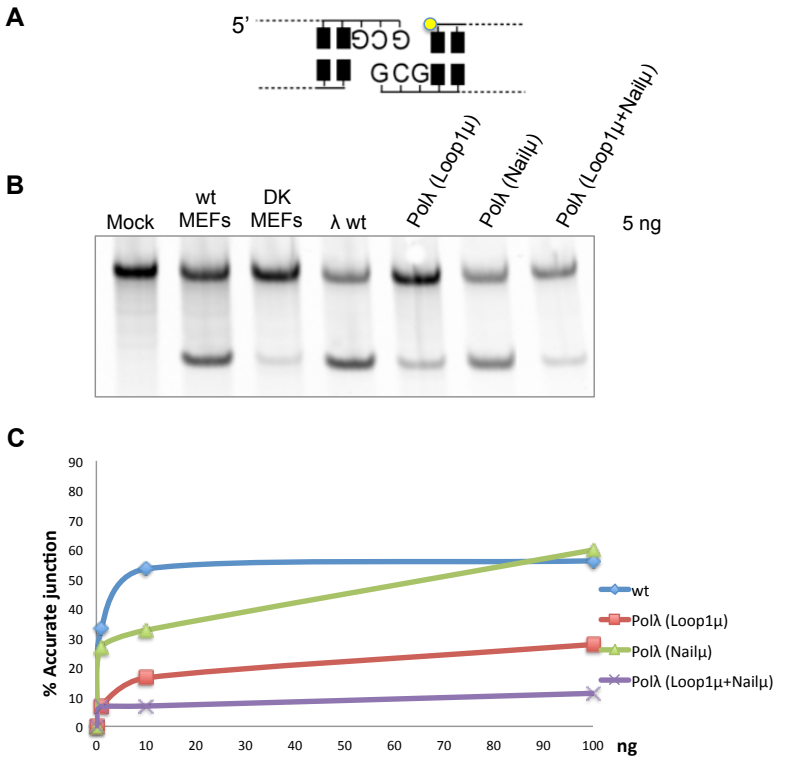

Figure 51. 3'GCG-overhangs (partially complementary substrate). A) Schematic representation of the substrate analyzed. Yellow dot indicates the presence of a downstream 5' phosphate. **B)** Polλ chimeras activity. From left to right: Mock as a negative control, represents the pool of 3 independent electroporation in wt MEFs, but with no final digest of the PCR fragment obtained; wt MEFs with no protein transfected are able to accurately fill the gap and solve the NHEJ product; DK MEFs with no protein. Polλ wt, Polλ(Nail*μ*), Polλ(Loop1*μ*) and Polλ(Loop1*μ*+Nail*μ*) were electroporated (5 ng in each case). C) Titration of NHEJ accuracy on this substrate. Graph represents the quantification of assays as shown in B) with different amounts of protein transfected shown in B) with different amounts of protein transfected.

5.3.3 3'G overhangs substrate (non-complementary substrate)

In the case of 3'G-overhang (Fig. 52), there is no end-complementarity to be used for bridging two DNA ends. According to previous results, performed *in vitro*, this susbtrate can only be efficiently handled by Pol*μ*, thanks to its specific Loop 1 region. Thus, we decided to test this kind of substrate in order to see if interchanging the specific regions of these proteins could affected their functionality. As shown in Figure 5.3.1.B, the NHEJ activity seen in wt MEFs is specifically lost in the DK MEFs, and only recovered at a significant level when electroporating wt Pol*μ*. Although we tried to titrate this substrate with increasing amounts of the chimeras, we couldn't get any remarkable result. That implies that Pol*μ*´s ability to connect and polymerize across non-complementary ends cannot be conferred to Polλ simply by swapping loop1 and Nail domains.

Taken all together, these results confirm the importance of the Loop 1 and Nail regions to confer the NHEJ specificity required in each case. In the case of 3'GCGA and 3'GCG overhangs, we demonstrated that the loss/interchange of these specific regions made Polλ less competent to perform NHEJ. It is interesting that in the case of Polλ(Loop1*μ*) the activity decreases drastically comparing to wild type protein, but in the case of Polλ(Nail*μ*) not that much. Interestingly, the double chimera was severely affected, leading us to think that the loss of the ability to handle partially complementary ends (a requisite for Polλ), could lead to a gain of function perhaps mimicking Pol*μ*´s ability to deal with non-compatible ends (studied here with a 3'G-overhang). However, whereas the cognate Loop1 and Nail regions of Pol*μ* confers this enzyme the ability to join non--compatible ends,

importing any or both of these regions to Polλ didn't allow the new chimeras to perform NHEJ in this context.

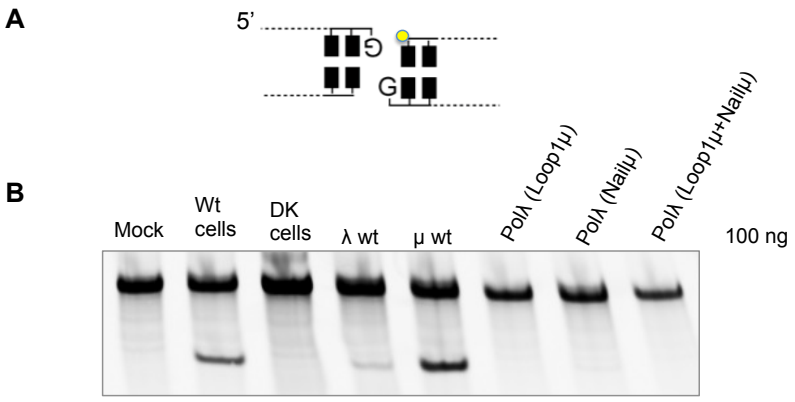

Figure 52. 3'G overhangs (non-complementary substrate). A) Schematic representation of the substrate analyzed. Yellow dot indicates the presence of a downstream 5' phosphate. **B)** Polλ chimeras show no activity in a Pol*μ* specific context. From left to right: Mock as a negative control, represents an independent electroporation in wt MEFs, but with no final digest of the PCR fragment obtained; wt MEFs with no protein transfected; DK MEFs with no protein transfected. Polλ wt, Pol*μ* wt, Polλ(Nail*μ*), Polλ(Loop1*μ*) and Polλ(Loop1*μ*+Nail*μ*) were electroporated in a dose of 100 ng in this case.

5.4 Effect of phosphorylation of Polλ on NHEJ activity *in vivo*

In order to maintain genomic integrity, cells have developed multiple surveillance pathways programmed to be active after DNA damage conforming the DNA damage response (DDR) (Bartek and Lukas 2007). When DSB occurs, a series of well-organized post-translational modifications recognize and amplify the primary signal to different effectors that coordinate DNA repair and other cellular events (cell cycle, gene expression...) (Zhou and Elledge 2000). Among all of them, protein phosphorylation is one of the post-translational modifications more extensively studied. During DSBs, ATM and DNA-PKs are triggered by the DDR: ATM is a crucial upstream event in the first steps of DSB, but on the contrary, DNA-PK participates particularly in the regulation of canonical NHEJ (Neal et al. 2014).

A large-scale proteomics analysis published on 2007, they identified consensus ATM and ATR phosphorylation motif sites in proteins responsive to DNA damage. In that work, ATM and/or ATR were proposed to phosphorylate Polλ (Matsuoka et al. 2007). ATM and ATR share substrate specificity, as they are able to recognize the same motifs: Ser-Gln (SQ) and Thr-Gln (TQ).

In a recent work published our lab (Ruiz et al. 2013), it was shown that Poλ's closest homolog in yeast, Pol4, is phosphorylated by Tel1 (homolog to human ATM) after DSB induction and, in addition, this kinase is able to regulate Pol4 during NHEJ. These results lead us to wonder whether ATM or DNA-PKs regulated Polλ during DDR.

In an ongoing project leaded by Jose F. Ruiz in collaboration with our laboratory, he has shown that Polλ can be phosphorylated by DNA-PKs during DDR response. Moreover, this phosphorylation seems to be aimed to its N-terminal region, specifically in Thr188 and Thr204 residues (data not shown, being prepared for submission).

In order to understand of the importance these residues, different phosphorylation mutants have been designed: firstly, these two threonines were mutated to non-phosphorylable alanine residues (A), and secondly, to phosphomimick glutamic acid residues (E) that imitate the effect of phosphorylation modification. With all these previous data, we thought that it would be interesting to

take advantage of the novel methodology developed in the laboratory of Prof. Ramsden for the *in vivo* analysis of NHEJ substrates, and analyze whether these punctual modifications in Polλ have any impact on its NHEJ activity *in vivo*.

5.4.1 3'GCCA-overhang (partially complementary substrate)

As mention before, 3'GCAC-overhang substrate is Polλ-specific, with a 2--nucleotide complementary microhomology and a 2 nucleotide gap (Figure 53A). We used wt MEFs with no protein as a positive control of the reaction (Figure 53B; second lane on the left). We observed a highly accurate junction in this case. In contrast, DK MEFs lacking both polymerases, λ and *μ*, with no protein transfected by electroporation (third lane on the left) are not able to perform an accurate junction of the substrate. The point mutants described above were thus analyzed in the context of DK MEFs in order to obtain a neat result from the protein activity itself.

As shown Fig. 53B, the proportion between non-accurate activity (upper band) and accurate gap polymerization (lower band) showed that the efficiency of these phosphorylation mutants was similar compared to Polλ wt protein, but apparently higher in the case of the phosphomimicking mutant T204E. In this case, figure shows an experiment performed in non-saturating conditions (0,2 ng of transfected protein, instead of 1 ng), because we were looking for slight (perhaps physiological) differences in enzymatic activity. Under these conditions, mutants T1881, T204A and T1881/T204A (to non-phosphorylable residues) and mutant T188E (phosphomimicking) showed similar activity to Polλ wt. However, as mentioned before, the other phosphomimicking mutant (T204E), showed much more accuracy activity than Polλ wt.

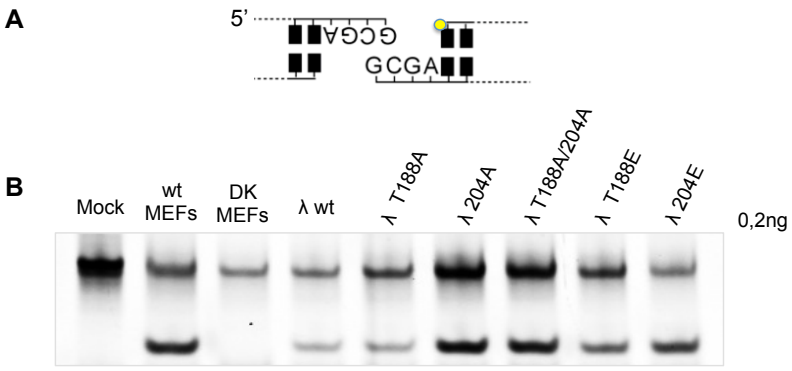

Figure 53. 3'GCAG-overhang (partially complementary substrate). A) Schematic representation of the substrate analyzed. Yellow dot indicates the presence of a downstream 5' phosphate. **B)** Polλ phosphorylation mutants activity in a Polλ-specific sequence context. From left to right: Mock as a negative control, represents the pool of 3 independent electroporation in wt MEFs; wt MEFs with no protein transfected; DK MEFs with no protein transfected. Polλ wt, λ T188A, λ T204A, λ T188AT204A, λ T188E, λ T204E were electroporated (0,2 ng in each case).

With this promising result obtained, we decided to titrate the T204E mutant against Polλ wt to confirm this result. Figure 54 confirms that this enhanced activity remained present even when using small amounts of protein. T204E NHEJ accuracy almost doubles that of the Polλ wt protein, being able to saturate the reaction at 0,2 ng. This interesting result in which the NHEJ capacity is altered in a phosphomimicking mutant seems to indicate that specific phosphorylation events can regulate Polλ's NHEJ activity. Further studies should be done in order to obtain a deep understanding of the importance of this residue in the ability of Polλ to perform gap-filling DNA synthesis mediated during NHEJ.

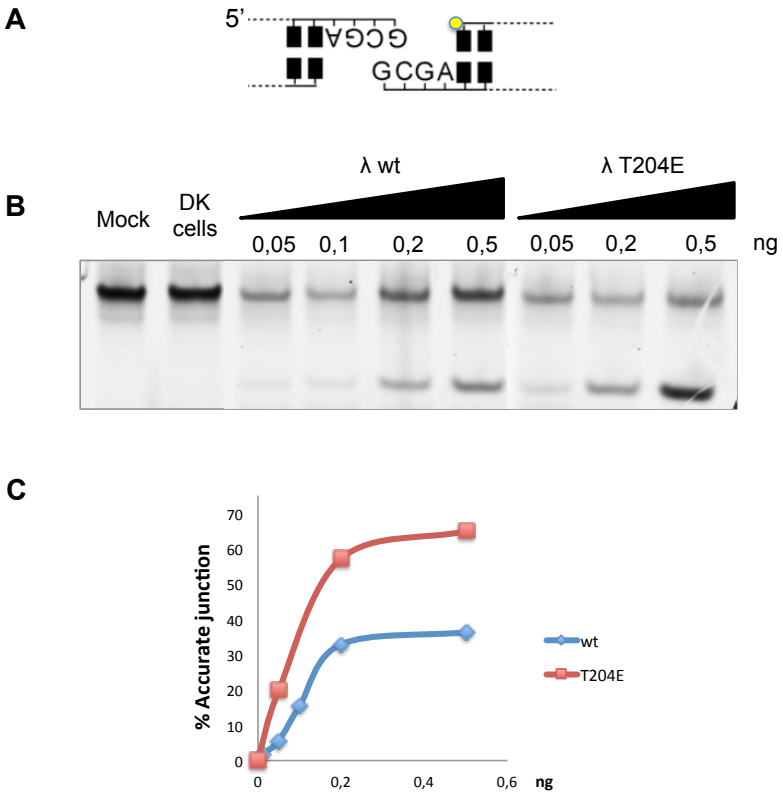

Figure 54. 3'GCAG partially complementary substrate. A) Schematic representation of the substrate analyzed. Yellow dot represents the presence of a downstream 5' phosphate. **B)** Polλ wt titration against λ T204E. From left to right: Mock as a negative control, represents the pool of 3 independent electroporation in wt MEFs; DK MEFs with no protein transfected. C) Graph represents the quantification of assays as shown in B) with different amounts of protein transfected.

5.4.2 3'GCC-overhang (partially complementary substrate)

In the case of the 3'GCG-overhang substrate (Fig. 55A), both polymerases, Polλ and Pol*μ*, are able to perform NHEJ when there is a 2-nt complementary microhomology and 1 nt gap, being Polλ more efficient than Pol*μ* (data not shown). In this case, we observed a similar pattern in the behavior of the phosphorylation mutants compared to Polλ wt. This result did not show specific differences among the mutants as when using the 3'GCGA-overhang substrate. As shown in Fig. 55B, we electroporated 0,5 ng of each protein to measure subtle differences in NHEJ under non-saturating conditions. The 3'GCG-overhang produces a 1 nucleotide gap and, therefore, is not Polλ-specific but it can be alternatively handled by Pol*μ*. Comparing the results obtained with both substrates

(3'GCGA- overhang versus 3'GCG-overhang), it appears that T204 phosphorylation could be more relevant to regulate the activity on the specific substrate of Polλ (a 2 nucleotide gap).

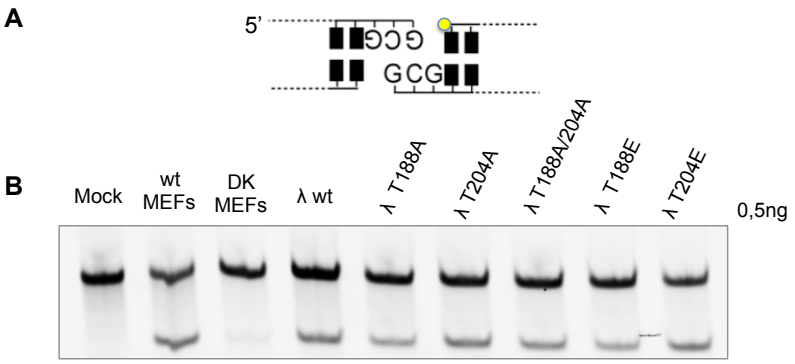

Figure 55. 3'GCG-overhang (partially complementary substrate). A) Schematic representation of the substrate analyzed. Yellow dot indicates the presence of a downstream 5' phosphate. **B)** Polλ phosphorylation mutants activity. From left to right: Mock as a negative control, represents the pool of 3 independent electroporation in wt MEFs, but with no final digest of the PCR fragment obtained; wt MEFs with no protein transfected are able to accurately fill the gap and solve the NHEJ product; DK MEFs with no protein transfected are not able to join and fill the substrate and show no accurate junction at all. Polλ wt, λ T188A, λ T204A, λ T188AT204A, λ T188E, λ T204E were electroporated (0,5 ng in each case).

DISCUSSION

1 Evolution of the X family of DNA polymerases

DNA polymerases have been categorized into four different groups attending to their biochemical properties and to the biological processes in which they are involved. Eukaryotic organisms have four families: A family (Polγ, Polθ and Polν), B family (Polα, Polδ, Polε and Polζ), X family (Polß, Polλ, Polμ and TdT) and Y family (Polη, Polι, Polκ and Rev1).

X Family members are present in all monophyletic taxa: Eukaria, Bacteria and Archea; even in virus whose genome is DNA(Oliveros et al. 1997). The high degree of conservation at primary and tridimensional structure suggests that their evolution comes from a common ancestor. Higher eukaryotes present more than one member of this X Family. In contrast, there are some organisms like Caenorhabditis elegans and Droshopila melanogaster (Burgers et al. 2001) with no reported members of this family. Yeasts have only one member of this family, Pol4. Both Pol4 from S. cerevisae (ScPol4) and S. pombe (SpPol4) present a core structure ß-like, additional domains such as BRCT and Ser/Pro, and both have dRP lyase activity (Bebenek et al. 2005; Gonzalez-Barrera et al. 2005). Based on sequence identity, we can argue that ScPol4 is Polλ's orthologous in humans (24% sequence identity) and ScPol4 is Pol*μ*'s orthologoue (27% sequence identity).

All X family members share a significant level of similarity in primary and tridimensional structure, thus indicating that they are truly homologous, derived from a common ancestor. The phylogenetic relationships between the known members of X family from different organisms is shown in Fig. 56. The evolution to have several members in superior organisms consequently determines the different mechanisms of DNA repair in which they participate.

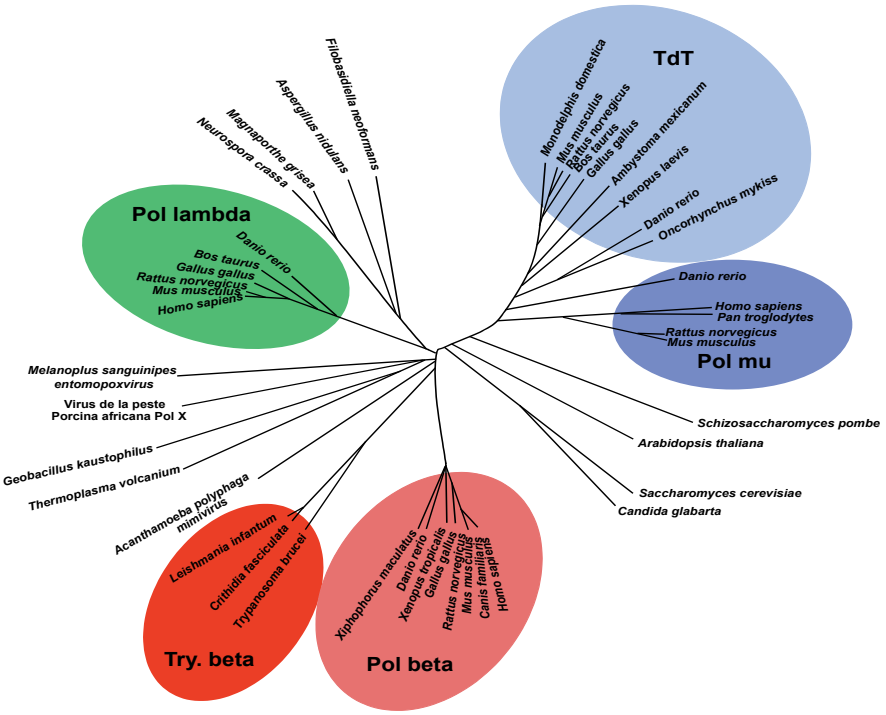

Figure 56. Evolutionary relationships between family X members. An unrooted phylogenetic tree built using a primary sequence alignment of a segment of the catalytic domain. Different enzymes are grouped (shaded areas) into the five main enzyme classes in the family: Polß, Pol λ, Polμ, TdT, and trypanosomatid (Try) Polß-like enzymes.

2 DNA expansions generated by human Pol*μ* on iterative sequences

Indels (insertions and deletions) are common errors produced during DNA replication and repair, associated with different human pathologies including cancer and diseases associated with expansion of repeats. All polymerases studied to date generate indels during DNA synthesis in vitro {Bloom, 1997 #5}, but with very different frequency. Thus, although X family members Polß, Polλ, and Pol*μ* all generate single-base deletions during DNA synthesis {Bebenek, 2003 #21;Kunkel, 1985 #22;Zhang, 2001 #9}, Polλ has a much higher deletion rate, whose structural basis has been already proposed (Bebenek and Kunkel 1990). The first explanatory hypothesis for the production of indels was introduced by Streisinger et al. (Streisinger et al. 1966), describing these frameshift mutations were described as byproducts of strand slippage in repetitive DNA sequences. Other two models have been proposed since then, namely "direct misincorporation misalignment", in which a polymerase introduces an initial mismatch that causes the primer terminus to be subsequently realigned {Bebenek, 1990 #41;Kunkel, 1988 #42} and "dNTP-stabilized misalignment", in which the selection of a dNTP that is complementary to a distant template base could trigger the deletion {Bloom, 1997 #43;Efrati, 1997 #44}.

The results presented here demonstrate that human Pol*μ* can catalyse large nucleotide expansions when copying a repeated templating base in the vicinity of a 5'P. Based on our findings with different sequence contexts, we propose a specific model for Pol*μ*-mediated generation of the expansions during gap-filling that requires: 1) initial dislocation of the template strand; 2) generation of a mismatch/distortion, that will trigger nucleotide expansion (Figure 57B,C). Initial template dislocation can be either facilitated by slippage, when the primer-terminus is complementary to the first nucleotide at the gap (Figure 57B), or stabilized by the incoming nucleotide (dNTP-mediated; Figure 57C); in both cases, after initial dislocation (stage 1), the gap is filled and a mismatch is left behind (stage 2), and then expansion occurs (stage 3). However, such expansions are not simply the result of Streisinger´s "strand slippage": if the sequence to be copied is formed by the three same nucleotides (Figure 57A), the expansion hardly happens because the mismatch/distortion that could trigger further nucleotide incorporation beyond gap-filling is not allowed to occur.

Such gaps, eventually containing distortions, are common substrates at the second step of NHEJ, as they are generated after repairing the first strand of the DSB. Moreover, our results indicate that our model for the production of expansions of iterative dinucleotides is also valid during the first step of NHEJ (Figure 57F), where the critical requisite of generating a distortion upstream the primer-terminus is expected to occur during end-bridging and search for microhomology.

2.1 Relationship between terminal transferase and the generation of sequence expansions.

In most DNA-dependent DNA polymerases, proper positioning of the 3' terminus is indirectly dictated by the enzyme's avidity for the templating base, thus configuring a binary complex ready to select the incoming nucleotide (ternary complex). Eventually, when no template base is available (blunt or 3'-protruding ends, or when a gap has been fulfilled), any further nucleotide addition is

unfavored, due to deficient translocation of the 3' terminus, thus precluding addition of extra nucleotides. Template instruction is a general feature of most members of the X family, with the exception of TdT. Interestingly, Pol*μ* shows hybrid biochemical properties: it is strongly activated by a template DNA chain (Dominguez et al. 2000), but it has an intrinsic terminal transferase activity, although weaker than TdT.

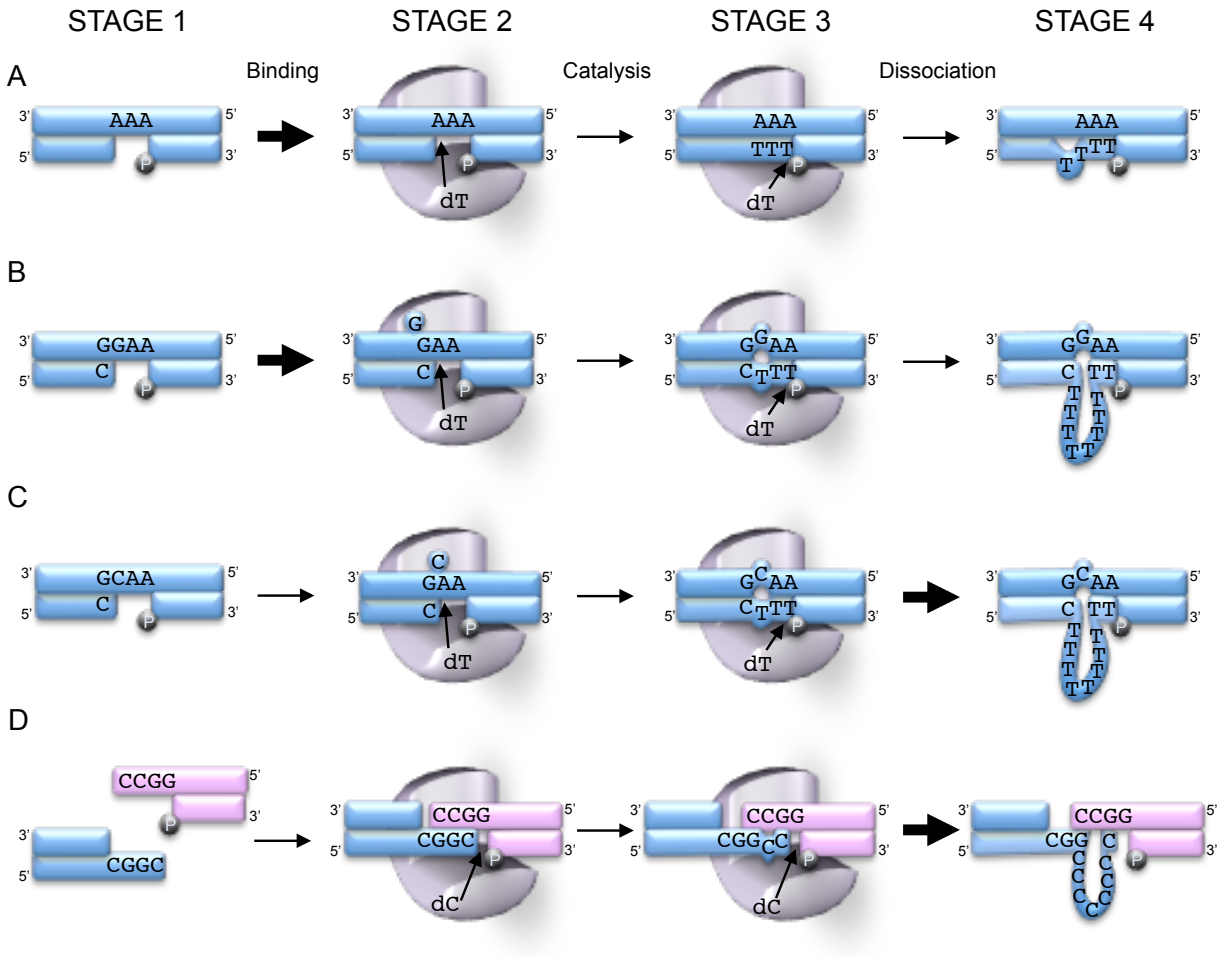

Figure 57. Mechanistic model for dinucleotide expansions generated by human Pol*μ*. Thick arrows indicate more efficient reactions, whereas thin arrows are related to slower or less favorable reactions. A) Trinucleotide conformed by the same nucleotide. In this case, no distortion associated to gap filling is generated, thus precluding a large expansion. B) After polymerase binding and realignment of the primer terminus, a "slippage-mediated" dislocation is formed, creating a template distortion. In this situation, a large expansion reaction is observed. C) In this case the distortion is induced by a "dNTP-selection mediated" dislocation of the template strand, again resulting in the generation of large sequence expansions. D) In a NHEJ context, a repeated nucleotide neighbour to the 5'P can induce nucleotide expansions by Pol*μ*, although in this case, a pre-existing stable distortion or impairing is not strictly required.

A specific histidine residue, conserved between Pol*μ* (His329) and TdT (His342) (Fig. 14), but absent in Polß (Gly189) or Polλ (Gly426), confers terminal transferase activity as it is crucial and responsible for proper positioning of the primer terminus and the incoming nucleotide in the absence of a template (Moon et al. 2007). Mutating this histidine in Pol*μ* (Andrade et al. 2009; Moon et al. 2007), and TdT {Romain, 2009 #48} substantially reduced template-independent activity. As shown here, elimination of His329 rendered Pol*μ* unable to perform sequence expansions in the context of

a gap. Therefore, the specific role of His329 during Pol*μ*´s catalytic cycle, facilitating primer translocation and non-templated nucleotide insertion (terminal transferase) has two sides, being beneficial for NHEJ of incompatible-ends but allowing, as a collateral effect, the eventual generation of large sequence expansions through the very same mechanism of favoured primer translocation. Besides, Pol*μ*´s terminal transferase activity is negatively regulated by Arg387 (10), acting as a brake for the necessary movement of the primer (thus counteracting His329), to limit excessive nucleotide additions before end bridging. The role of this residue in a non-distorted gap would be positive in terms of genome stability, because a braked primer translocation would help to reduce the number of extra nucleotide units added beyond gap-filling (Figure 43A). However, in a physiological context of DSB repair, where NHEJ produces gaps with eventual distortions (shown here to be a requisite for expansion), Arg^{387} might not be able to maintain the contacts with the primer, allowing unbraked translocation and facilitating nucleotide expansion. In summary, our site-directed mutagenesis results support that the same mechanism that provides Pol*μ* with the ability to perform untemplated insertion of nucleotides (terminal transferase), beneficial for NHEJ of non-complementary ends, has an unexpected downside, since it also allows Pol*μ* to generate large sequence expansions in the context of repair reactions.

2.2 Pol*μ*, a candidate to generate mono- and di-nucleotide expansions *in vivo*.

The genome of most organisms thus far examined contains many tracts of repetitive DNA called microsatellites. The discovery that a number of human diseases are the direct consequence of mutations within such repeats has triggered considerable interest in the mechanisms that change the number of copies of repeated DNA sequences. DNA expansions in mono- and dinucleotide repeats are more likely to be deleterious to the cell by causing not only addition mutations but also frameshift mutations. Current models of DNA repeat instability involve DNA polymerase slippage at these iterative tracts, which are normally associated with mutation hot-spots. Which polymerases are responsible for expansions? Initial efforts were oriented to measure DNA polymerase-catalyzed “reiterative replication” of repeat sequences with replicative polymerases {Lyons-Darden, 1999 #50;Petruska, 1998 #51;Sinden, 2002 #33;Canceill, 1999 #53;Sinden, 1992 #52}, but evidence soon indicated that those lacking proofreading and also strand displacement capabilities are better candidates {da Silva, 2000 #55;Hartenstine, 2002 #54;Kunkel, 1994 #49}. Moreover, other results indicate that sequence expansions could be linked to DNA damage (Kovtun et al. 2007), a process causatively related with ageing {Stadtman, 1992 #57;Cardozo-Pelaez, 1999 #56}. That could be a vicious cycle, as it is quite possible that repetitive DNA is a better target for DNA damage than normal DNA. Repair substrates as short gaps are produced *in vivo* during base excision repair, as well as during the final steps of nucleotide excision repair and post-replication mismatch repair. More specifically, DNA polymerases as Pol*μ* are able to configure gap-like substrates during NHEJ. In all these substrates, the presence of a downstream strand would lead to the “stalling” of the polymerization reaction (Hartenstine et al. 2002), thus providing sufficient time for realigning the primer strand and triggering expansive nucleotide insertion.

Our results suggest that Pol*μ* can generate the expansion of mononucleotide tracts during these repair reactions *in vivo*, given the appropriate sequence context. It is not yet known whether homopolymeric runs are more prone to DSBs than non-iterative sequences, but the possibility can be easily envisaged, due to the ssDNA-containing secondary structures that these sequences can adopt. As derived from our work, in the case of a DSB occurring at a site containing an iterative sequence as short as a single dinucleotide, the outcome of a Pol*μ*-mediated repair reaction would result in the generation of frameshifts and sequence expansions. This could in turn lead to an increased risk of microsatellite and genome instability, events that have been related to cancer and other illnesses such as neurodegenerative syndromes.

3 Effect of Polλ depletion on CAG somatic expansion in a Huntington´s disease mouse model

Several DNA repair mechanisms have been proposed to be involved in trinucleotide repeat (TNR) somatic expansion involved in HD. HD is an autosomal dominant progressive and fatal inherited neurodegenerative disorder caused by a polyglutamine repeat expansion (CAG) in the coding region of the Huntingtin (HTT) gene. The concise mechanism of somatic expansion has not been yet elucidated.

Msh2 and Msh3, proteins that participate in MMR have been involved in HD, demonstrating that contractions and expansions are suppressed in their absence (Mason et al. 2014). This suggests a possible role of MMR to promote CAG/CTG repeat expansion (Dragileva et al. 2009; Kovalenko et al. 2012; Kovtun et al. 2001; Manley et al. 1999; Tome et al. 2013). But MMR is not the only mechanism of DNA repair proposed to participate in HD; BER has been also involved. DNA Polß has been involved with TNR through a slippage mechanism, and besides through its dRP lyase activity in coordination with FEN. When Polß is not able to properly remove an oxidized dRP residue, it might be a lack of coordination between Polß and FEN1 leads to triplet expansion (Matsumoto et al. 1994;(Liu et al. 2009; Petruska et al. 1998). Moreover, oxidative damage has been related to aging (Cardozo-Pelaez et al. 1999), and also with repeat expansion in the brain (Kovtun et al. 2007). The BER enzyme OGG1, a glycosidase involved in the removal of one of the most common DNA oxidative damages, 8oxoG, was recently linked to somatic CAG/CTG repeat expansion, creating ssDNA breaks. As CAG repeats are sequences very susceptible to be oxidized and Polλ is implicated in BER, we reasoned that this DNA polymerase might be implicated in the promotion of CAG repeat expansion in somatic cells in HD context.

In addition, Reactive Oxigen Species (ROS) are recognized to have a very important role in the onset of trinucleotide repeat instability in conditions like Huntington disease (McMurray 2010). Many organisms have developed a system to overcome this lesion consisting of three BER proteins: OGG1 (8-oxo-G DNA glycosylase) MutYH (MutY glycosylase homolog) and MTH1 (8-oxo-dGTPase). Interestingly, it has been demonstrated that in cells exposed to ROS, MutYH and Polλ colocalize to sites of 8oxoG lesions. Polλ has been identified to play an important role in repair of oxidative damage, especially in the correction of the pair 8oxoG:A to 8oxoGC, and MEFs deficient in

Polλ enter prematurely in senescence when cultured in oxidative stress conditions, 20% O_2 (Bertocci et al. 2003). Additionally, there is specific recruitment of MutYH, Polλ, PCNA, FEN1 and DNA ligases I and III in human cell extracts containing DNA A:8oxoG mispair (van Loon and Hubscher 2009).

Recently, it has been proposed that oxidative stress could be responsible for activate repair systems that lead to triplet sequences expansion. One recent study describes the impact of a single-nucleotide polymorphisms (SNPs) in OGG1 on the age at onset of Huntington's disease (Berger et al. 2013). This SNP has been associated with lower 8oxoG repair activity emphasizing the potential role of oxidative stress in determining the age at onset of HD.

Our results coincide with those described in a recent paper that describes a possible role for Neil1 in somatic CAG expansion (Mollersen et al. 2012). Neil1 is one of four mammalian DNA glycosylases involved in removing oxidized lesions as part of BER. Although Neil1 prefers cytosine-derived lesions, shares substrate specificities with Ogg1, including 8oxoG lesions. In this study, R6/1; Neil1$^{-/-}$ mice present both somatic TNR expansions in several organs and reduced germline expansions in R6/1 as we observed. Interestingly, they don't mention anything related to the effects this might have on that mice. In contrast, we analyzed HD phenotype in R6/1, as we observed in our study. However, no mention is made about any effect that this might have on that mice. In contrast, we analyzed HD phenotype in R6/1; Polλ$^{-/-}$ mice, but there was no effect in weight loss or motor impairment. The downregulation of glycosylases (Ogg1, Neil1) has been involved in the accumulation of base damage within CAG tracts that can ultimately drive TNR expansions, but it is also important to consider the role of Polλ in the repair of oxidative damage to maintain genomic stability. If oxidative damage is correlated with TNR expansions, Polλ might play a role in this process.

Using the 'Search Tool for the Retrieval of INteracting Genes/proteins' (STRING v9.0) (Szklarczyk et al. 2011) analysis to interrogate the protein interaction network centered at Polλ, we noted that the resulting network highlights PCNA and FEN, components of DNA repair (Fig. 58). Polλ's interaction with FEN1, combined with the role of Polλ in oxidative damage, suggests a similar coordination to the one described between Polß and FEN1, thus, implicating Polλ in TNR expansions.

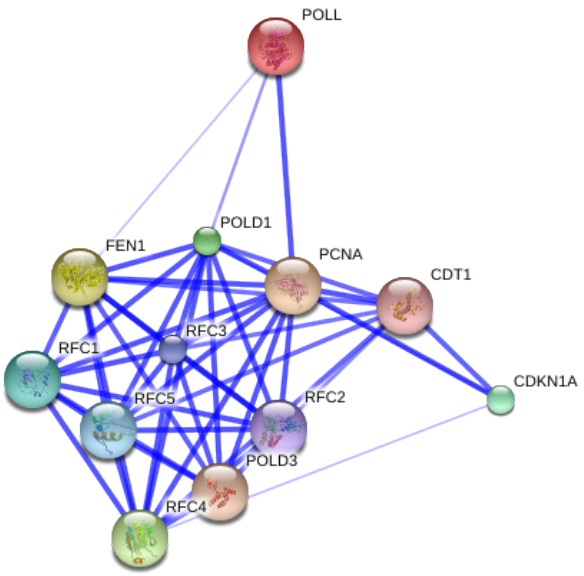

Figure 58. STRING protein interaction network centered on Polλ.

In summary, we should consider the dual role Polλ in HD, as concluded from our study. On one hand, the absence of Polλ in R6/1 mice diminishes the number of triplet expansions transmitted to successive generations and reduces the area of huntingtin inclusions, but contrary to our expectations, prevention of this expansion does not preclude disease progression. Polλ appears to be necessary to "count and copy" faithfully any repeated sequences, thus also contributing to the maintenance of the expanded sequence. On the other hand, as mentioned before, Polλ is also very important in the repair of oxidative damage; consequently, the asbsence of Polλ might increase the accumulation of oxidative damage left unrepaired in these mice (similarly to the case of the variant OGG1), thus leading to an impact on HD, independently of the CAG-repeat number and associating oxidative stress with the severity of HD.

4 Analysis of genetic instability in Mouse Embryonic Cells (MEFs) double deficient in Polλ and Polμ

In general, cells deficient in DNA repair factors are sensitive to genotoxic agents. Considering this, we evaluated the sensitivity of MEFs deficient in Polλ, Pol*μ* or both to different drugs.

As it was previously described, MEFs deficient in NHEJ factors present diminished proliferative capability (Espejel and Blasco 2002; Vogel et al. 1999) and a severe DNA repair deficiency, promoting global premature replicative senescence (Sekiguchi and Ferguson 2006). Moreover, Pol*μ* and Polλ KO MEFs enter earlier in senescence than wt cells (Lucas et al. 2009b). Here, we report that DK MEFs enter in senescence earlier than wt MEF, as we concluded using both the 3T3 protocol and ß-gal associated senescence assay (chapter 2 of the Results section). DK MEFs show 3-times higher ß-gal associated senescence than wt MEFs.

We analyzed the sensitivity of these MEFs to different drugs related to DNA damage: from oxidative agents (TBH, H_2O_2) to nucleoside analogous used in medicine as a chemotherapeutical agents (Cytarabine, Fludarabine, Etoposide) and to gamma radiation. In gamma radiation, MEFs lacking Polλ or Pol*μ* were not sensitive, whereas DK MEFs, deficient in both DNA polymerases, were extremely sensitive to gamma radiation compared to wt.

In the case of H_2O_2, we found that KOλ and DK MEFs were sensitive to this agent whereas wt and KO*μ* MEFs were not. This corroborates the previous results obtained by (Tano et al 2007), where they found that KOλ MEFs were sensitive to this agent. Interestingly, this result is repeated in the case of DK MEFs but not in KO*μ*, suggesting that this kind of damage seems to be repaired only by Polλ. In the case of TBH, KOλ and KO*μ* behaved very similar, indicating that both polymerases seem to be involved in the repair of this damage. This is confirmed by the effect in DK MEFs, where the survival is much lower than in the case of the simple KOs.

Curcumin was described to be a selective inhibitor of Polλ (Takeuchi et al. 2006). Previous data from our lab confirmed that Pol*μ* was also inhibited by curcumin (not shown). The strong sensitivity to this compound presented by DK MEFs indicates that curcumin damage might involve more repair

genes than Polλ and Pol*μ*, or that the DNA damage is so massive that Polλ and Pol*μ* might be required to solve it.

When using Fludarabine, all the MEFs were sensitive to this drug, especially in KOλ and DK whereas the effect was milder in KO*μ*. This suggests that both polymerases were involved in the tolerance of this compound, being Polλ more involved in the process. In contrast, when using AraC we found that the single deficiency of one polymerase didn't compromise cell survival, but on the other hand, when both of them were absent in DK, cell survival fell drastically. This might indicate some kind compensation in the single KOs that cannot occur in the case of the DK.

Cisplatin treatment presented a strong effect in KO*μ* MEFs, being as sensitive as DK MEFs. It has been described that Pol*μ* is able to bypass this kind of lesion (Havener et al. 2003), so our result confirms the importance *in vivo* of Pol*μ* in the ability to bypass cisplatin adducts.

Thus, using etoposide, a drug that produces DSBs DK MEFs clearly showed a persistent DNA damage. The use of different damaging agents have shown *in vivo* the non-overlapping functions of Polλ and Pol*μ* when facing DNA damage, as single KO are sensitive to different drugs and the use of the DK MEFs have confirmed that there is no redundancy on their functions. These experiments support that the absence of the two DNA polymerases involved in NHEJ, Polλ and Pol*μ*, lead to a severe defect in genomic instability in a cellular context compromising the maintenance of genomic integrity and therefore, cell survival.

One of the first questions that arise was about the possible overexpression of the other PolX in the single KO in order to compensate and balance this absence. For this, we analyzed PolX relative expression in MEFs (not shown). Interestingly, the lack of one of both of these two polymerases didn't involve an increase in the expression of the other polymerase present in the single models neither did Polß. This could be explained because this result was obtained in the absence of DNA damage, which could trigger this polymerases' expression, and therefore, their expression in cells. It would be interesting to analyze in the future how these polymerases expression is balanced (or not) depending on the damage the cell receives, in order to obtain very specific drugs to inhibit them.

4.1 Lack of Polλ and Pol*μ* compromises cell cycle

NHEJ is the prominent pathway for DSB repair because of the absence of a sister chromatid, is active during all stages of cell cycle and can be error-prone, but its efficiency is the highest during G2/M. In late S and G2 phases, even though NHEJ remains functional, there is an increase in the repair of DSB by HR when a homologous sister chromosome or chromatid is available for direct base.pairing to effect error-free repair of a DNA DSB (Mao et al. 2008; Natarajan et al. 2008; Takashima et al. 2009; Takata et al. 1998). Previous reports amount that only about 15% of the DSB repaired in G2 is done by HR (Fig. 45) (Beucher et al. 2009). DNA-damage signaling activates several cell cycle checkpoints and deficiency in genes involved in DDR such as H2AX (Fernandez-Capetillo et al. 2002) Mdc1 (Lou et al. 2006) Rnf8 Kolas (Kolas et al. 2007) and 53bp1 (Fernandez-Capetillo et al. 2002) lead to a defect in the G2/M checkpoint. Cell cycle analyses of wild-type and

DK MEFs at 4 h post-etoposide treatment indicated that a higher proportion of the DK MEFs was found at the G2/M phase. Here we report that the absence of two polymerases involved in NHEJ, λ and *μ*, lead to a defect in the G2/M checkpoint when both of them are not present. Interestingly, although their biochemical properties characterized *in vitro* demonstrate that they have different cognate substrates, in the case of the single models deficiency we find a mild defect in G2/M arrest suggesting that there might be some kind of compensation that helps these cells to overcome the deficiency of one polymerase, and consequently, allow the cells to progress in G2/M checkpoint, whereas in the case of DK MEFs, when both of them are absent, DK MEFs are not capable of overcome the damage produced due to NHEJ inefficiency thus, increasing G2/M checkpoint and leading to G2/M arrest (Fig. 59).

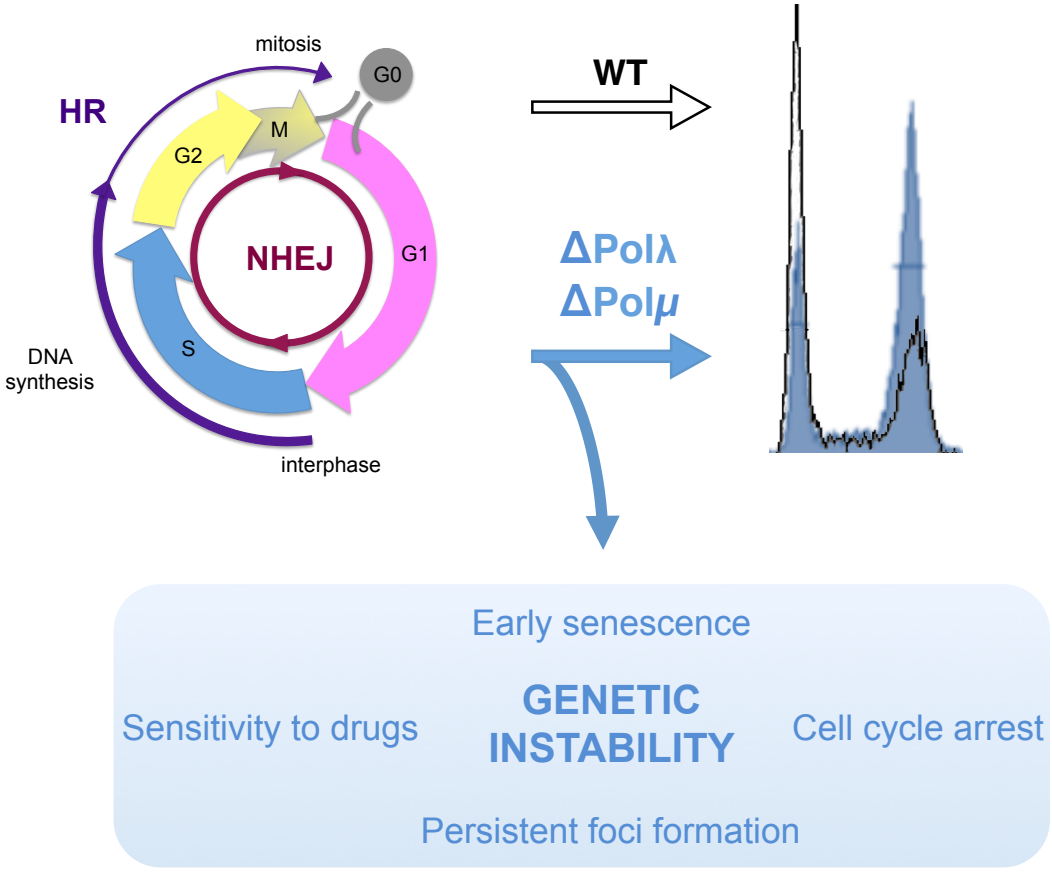

Figure 59. Lack of Polλ and Pol*μ* compromises cell cycle. Upper part, left: Comparative strength of NHEJ vs. HR along the different phases of the cell cycle. The letter size illustrates the comparative contribution of the two mechanisms in each phase. When NHEJ is compromised, cell cycle arrest in G2/M. **Upper part, right:** Comparative cell cycle distribution in wt MEFs (Black line) vs. DK MEFs (blue). DK MEFs arrest in G2/M, leading to genetic instability.

NHEJ employs multiple strategies for damage processing that can be grouped in three categories: tolerance; end cleaning and short parch repair; and end remodeling and long patch repair (Fig. 60). These strategies are distinguishable by the specificity and extent of the end processing steps prior to ligation. The type(s) of damage present at the DNA ends might determine the way NHEJ chooses each strategy. Nevertheless, the complexity of the NHEJ mechanism, and the large number of processing factors involved, rquires a hierarchically model, that selects the more conservative processing to minimize sequence loss. Considering that the goal of NHEJ is retaining the DNA

sequence as much as possible, direct ligation would be the first choice to tolerate the damage; then, damage-specific end cleaning and short-patch excision would be a second choice and finally, long-patch excision.

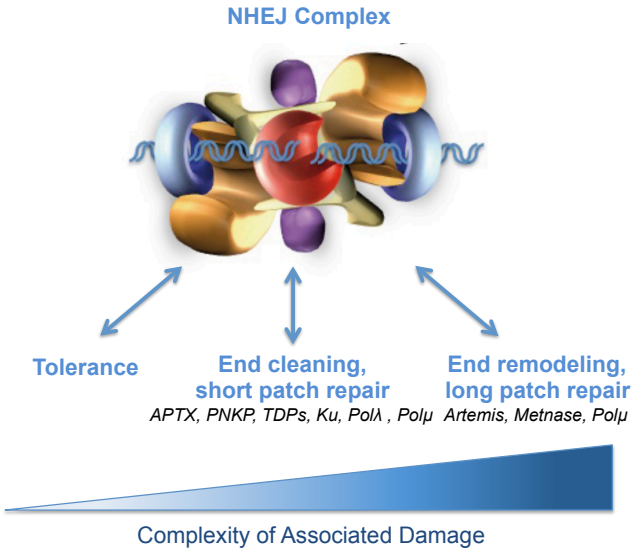

Figure 60. NHEJ may employ these strategies hierarchically. The choice and transition from one strategy to the next is likely determined by the complexity of damage at the ends. The NHEJ core complex is shown as described in Fig. XX. *(Adapted from Waters et al. 2014)*

Post-translational modifications could facilitate all these sequential decisions, modifying modifying the NHEJ complex. Among all of them, protein phosphorylation is one of the best post-translational modifications studied. During DSBs, ATM and DNA-PKs are triggered in the DDR: ATM is a crucial upstream event in the first steps of DSB, but on the contrary, DNA-PK participates particularly in the regulation of canonical NHEJ (Neal et al. 2014). DNA-PKcs kinase activity has been implicated as the primary factor that could determine the choice of strategy and processing factor in NHEJ. Interestingly, there are over 30 different phosphorylation sites in DNA-PKcs, thus meaning that DNA-PKcs autophosphorylation is one of the most relevant targets to promote the rearrangements of these proteins at DNA ends as well as end accessibility. Several studies have described that mutations at different sites in DNA-PK have distinct effects on processing, indicating that phosphorylation acts as a modulator of the NHEJ activity (reviewed in (Dobbs et al. 2010). Moreover, DNA-PKcs have been described to modify the function of many factors involved in NHEJ through phosphorylation (although sometimes ATM also participates): Artemis, PNKP, WRN, Tdp1 and XRCC4-XLF-LigIV (Williams et al. 2014).

These evidences led us to think that Polλ and Pol*μ* might be regulated by this kind of phosphorylation too. They share multiple characteristics that could be aimed fro phosphorylation: their BRCT domain allow them to interact with other factors in NHEJ; their functions appear to be redundant at some points, but some overlapping in their substrate specificity indicates that they are able to cooperate depending on the situation they have to deal with. All of these considerations

made us think that a regulation by phosphorylation might be key to balance between these two DNA polymerases in NHEJ.

Recent results from our lab (Ruiz et al. 2013) show that Polλ's closest homolog in yeast, Pol4, is phosphorylated by Tel1 (homolog to human ATM) after DSB induction, thus potentially regulating Pol4 during NHEJ. These results lead us to wonder whether ATM or DNA-PKs could regulate Polλ during DDR.

In a large-scale proteomics analysis published on 2007, they identified consensus ATM and ATR phosphorylation motif sites were identified in proteins responsive to DNA damage. In that work, ATM and/or ATR were proposed to phosphorylate Polλ (Matsuoka et al. 2007). ATM and ATR share substrate specificity, as they are able to recognize the same motifs: Ser-Gln (SQ) and Thr-Gln (TQ). Taking this into consideration, we searched in phosphosite (www.phosphosite.org) for specific residues that might be candidates to be regulated by phosphorylation and Polλ presented several phosphorylation sites.

Polλ can be also phosphorylated by DNA-PKs during DDR response and moreover, this phosphorylation appears to be targetted to its N-terminal region, specifically in Thr188 and Thr204 residues. Ongoing work in our lab, studying phosphomimicking mutants,supports a possible role of the residue T204 in NHEJ regulation. We have obtained very promising results analyzing the activity of these mutant in NHEJ *in vivo*. Interestingly, it seems that specific phosphorylation can enhance Polλ's activity during NHEJ. This phosphorylation might improve its interaction with other NHEJ factors and its gap filling DNA-synthesis. With these results and considering all the similarities between Polλ and Pol*μ*, we believe that Pol*μ* must be also regulated by phosphorylation. Thus, future work will follow this experimental approach to analyze *in vivo* Pol*μ* phosphomimicking mutants in order to decipher if phosphorylation either enhances or restricts Pol*μ* specific activity.

Recent studies have also shown that Polλ and Pol*μ* are regulated by Cdk phosphorylation. In the case of Polλ, it has been shown that protein stability is regulated during the cell cycle (in the late S and G2 phases) by Cdk-mediated phosphorylation (Markkanen et al. 2011; Wimmer et al. 2008) to allow efficient DNA repair and translesion synthesis during and after replication.

On the other hand, Pol*μ* could be regulated in vivo by phosphorylation of the BRCT domain, affecting the function of loop1. This might lead to a negative regulation of Pol*μ* at specific cell-cycle phases (S and G2), when these promiscuous functions might be harmful to the cell (Esteban et al. 2013). Interestingly, this suggests that Cdk complexes could be a general way to regulate the specific or multiple functions of these polymerases during DNA repair. The target Pol*μ* residues are very close to a DNA binding region required for NHEJ activity. Therefore, and taking into account the promising results we obtained with the phosphomimicking mutants in Polλ, it would be interesting to test how the corresponding Cdk-phosphomimicking mutants affect NHEJ *in vivo* (fig. 61).

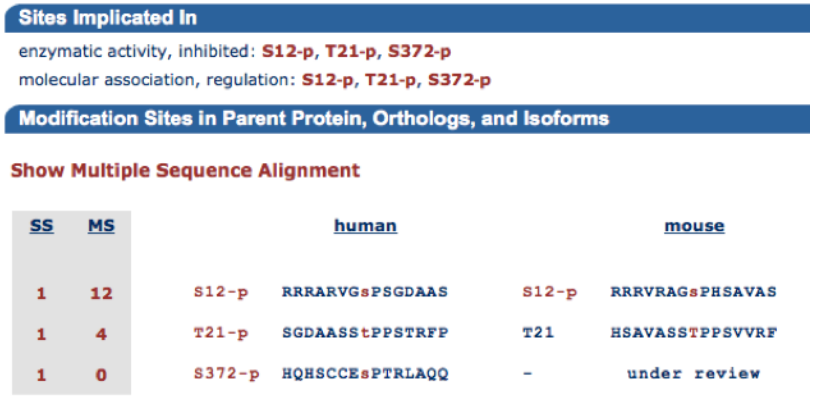

Sites Implicated In

enzymatic activity, inhibited: **S12-p**, **T21-p**, **S372-p**

molecular association, regulation: **S12-p**, **T21-p**, **S372-p**

Modification Sites in Parent Protein, Orthologs, and Isoforms

Show Multiple Sequence Alignment

SS	MS	human		mouse	
1	12	S12-p	RRRARVGsPSGDAAS	S12-p	RRRVRAGsPHSAVAS
1	4	T21-p	SGDAASStPPSTRFP	T21	HSAVASSTPPSVVRF
1	0	S372-p	HQHSCCEsPTRLAQQ	-	under review

Figure 61. Phosphorylation sites predicted for Pol*μ*. Results obtained from www.phosphosite.org.

Is the balance between Polλ and Pol*μ* relevant in cancer and disease? Here we have discussed the possible *in vivo* roles of these polymerases in NHEJ, how their non-redundant roles still has to be deciphered *in vivo*, and how they can be regulated by phosphorylation. But, do they have a direct impact in disease?

4.2 Is there a balance between Polλ and Pol*μ* relevant in cancer?

COSMIC is a catalogue of somatic mutations in cancer developed in UK (http://cancer.sanger.ac.uk/cancergenome/projects/cosmic/). This database is designed to store and display somatic mutation information and related details and information related to human cancers. It contains information on publications, samples and mutations that can query by tissue, histology or gene.

Copy number variation (CNV) can be defined as the number of copies (gain or loss) of a particular gene in the genotype of an individual. CNV has recently emerged as an important tool in understanding heritable source of human genomic differences. It has been shown to contribute to genetic susceptibility of various common and complex diseases. Recent evidence shows that the gene copy number can be elevated in cancer cells. Fig. 62 shows a table of primary tissues with percentage CNV for DNA Polλ (A) and Pol*μ* (B). The CNV data is represented for both loss (orange) and gain (blue) in histogram and total number of samples analyzed (tested column).

It is highly remarkable that in the case of Polλ and with the exception of endometrium, there is a general loss in the cancer tissues tested. On the contrary, Pol*μ* presents a gain of CNV in most of the tissues shown. Comparing both polymerases we might think that there is a correlation or balance among them in the tissues analyzed. Polλ, which seems to be the most faithful polymerase able to maintain DNA integrity in delicate situations thanks to its ability to deal with repeated sequences or long gaps with some complementarity in NHEJ, has a loss in cancer tissues. This loss is counteracted with the gain of Pol*μ* in the same tissues. In this thesis we described a mutagenic behavior for Pol*μ* in a specific sequence context that could result in the generation of frameshifts and

A

Cosmic » Gene » Analysis » POLL

Tissue	Copy Number Variation	
	Variant %	Tested
Endometrium		246
NS		30
Ovary		462
Lung		476
Breast		852
Kidney		300
Large intestine		486
Haematopoietic and lymphoid		192
Central nervous system		411
Pancreas		29

B

Cosmic » Gene » Analysis » POLM

Tissue	Copy Number Variation	
	Variant %	Tested
Central nervous system		411
Large intestine		486
Lung		476
Kidney		300
Ovary		462
Breast		852
NS		30
Endometrium		246
Pancreas		29
Haematopoietic and lymphoid		192

Figure 62. COSMIC analysis of Copy Number Variations (CNV) in human DNA Polλ (A) and Pol*μ* (B). The CNV data is represented for both loss (orange) and gain (blue) in histogram and total number of samples analyzed (tested column).

sequence expansions. If cancer cells take advantage of this ability, it makes sense that cancer tissues present a gain of CNV in Pol*μ*, meaning that it contributes to create genomic instability in these tissues. Interestingly, in a study analyzing Polλ expression in bronchial tissues from smokers, expression correlated with the amount of smoking in normal tissues, but not in cancer tissues; and lack of Polλ expression in heavy smokers was linked to an advanced tumor stage (Ohba et al. 2009).

Besides, a single nucleotide polymorphism in Polλ has been associated to rectal cancer, and the corresponding mutation displays a mutator phenotype, and compromises the NHEJ pathway (Capp et al. 2010; Terrados et al. 2009). It is a{, #0;Capp, 2010 #85}lso remarkable that Polλ, which participates in the tolerance of 8oxoG lesions, loses CNV in cancer breast, lung, ovarian, and colorectal cancer. The most frequent mutations found in these cancers are G:C to T:A transversion mutations (Greenman et al. 2007; Pleasance et al. 2010), confirming the importance of this polymerase to avoid the mutagenicity caused by the formation of 8oxoG:dAMP mispairs during DNA replication.

In the fight for cancer, many approaches are commonly used: from surgical approaches to radiotherapy or chemotherapy by using different cytotoxic drugs. Cancer survival and treatment response to radiotherapy or cytotoxic drugs have been often related to sequence duplications in DNA repair involving DNA polymerases. Hence, DNA polymerases seem to be a potential target for inhibitors for improving the efficacy of cancer therapy, and consequently, survival rate amongst patients. Recently it has been described an additive or synergistic effect in human colorectal cancer cells combining H_2O_2 and TMZ treatments, suggesting that there are compounds able to enhance the sensitivity of these cells to this combined therapy and thus, having the potential to reduce the dosage of DNA damaging agents (Strittmatter et al. 2014). Besides, the study of the contribution of the different DNA polymerases in every type of cancer might lead to select them as clinical biomarkers for particular cancer therapies.

Recently, different methods that link DNA repair and prognosis in cancer have been described. In the first study based on Multiple Myeloma (MM) patients, a DNA repair score (DRScore) obtained from a consensus list of 84 DNA repair genes, resulted to be strongly predictive for both patients' event-free and overall survival. From that consensus list of 84 DNA repair genes, 17 had a bad prognostic value and 5 a good prognostic value for both event-free and overall survival of previously-untreated MM patients. Interestingly, Polλ is one of the 5 genes with good prognosis, confirming that the presence of this polymerase benefits DNA repair and prevents cells from genetic instability. A second study describes a method to quantify the efficiency of DNA repair pathways in the context of cancer therapy. The recombination proficiency score (RPS) is based on the expression levels for four genes involved in DNA repair pathway (Rif1, PARI, RAD51, and Ku80); a high expression of these genes yields a low RPS, increasing mutagenesis, clinical features and inferior survival rates for patients, suggesting that HR suppression contributes to the genomic instability that fuels malignant progression. The method was validated in patients with breast or non-small cell lung carcinomas. This adverse prognosis associated with low RPS was diminished if patients received adjuvant chemotherapy, suggesting that HR suppression and associated sensitivity to platinum-based drugs counteract the adverse prognosis associated with low RPS (Escudero et al. 2014). This equilibrium in NHEJ/HR was confirmed in a recent paper where Polμ deficiency triggers a lineage specific compensatory increase in HR activity (Escudero et al. 2014).

In next future it would be interesting to analyze expression of HR genes in our DK mouse model to evaluate if the deficiency of these two polymerases stimulate the expression of genes involved in HR in order to counterbalance the absence of these proteins involved in NHEJ. Besides, as the HR overexpression is lineage specific, it would be interesting to check if this increase in gene expression of HR genes coincides with tissues where NHEJ proteins are downregulated, expanding this analysis to different diseases like cancer.

DRS score, RPS or the balance between NHEJ and HR are some examples of what the future holds for medicine. These advances might help to select which therapies will be effective for individual patients, thereby enabling more personalized care. The involvement of these two DNA

polymerases in specific cancers will help to elucidate a more personalized treatment by choosing target-specific drugs.

Medicine is becoming more and more personalized, individualizing treatment for each patient. Continuing the study of these polymerases and their potential use as clinical biomarkers to select for certain combined chemotherapies and radiotherapy, with the ultimate goal of individualizing cancer treatment, will help to improve in noninvasive cancer treatment and specially, in specific treatment-resistant tumors.

CONCLUSIONES

1. Proponemos un modelo de expansión de dinucleótidos mediado por Pol*μ* en función del contexto de secuencia. En este modelo Pol*μ* requiere diferentes substratos de DNA, incluidos aquellos que pueden mimetizar los intermediarios de NHEJ.

2. Además, nuestro estudio mecanístico señaló los residuos His329 y Arg387 de Pol*μ* humana como responsables de la regulación de la expansión de nucleótidos que ocurre durante las transiciones de reparación de DNA, o bien promoviendo o bien bloqueando, respectivamente, mediante polimeración iterativa.

3. la ausencia de Pol*μ* puede provocar una reparación menos eficiente en NHEJ pero más conservadora en el cerebro de ratones de edad avanzada. Utilizando extractos de tejidos de ratones deficientes en Pol*μ* demostramos una reducción en la tasa de error en la síntesis en los ratones Pol$\mu^{-/-}$ cuando soportan lesiones de tipo 8oxoG.

4. Polλ puede estar implicado en las expansiones somáticas en la enfermedad de Huntington (HD). Combinamos ratones R6/1(N-mutante Htt) con ratones deficientes de Polλ. El análisis somático de la expansión revela que Polλ está implicada en este proceso, ya que los ratones R6/1;Polλ-/- muestran una menor expansión somática de CAG e incluso lo transmiten a sucesivas generaciones.

5. Además, el área de las inclusiones de huntingtina está reducida en los ratones R6/1;Polλ-/-, pero contrariamente a lo esperado, la prevención de esta expansión no disminuye la progresión de la enfermedad en características como la deficiencia motora o la pérdida de peso.

6. Hemos desarrollado un modelo de ratón deficiente en ambas polimerasas, el cual era tanto viable como fértil. Obtuvimos fibroblastos embrionarios de ratón (MEFs) deficientes en Polλ, Pol*μ* o en ambas (DK).

7. Los MEFs procedentes del doble KO son más sensibles a diferentes agentes de daño al DNA (desde agentes oxidantes (TBH, H_2O_2) a análogos de nucleósidos utilizados en medicina como agente quimioterapéuticos (Citarabina, Fludarabina, Etopósido), así como su supervivencia frente a radiación ionizante) que los MEFs control procedentes de ratones silvestres, indicando una mayor inestabilidad genómica debido a la ausencia de estas dos polimerasas.

8. Los MEFs DK presentan un daño persistente en el DNA en tiempo y el ciclo celular se ve drásticamente afectado provocando un mayor arresto en G2/M. Los MEFs DK entran en senescencia antes que los MEFs control.

9. Hemos desarrollado varias quimeras intercambiando dos dominios específicos: “Loop 1”, presente de manera específica en Pol*μ* y TdT confiriendo un rol muy importante a Pol*μ* tanto en NHEJ como en la actividad transferasa terminal, y un dominio “nail” presente en Polλ que interactúa con la hebra molde. En esta tesis hemos podido evaluar *in vivo* estas quimeras confirmando la importancia de estos residuos reconociendo la secuencia en el contexto de NHEJ.

10. También hemos demostrado también que la fosforilación de ciertos residuos específicos aumenta la actividad de las polimerasas λ durante NHEJ.

CONCLUSIONS

1. Polμ requires an initial dislocation that must be subsequently stabilized, to generate large sequence expansions at different DNA substrates, including those that mimic NHEJ intermediates.
2. Our mechanistic studies pointed at human Polμ residues His329 and Arg387 as responsible for regulating nucleotide expansions occurring during DNA repair transactions, either promoting or blocking, respectively, iterative polymerization.
3. The absence of Polμ could provoke a less efficient but more conservative NHEJ repair in the brain of old mice. By using tissue extracts from mice deficient in Polμ, we demonstrated a reduced error-prone synthesis in the Polμ-KO mice when tolerating 8oxoG lesions.
4. Polλ might be implicated in the promotion of CAG repeat expansion in somatic cells in Huntington's disease. We combined R6/1(N-mutant Htt) mice with Polλ knockout mice. Analysis of somatic expansion reveals that Polλ is implicated in this process, since R6/1;Polλ$^{-/-}$ mice showed lower CAG repeat somatic expansion and even contraction transmitted to successive generations.
5. In addition, the area of huntingtin inclusions is reduced in R6/1;Polλ$^{-/-}$ mice, but contrary to expect, prevention of this expansion does not preclude disease progression such as motor impairment or weight loss.
6. We have developed a mouse model deficient in both polymerases, which is viable and fertile. We have obtained Mouse Embryonic Fibroblasts (MEFs) deficient in ether Polλ, Polμ or in both (Double KO).
7. DK MEFs present more genetic instability than wt MEFs. DK MEFs are more sensitive to drugs related to DNA damage: from oxidative agents (TBH, H_2O_2) to nucleoside analogous used in medicine as a chemotherapeutical agents (Cytarabine, Fludarabine, Etoposide). Double KO MEFs are three times more sensitive to ionizing radiation than wt MEFs.
8. DK MEFs present persistent DNA damage in time and cell cycle is drastically affected provoking major arrest in G2/M. DK MEFs entry in senescence earlier than wt MEFs.
9. We have developed various chimeras interchanging two specific domains: 'Loop 1', specifically present in Polμ and TdT which confers an important role in Polμ's NHEJ and terminal transferase activity; and a 'nail' domain present in Polλ that interacts with the template strand. We have demonstrated *in vivo* the importance of these two residues involved in NHEJ.
10. We have also demonstrated *in vivo* that the phosphorylation of specific residues enhances Polλ's activity during NHEJ.

BIBLIOGRAPHY

Ahnesorg, P., Smith, P., and Jackson, S. P. (2006), 'XLF interacts with the XRCC4-DNA ligase IV complex to promote DNA nonhomologous end-joining', *Cell,* 124 (2), 301-13.
Allinson, S. L., Dianova, II, and Dianov, G. L. (2001), 'DNA polymerase beta is the major dRP lyase involved in repair of oxidative base lesions in DNA by mammalian cell extracts', *The EMBO journal,* 20 (23), 6919-26.
Amoroso, A., et al. (2008), 'DNA polymerases and oxidative damage: friends or foes?', *Current molecular pharmacology,* 1 (2), 162-70.
Andrade, P., et al. (2009), 'Limited terminal transferase in human DNA polymerase mu defines the required balance between accuracy and efficiency in NHEJ', *Proc Natl Acad Sci U S A,* 106 (38), 16203-8.
Arana, M. E., et al. (2008), 'Low-fidelity DNA synthesis by human DNA polymerase theta', *Nucleic acids research,* 36 (11), 3847-56.
Babu, J. R., et al. (2003), 'Rae1 is an essential mitotic checkpoint regulator that cooperates with Bub3 to prevent chromosome missegregation', *The Journal of cell biology,* 160 (3), 341-53.
Bacolla, A. and Wells, R. D. (2004), 'Non-B DNA conformations, genomic rearrangements, and human disease', *The Journal of biological chemistry,* 279 (46), 47411-4.
Bartek, J. and Lukas, J. (2007), 'DNA damage checkpoints: from initiation to recovery or adaptation', *Current opinion in cell biology,* 19 (2), 238-45.
Bassing, C. H. and Alt, F. W. (2004), 'The cellular response to general and programmed DNA double strand breaks', *DNA repair,* 3 (8-9), 781-96.
Bebenek, K. and Kunkel, T. A. (1990), 'Frameshift errors initiated by nucleotide misincorporation', *Proceedings of the National Academy of Sciences of the United States of America,* 87 (13), 4946-50.
--- (2004), 'Functions of DNA polymerases', *Advances in protein chemistry,* 69, 137-65.
Bebenek, K., et al. (2003), 'The frameshift infidelity of human DNA polymerase lambda. Implications for function', *The Journal of biological chemistry,* 278 (36), 34685-90.
Bebenek, K., et al. (2005), 'Biochemical properties of Saccharomyces cerevisiae DNA polymerase IV', *The Journal of biological chemistry,* 280 (20), 20051-8.
Bebenek, K., et al. (2001), '5'-Deoxyribose phosphate lyase activity of human DNA polymerase iota in vitro', *Science,* 291 (5511), 2156-9.
Ben-Porath, I. and Weinberg, R. A. (2005), 'The signals and pathways activating cellular senescence', *The international journal of biochemistry & cell biology,* 37 (5), 961-76.
Bennett, R. A., et al. (1997), 'Interaction of human apurinic endonuclease and DNA polymerase beta in the base excision repair pathway', *Proceedings of the National Academy of Sciences of the United States of America,* 94 (14), 7166-9.
Berger, F., et al. (2013), 'The impact of single-nucleotide polymorphisms (SNPs) in OGG1 and XPC on the age at onset of Huntington disease', *Mutation research,* 755 (2), 115-9.
Bertocci, B., et al. (2006), 'Nonoverlapping functions of DNA polymerases mu, lambda, and terminal deoxynucleotidyltransferase during immunoglobulin V(D)J recombination in vivo', *Immunity,* 25 (1), 31-41.
Bertocci, B., et al. (2003), 'Immunoglobulin kappa light chain gene rearrangement is impaired in mice deficient for DNA polymerase mu', *Immunity,* 19 (2), 203-11.
Bertocci, B., et al. (2002), 'Cutting edge: DNA polymerases mu and lambda are dispensable for Ig gene hypermutation', *Journal of immunology,* 168 (8), 3702-6.
Beucher, A., et al. (2009), 'ATM and Artemis promote homologous recombination of radiation-induced DNA double-strand breaks in G2', *The EMBO journal,* 28 (21), 3413-27.
Biade, S., et al. (1998), 'Impairment of proliferating cell nuclear antigen-dependent apurinic/apyrimidinic site repair on linear DNA', *The Journal of biological chemistry,* 273 (2), 898-902.

Boudsocq, F., et al. (2004), 'Investigating the role of the little finger domain of Y-family DNA polymerases in low fidelity synthesis and translesion replication', *The Journal of biological chemistry,* 279 (31), 32932-40.

Boule, J. B., Rougeon, F., and Papanicolaou, C. (2001), 'Terminal deoxynucleotidyl transferase indiscriminately incorporates ribonucleotides and deoxyribonucleotides', *The Journal of biological chemistry,* 276 (33), 31388-93.

Braithwaite, D. K. and Ito, J. (1993), 'Compilation, alignment, and phylogenetic relationships of DNA polymerases', *Nucleic acids research,* 21 (4), 787-802.

Braithwaite, E. K., et al. (2005a), 'DNA polymerase lambda mediates a back-up base excision repair activity in extracts of mouse embryonic fibroblasts', *The Journal of biological chemistry,* 280 (18), 18469-75.

Braithwaite, E. K., et al. (2005b), 'DNA polymerase lambda protects mouse fibroblasts against oxidative DNA damage and is recruited to sites of DNA damage/repair', *The Journal of biological chemistry,* 280 (36), 31641-7.

Brissett, N. C., et al. (2011), 'Structure of a preternary complex involving a prokaryotic NHEJ DNA polymerase', *Molecular cell,* 41 (2), 221-31.

Brook, J. S., et al. (2009), 'Familial and non-familial smoking: effects on smoking and nicotine dependence', *Drug and alcohol dependence,* 101 (1-2), 62-8.

Burgers, P. M., et al. (2001), 'Eukaryotic DNA polymerases: proposal for a revised nomenclature', *J Biol Chem,* 276 (47), 43487-90.

Cabaniols, J. P., et al. (2001), 'Most alpha/beta T cell receptor diversity is due to terminal deoxynucleotidyl transferase', *The Journal of experimental medicine,* 194 (9), 1385-90.

Caldecott, K. W., et al. (1996), 'XRCC1 polypeptide interacts with DNA polymerase beta and possibly poly (ADP-ribose) polymerase, and DNA ligase III is a novel molecular 'nick-sensor' in vitro', *Nucleic acids research,* 24 (22), 4387-94.

Campisi, J., et al. (2001), 'Cellular senescence, cancer and aging: the telomere connection', *Experimental gerontology,* 36 (10), 1619-37.

Cann, I. K. and Ishino, Y. (1999), 'Archaeal DNA replication: identifying the pieces to solve a puzzle', *Genetics,* 152 (4), 1249-67.

Cao, J., et al. (2006), 'Mitochondrial and nuclear DNA damage induced by curcumin in human hepatoma G2 cells', *Toxicological sciences : an official journal of the Society of Toxicology,* 91 (2), 476-83.

Capp, J. P., et al. (2010), 'The R438W polymorphism of human DNA polymerase lambda triggers cellular sensitivity to camptothecin by compromising the homologous recombination repair pathway', *Carcinogenesis,* 31 (10), 1742-7.

Cardozo-Pelaez, F., et al. (1999), 'Oxidative DNA damage in the aging mouse brain', *Movement disorders : official journal of the Movement Disorder Society,* 14 (6), 972-80.

Catapano, C. V., Chandler, K. B., and Fernandes, D. J. (1991), 'Inhibition of primer RNA formation in CCRF-CEM leukemia cells by fludarabine triphosphate', *Cancer research,* 51 (7), 1829-35.

Chappell, C., et al. (2002), 'Involvement of human polynucleotide kinase in double-strand break repair by non-homologous end joining', *The EMBO journal,* 21 (11), 2827-32.

Chen, L., et al. (2000), 'Interactions of the DNA ligase IV-XRCC4 complex with DNA ends and the DNA-dependent protein kinase', *The Journal of biological chemistry,* 275 (34), 26196-205.

Covo, S., Blanco, L., and Livneh, Z. (2004), 'Lesion bypass by human DNA polymerase mu reveals a template-dependent, sequence-independent nucleotidyl transferase activity', *J Biol Chem,* 279 (2), 859-65.

Daley, J. M., et al. (2005), 'DNA joint dependence of pol X family polymerase action in nonhomologous end joining', *The Journal of biological chemistry,* 280 (32), 29030-7.

de Laat, W. L., Jaspers, N. G., and Hoeijmakers, J. H. (1999), 'Molecular mechanism of nucleotide excision repair', *Genes & development,* 13 (7), 768-85.

Dianova, II, et al. (2004), 'XRCC1-DNA polymerase beta interaction is required for efficient base excision repair', *Nucleic acids research,* 32 (8), 2550-5.
Dobbs, T. A., Tainer, J. A., and Lees-Miller, S. P. (2010), 'A structural model for regulation of NHEJ by DNA-PKcs autophosphorylation', *DNA repair,* 9 (12), 1307-14.
Dogliotti, E., et al. (2001), 'The mechanism of switching among multiple BER pathways', *Progress in nucleic acid research and molecular biology,* 68, 3-27.
Dominguez, O., et al. (2000), 'DNA polymerase mu (Pol mu), homologous to TdT, could act as a DNA mutator in eukaryotic cells', *The EMBO journal,* 19 (7), 1731-42.
Dragileva, E., et al. (2009), 'Intergenerational and striatal CAG repeat instability in Huntington's disease knock-in mice involve different DNA repair genes', *Neurobiology of disease,* 33 (1), 37-47.
Duvauchelle, J. B., et al. (2002), 'Human DNA polymerase mu (Pol mu) exhibits an unusual replication slippage ability at AAF lesion', *Nucleic Acids Res,* 30 (9), 2061-7.
Escudero, B., et al. (2014), 'Polmu deficiency increases resistance to oxidative damage and delays liver aging', *PloS one,* 9 (4), e93074.
Espejel, S. and Blasco, M. A. (2002), 'Identification of telomere-dependent "senescence-like" arrest in mouse embryonic fibroblasts', *Experimental cell research,* 276 (2), 242-8.
Esteban, V., Martin, M. J., and Blanco, L. (2013), 'The BRCT domain and the specific loop 1 of human Polmu are targets of Cdk2/cyclin A phosphorylation', *DNA Repair (Amst),* 12 (10), 824-34.
Esteva, F. J., et al. (2001), 'Chemotherapy of metastatic breast cancer: what to expect in 2001 and beyond', *The oncologist,* 6 (2), 133-46.
Estey, E., et al. (1987), 'Variables predicting response to high dose cytosine arabinoside therapy in patients with refractory acute leukemia', *Leukemia,* 1 (8), 580-3.
Fernandez-Capetillo, O., et al. (2002), 'DNA damage-induced G2-M checkpoint activation by histone H2AX and 53BP1', *Nature cell biology,* 4 (12), 993-7.
Fortini, P., et al. (2003), '8-Oxoguanine DNA damage: at the crossroad of alternative repair pathways', *Mutation research,* 531 (1-2), 127-39.
Garcia-Diaz, M., et al. (2001), 'Identification of an intrinsic 5'-deoxyribose-5-phosphate lyase activity in human DNA polymerase lambda: a possible role in base excision repair', *J Biol Chem,* 276 (37), 34659-63.
Garcia-Diaz, M., et al. (2006), 'Structural analysis of strand misalignment during DNA synthesis by a human DNA polymerase', *Cell,* 124 (2), 331-42.
Garcia-Diaz, M., et al. (2000), 'DNA polymerase lambda (Pol lambda), a novel eukaryotic DNA polymerase with a potential role in meiosis', *Journal of molecular biology,* 301 (4), 851-67.
Garcia-Diaz, M., et al. (2002), 'DNA polymerase lambda, a novel DNA repair enzyme in human cells', *J Biol Chem,* 277 (15), 13184-91.
Garcia-Escudero, R., et al. (2003), 'DNA polymerase X of African swine fever virus: insertion fidelity on gapped DNA substrates and AP lyase activity support a role in base excision repair of viral DNA', *Journal of molecular biology,* 326 (5), 1403-12.
Gilfillan, S., et al. (1993), 'Mice lacking TdT: mature animals with an immature lymphocyte repertoire', *Science,* 261 (5125), 1175-8.
Gonitel, R., et al. (2008), 'DNA instability in postmitotic neurons', *Proceedings of the National Academy of Sciences of the United States of America,* 105 (9), 3467-72.
Gonzalez-Barrera, S., et al. (2005), 'Characterization of SpPol4, a unique X-family DNA polymerase in Schizosaccharomyces pombe', *Nucleic Acids Res,* 33 (15), 4762-74.
Goodarzi, A. A. and Jeggo, P. A. (2009), "A mover and a shaker': 53BP1 allows DNA doublestrand breaks a chance to dance and unite', *F1000 biology reports,* 1, 21.
Gottlieb, T. M. and Jackson, S. P. (1993), 'The DNA-dependent protein kinase: requirement for DNA ends and association with Ku antigen', *Cell,* 72 (1), 131-42.

Gozalbo-Lopez, B., et al. (2009), 'A role for DNA polymerase mu in the emerging DJH rearrangements of the postgastrulation mouse embryo', *Mol Cell Biol,* 29 (5), 1266-75.
Grabarz, A., et al. (2012), 'Initiation of DNA double strand break repair: signaling and single-stranded resection dictate the choice between homologous recombination, non-homologous end-joining and alternative end-joining', *American journal of cancer research,* 2 (3), 249-68.
Grawunder, U., et al. (1997), 'Activity of DNA ligase IV stimulated by complex formation with XRCC4 protein in mammalian cells', *Nature,* 388 (6641), 492-5.
Greenman, C., et al. (2007), 'Patterns of somatic mutation in human cancer genomes', *Nature,* 446 (7132), 153-8.
Gryk, M. R., et al. (2002), 'Mapping of the interaction interface of DNA polymerase beta with XRCC1', *Structure,* 10 (12), 1709-20.
Guirouilh-Barbat, J., et al. (2007), 'Defects in XRCC4 and KU80 differentially affect the joining of distal nonhomologous ends', *Proceedings of the National Academy of Sciences of the United States of America,* 104 (52), 20902-7.
Hartenstine, M. J., Goodman, M. F., and Petruska, J. (2002), 'Weak strand displacement activity enables human DNA polymerase beta to expand CAG/CTG triplet repeats at strand breaks', *The Journal of biological chemistry,* 277 (44), 41379-89.
Hartlerode, A. J. and Scully, R. (2009), 'Mechanisms of double-strand break repair in somatic mammalian cells', *The Biochemical journal,* 423 (2), 157-68.
Havener, J. M., et al. (2003), 'Translesion synthesis past platinum DNA adducts by human DNA polymerase mu', *Biochemistry,* 42 (6), 1777-88.
Hefferin, M. L. and Tomkinson, A. E. (2005), 'Mechanism of DNA double-strand break repair by non-homologous end joining', *DNA repair,* 4 (6), 639-48.
Hentges, P., et al. (2006), 'Evolutionary and functional conservation of the DNA non-homologous end-joining protein, XLF/Cernunnos', *The Journal of biological chemistry,* 281 (49), 37517-26.
Hirose, F., et al. (1989), 'Difference in the expression level of DNA polymerase beta among mouse tissues: high expression in the pachytene spermatocyte', *Experimental cell research,* 181 (1), 169-80.
Irani, K., et al. (1997), 'Mitogenic signaling mediated by oxidants in Ras-transformed fibroblasts', *Science,* 275 (5306), 1649-52.
Ishiguro, H., et al. (2001), 'Age-dependent and tissue-specific CAG repeat instability occurs in mouse knock-in for a mutant Huntington's disease gene', *Journal of neuroscience research,* 65 (4), 289-97.
Ito, J. and Braithwaite, D. K. (1991), 'Compilation and alignment of DNA polymerase sequences', *Nucleic acids research,* 19 (15), 4045-57.
Jonson, I., Ougland, R., and Larsen, E. (2013), 'DNA repair mechanisms in Huntington's disease', *Molecular neurobiology,* 47 (3), 1093-102.
Juarez, R., et al. (2006), 'A specific loop in human DNA polymerase mu allows switching between creative and DNA-instructed synthesis', *Nucleic Acids Res,* 34 (16), 4572-82.
Karanjawala, Z. E., et al. (2002), 'Oxygen metabolism causes chromosome breaks and is associated with the neuronal apoptosis observed in DNA double-strand break repair mutants', *Current biology : CB,* 12 (5), 397-402.
Keating, M. J., et al. (1982), 'A prognostic factor analysis for use in development of predictive models for response in adult acute leukemia', *Cancer,* 50 (3), 457-65.
Kirouac, K. N. and Ling, H. (2011), 'Unique active site promotes error-free replication opposite an 8-oxo-guanine lesion by human DNA polymerase iota', *Proceedings of the National Academy of Sciences of the United States of America,* 108 (8), 3210-5.
Kolas, N. K., et al. (2007), 'Orchestration of the DNA-damage response by the RNF8 ubiquitin ligase', *Science,* 318 (5856), 1637-40.

Komori, T., et al. (1993), 'Lack of N regions in antigen receptor variable region genes of TdT-deficient lymphocytes', *Science,* 261 (5125), 1171-5.
Kornberg, A. (1957), 'Enzymatic synthesis of deoxyribonucleic acid', *Harvey lectures,* 53, 83-112.
Kovalenko, M., et al. (2012), 'Msh2 acts in medium-spiny striatal neurons as an enhancer of CAG instability and mutant huntingtin phenotypes in Huntington's disease knock-in mice', *PloS one,* 7 (9), e44273.
Kovtun, I. V., Therneau, T. M., and McMurray, C. T. (2000), 'Gender of the embryo contributes to CAG instability in transgenic mice containing a Huntington's disease gene', *Human molecular genetics,* 9 (18), 2767-75.
Kovtun, I. V., Goellner, G., and McMurray, C. T. (2001), 'Structural features of trinucleotide repeats associated with DNA expansion', *Biochemistry and cell biology = Biochimie et biologie cellulaire,* 79 (3), 325-36.
Kovtun, I. V., et al. (2007), 'OGG1 initiates age-dependent CAG trinucleotide expansion in somatic cells', *Nature,* 447 (7143), 447-52.
Kramer, K. M., et al. (1994), 'Two different types of double-strand breaks in Saccharomyces cerevisiae are repaired by similar RAD52-independent, nonhomologous recombination events', *Molecular and cellular biology,* 14 (2), 1293-301.
Kubota, Y., et al. (1996), 'Reconstitution of DNA base excision-repair with purified human proteins: interaction between DNA polymerase beta and the XRCC1 protein', *The EMBO journal,* 15 (23), 6662-70.
Kunkel, T. A. (1985), 'The mutational specificity of DNA polymerases-alpha and -gamma during in vitro DNA synthesis', *The Journal of biological chemistry,* 260 (23), 12866-74.
--- (2004), 'DNA replication fidelity', *The Journal of biological chemistry,* 279 (17), 16895-8.
--- (2009), 'Evolving views of DNA replication (in)fidelity', *Cold Spring Harbor symposia on quantitative biology,* 74, 91-101.
Lee, J. W., et al. (2004), 'Implication of DNA polymerase lambda in alignment-based gap filling for nonhomologous DNA end joining in human nuclear extracts', *J Biol Chem,* 279 (1), 805-11.
Lieber, M. R. (2008), 'The mechanism of human nonhomologous DNA end joining', *The Journal of biological chemistry,* 283 (1), 1-5.
Lieber, M. R., et al. (2004), 'The mechanism of vertebrate nonhomologous DNA end joining and its role in V(D)J recombination', *DNA repair,* 3 (8-9), 817-26.
Lindahl, T., et al. (1993), 'DNA joining in mammalian cells', *Cold Spring Harbor symposia on quantitative biology,* 58, 619-24.
Liu, Y., et al. (2009), 'Coordination between polymerase beta and FEN1 can modulate CAG repeat expansion', *The Journal of biological chemistry,* 284 (41), 28352-66.
Lobrich, M. and Jeggo, P. A. (2007), 'The impact of a negligent G2/M checkpoint on genomic instability and cancer induction', *Nature reviews. Cancer,* 7 (11), 861-9.
Locatelli, G. A., et al. (2010), 'Effect of 8-oxoguanine and abasic site DNA lesions on in vitro elongation by human DNA polymerase in the presence of replication protein A and proliferating-cell nuclear antigen', *The Biochemical journal,* 429 (3), 573-82.
Lopez Castel, A., Cleary, J. D., and Pearson, C. E. (2010), 'Repeat instability as the basis for human diseases and as a potential target for therapy', *Nature reviews. Molecular cell biology,* 11 (3), 165-70.
Lou, Z., et al. (2006), 'MDC1 maintains genomic stability by participating in the amplification of ATM-dependent DNA damage signals', *Molecular cell,* 21 (2), 187-200.
Lu, H. F., et al. (2009), 'Curcumin-induced DNA damage and inhibited DNA repair genes expressions in mouse-rat hybrid retina ganglion cells (N18)', *Neurochemical research,* 34 (8), 1491-7.

Lucas, D., et al. (2005), 'Polymerase mu is up-regulated during the T cell-dependent immune response and its deficiency alters developmental dynamics of spleen centroblasts', *Eur J Immunol,* 35 (5), 1601-11.
Lucas, D., et al. (2009a), 'Altered hematopoiesis in mice lacking DNA polymerase mu is due to inefficient double-strand break repair', *PLoS Genet,* 5 (2), e1000389.
--- (2009b), 'Altered hematopoiesis in mice lacking DNA polymerase mu is due to inefficient double-strand break repair', *PLoS genetics,* 5 (2), e1000389.
Ma, J. L., et al. (2003), 'Yeast Mre11 and Rad1 proteins define a Ku-independent mechanism to repair double-strand breaks lacking overlapping end sequences', *Molecular and cellular biology,* 23 (23), 8820-8.
Ma, Y., et al. (2004), 'A biochemically defined system for mammalian nonhomologous DNA end joining', *Molecular cell,* 16 (5), 701-13.
Maciejewski, M. W., et al. (2001), 'Solution structure of a viral DNA repair polymerase', *Nature structural biology,* 8 (11), 936-41.
Maga, G., et al. (2007), '8-oxo-guanine bypass by human DNA polymerases in the presence of auxiliary proteins', *Nature,* 447 (7144), 606-8.
Maga, G., et al. (2008), 'Replication protein A and proliferating cell nuclear antigen coordinate DNA polymerase selection in 8-oxo-guanine repair', *Proceedings of the National Academy of Sciences of the United States of America,* 105 (52), 20689-94.
Mahajan, K. N., et al. (2002), 'Association of DNA polymerase mu (pol mu) with Ku and ligase IV: role for pol mu in end-joining double-strand break repair', *Mol Cell Biol,* 22 (14), 5194-202.
Mangiarini, L., et al. (1997), 'Instability of highly expanded CAG repeats in mice transgenic for the Huntington's disease mutation', *Nature genetics,* 15 (2), 197-200.
Mangiarini, L., et al. (1996), 'Exon 1 of the HD gene with an expanded CAG repeat is sufficient to cause a progressive neurological phenotype in transgenic mice', *Cell,* 87 (3), 493-506.
Manley, K., et al. (1999), 'Msh2 deficiency prevents in vivo somatic instability of the CAG repeat in Huntington disease transgenic mice', *Nature genetics,* 23 (4), 471-3.
Mao, Z., et al. (2008), 'DNA repair by nonhomologous end joining and homologous recombination during cell cycle in human cells', *Cell cycle,* 7 (18), 2902-6.
Marintchev, A., et al. (2000), 'Domain specific interaction in the XRCC1-DNA polymerase beta complex', *Nucleic acids research,* 28 (10), 2049-59.
Markkanen, E., et al. (2011), 'Ubiquitylation of DNA polymerase lambda', *FEBS letters,* 585 (18), 2826-30.
Markkanen, E., et al. (2012a), 'A switch between DNA polymerases delta and lambda promotes error-free bypass of 8-oxo-G lesions', *Proceedings of the National Academy of Sciences of the United States of America,* 109 (50), 20401-6.
Markkanen, E., et al. (2012b), 'Regulation of oxidative DNA damage repair by DNA polymerase lambda and MutYH by cross-talk of phosphorylation and ubiquitination', *Proceedings of the National Academy of Sciences of the United States of America,* 109 (2), 437-42.
Martin, M. J., Juarez, R., and Blanco, L. (2012), 'DNA-binding determinants promoting NHEJ by human Polmu', *Nucleic Acids Res,* 40 (22), 11389-403.
Martin, M. J., et al. (2013), 'Ribonucleotides and manganese ions improve non-homologous end joining by human Polmu', *Nucleic Acids Res,* 41 (4), 2428-36.
Mason, A. G., et al. (2014), 'Expression levels of DNA replication and repair genes predict regional somatic repeat instability in the brain but are not altered by polyglutamine disease protein expression or age', *Human molecular genetics,* 23 (6), 1606-18.
Mastrianni, D. M., Tung, N. M., and Tenen, D. G. (1992), 'Acute myelogenous leukemia: current treatment and future directions', *The American journal of medicine,* 92 (3), 286-95.
Matsumoto, Y., Kim, K., and Bogenhagen, D. F. (1994), 'Proliferating cell nuclear antigen-dependent abasic site repair in Xenopus laevis oocytes: an alternative pathway of base excision DNA repair', *Molecular and cellular biology,* 14 (9), 6187-97.

Matsuoka, S., et al. (2007), 'ATM and ATR substrate analysis reveals extensive protein networks responsive to DNA damage', *Science,* 316 (5828), 1160-6.
McMurray, C. T. (1999), 'DNA secondary structure: a common and causative factor for expansion in human disease', *Proceedings of the National Academy of Sciences of the United States of America,* 96 (5), 1823-5.
--- (2010), 'Mechanisms of trinucleotide repeat instability during human development', *Nature reviews. Genetics,* 11 (11), 786-99.
Meek, K., et al. (2004), 'The DNA-dependent protein kinase: the director at the end', *Immunological reviews,* 200, 132-41.
Mladenov, E. and Iliakis, G. (2011), 'Induction and repair of DNA double strand breaks: the increasing spectrum of non-homologous end joining pathways', *Mutation research,* 711 (1-2), 61-72.
Mollersen, L., et al. (2012), 'Neil1 is a genetic modifier of somatic and germline CAG trinucleotide repeat instability in R6/1 mice', *Human molecular genetics,* 21 (22), 4939-47.
Moon, A. F., et al. (2007), 'Structural insight into the substrate specificity of DNA Polymerase mu', *Nat Struct Mol Biol,* 14 (1), 45-53.
Morgan, W. F., et al. (1996), 'Genomic instability induced by ionizing radiation', *Radiation research,* 146 (3), 247-58.
Nakamura, J. and Swenberg, J. A. (1999), 'Endogenous apurinic/apyrimidinic sites in genomic DNA of mammalian tissues', *Cancer research,* 59 (11), 2522-6.
Natarajan, A. T. (1993), 'Mechanisms for induction of mutations and chromosome alterations', *Environmental health perspectives,* 101 Suppl 3, 225-9.
Natarajan, A. T., et al. (2008), 'The type and yield of ionising radiation induced chromosomal aberrations depend on the efficiency of different DSB repair pathways in mammalian cells', *Mutation research,* 642 (1-2), 80-5.
Neal, J. A., et al. (2014), 'Unraveling the complexities of DNA-PK autophosphorylation', *Molecular and cellular biology*.
Nick McElhinny, S. A. and Ramsden, D. A. (2003), 'Polymerase mu is a DNA-directed DNA/RNA polymerase', *Molecular and cellular biology,* 23 (7), 2309-15.
Nick McElhinny, S. A., et al. (2005a), 'A gradient of template dependence defines distinct biological roles for family X polymerases in nonhomologous end joining', *Molecular cell,* 19 (3), 357-66.
--- (2005b), 'A gradient of template dependence defines distinct biological roles for family X polymerases in nonhomologous end joining', *Mol Cell,* 19 (3), 357-66.
Ohba, T., et al. (2009), 'Expression of an X-family DNA polymerase, pol lambda, in the respiratory epithelium of non-small cell lung cancer patients with habitual smoking', *Mutation research,* 677 (1-2), 66-71.
Oliveros, M., et al. (1997), 'Characterization of an African swine fever virus 20-kDa DNA polymerase involved in DNA repair', *The Journal of biological chemistry,* 272 (49), 30899-910.
Ollis, D. L., et al. (1985), 'Structure of large fragment of Escherichia coli DNA polymerase I complexed with dTMP', *Nature,* 313 (6005), 762-6.
Ortega, Z., Diaz-Hernandez, M., and Lucas, J. J. (2007), 'Is the ubiquitin-proteasome system impaired in Huntington's disease?', *Cellular and molecular life sciences : CMLS,* 64 (17), 2245-57.
Parrinello, S., et al. (2003), 'Oxygen sensitivity severely limits the replicative lifespan of murine fibroblasts', *Nature cell biology,* 5 (8), 741-7.
Petruska, J., Hartenstine, M. J., and Goodman, M. F. (1998), 'Analysis of strand slippage in DNA polymerase expansions of CAG/CTG triplet repeats associated with neurodegenerative disease', *The Journal of biological chemistry,* 273 (9), 5204-10.

Pfeiffer, P., Goedecke, W., and Obe, G. (2000), 'Mechanisms of DNA double-strand break repair and their potential to induce chromosomal aberrations', *Mutagenesis,* 15 (4), 289-302.

Picher, A. J., et al. (2006), 'Promiscuous mismatch extension by human DNA polymerase lambda', *Nucleic Acids Res,* 34 (11), 3259-66.

Pleasance, E. D., et al. (2010), 'A small-cell lung cancer genome with complex signatures of tobacco exposure', *Nature,* 463 (7278), 184-90.

Prakash, S., Johnson, R. E., and Prakash, L. (2005), 'Eukaryotic translesion synthesis DNA polymerases: specificity of structure and function', *Annual review of biochemistry,* 74, 317-53.

Prasad, R., Beard, W. A., and Wilson, S. H. (1994), 'Studies of gapped DNA substrate binding by mammalian DNA polymerase beta. Dependence on 5'-phosphate group', *The Journal of biological chemistry,* 269 (27), 18096-101.

Rafehi, H., et al. (2011), 'Clonogenic assay: adherent cells', *Journal of visualized experiments : JoVE,* (49).

Rai, K. R., et al. (2000), 'Fludarabine compared with chlorambucil as primary therapy for chronic lymphocytic leukemia', *The New England journal of medicine,* 343 (24), 1750-7.

Ramsden, D. A. (2011), 'Polymerases in nonhomologous end joining: building a bridge over broken chromosomes', *Antioxid Redox Signal,* 14 (12), 2509-19.

Ramsden, D. A. and Asagoshi, K. (2012), 'DNA polymerases in nonhomologous end joining: are there any benefits to standing out from the crowd?', *Environ Mol Mutagen,* 53 (9), 741-51.

Rosenberg, B. (1985), 'Fundamental studies with cisplatin', *Cancer,* 55 (10), 2303-l6.

Roth, D. B. and Wilson, J. H. (1986), 'Nonhomologous recombination in mammalian cells: role for short sequence homologies in the joining reaction', *Molecular and cellular biology,* 6 (12), 4295-304.

Ruiz, J. F., et al. (2013), 'Yeast pol4 promotes tel1-regulated chromosomal translocations', *PLoS Genet,* 9 (7), e1003656.

Ruiz, J. F., et al. (2001), 'DNA polymerase mu, a candidate hypermutase?', *Philos Trans R Soc Lond B Biol Sci,* 356 (1405), 99-109.

Ruiz, J. F., et al. (2003), 'Lack of sugar discrimination by human Pol mu requires a single glycine residue', *Nucleic Acids Res,* 31 (15), 4441-9.

Ruiz, J. F., et al. (2004), 'Overexpression of human DNA polymerase mu (Pol mu) in a Burkitt's lymphoma cell line affects the somatic hypermutation rate', *Nucleic Acids Res,* 32 (19), 5861-73.

Sale, J. E., Lehmann, A. R., and Woodgate, R. (2012), 'Y-family DNA polymerases and their role in tolerance of cellular DNA damage', *Nature reviews. Molecular cell biology,* 13 (3), 141-52.

Sawaya, M. R., et al. (1997), 'Crystal structures of human DNA polymerase beta complexed with gapped and nicked DNA: evidence for an induced fit mechanism', *Biochemistry,* 36 (37), 11205-15.

Schofield, M. J. and Hsieh, P. (2003), 'DNA mismatch repair: molecular mechanisms and biological function', *Annual review of microbiology,* 57, 579-608.

Sekiguchi, J. M. and Ferguson, D. O. (2006), 'DNA double-strand break repair: a relentless hunt uncovers new prey', *Cell,* 124 (2), 260-2.

Sharpless, N. E. and DePinho, R. A. (2004), 'Telomeres, stem cells, senescence, and cancer', *The Journal of clinical investigation,* 113 (2), 160-8.

Sherr, C. J. and DePinho, R. A. (2000), 'Cellular senescence: mitotic clock or culture shock?', *Cell,* 102 (4), 407-10.

Shimazaki, K., et al. (2012), 'p53 Retards cell-growth and suppresses etoposide-induced apoptosis in Pin1-deficient mouse embryonic fibroblasts', *Biochemical and biophysical research communications,* 422 (1), 133-8.

Showalter, A. K., et al. (2001), 'Solution structure of a viral DNA polymerase X and evidence for a mutagenic function', *Nature structural biology,* 8 (11), 942-6.
Shrivastav, M., De Haro, L. P., and Nickoloff, J. A. (2008), 'Regulation of DNA double-strand break repair pathway choice', *Cell research,* 18 (1), 134-47.
Singhal, R. K. and Wilson, S. H. (1993), 'Short gap-filling synthesis by DNA polymerase beta is processive', *The Journal of biological chemistry,* 268 (21), 15906-11.
Sobol, R. W., et al. (1996), 'Requirement of mammalian DNA polymerase-beta in base-excision repair', *Nature,* 379 (6561), 183-6.
Streisinger, G., et al. (1966), 'Frameshift mutations and the genetic code. This paper is dedicated to Professor Theodosius Dobzhansky on the occasion of his 66th birthday', *Cold Spring Harbor symposia on quantitative biology,* 31, 77-84.
Strittmatter, T., et al. (2014), 'Expanding the scope of human DNA polymerase lambda and beta inhibitors', *ACS chemical biology,* 9 (1), 282-90.
Sugo, N., et al. (2000), 'Neonatal lethality with abnormal neurogenesis in mice deficient in DNA polymerase beta', *The EMBO journal,* 19 (6), 1397-404.
Sugo, N., et al. (2004), 'p53 Deficiency rescues neuronal apoptosis but not differentiation in DNA polymerase beta-deficient mice', *Molecular and cellular biology,* 24 (21), 9470-7.
Szklarczyk, D., et al. (2011), 'The STRING database in 2011: functional interaction networks of proteins, globally integrated and scored', *Nucleic acids research,* 39 (Database issue), D561-8.
Takashima, Y., et al. (2009), 'Dependence of DNA double strand break repair pathways on cell cycle phase in human lymphoblastoid cells', *Environmental and molecular mutagenesis,* 50 (9), 815-22.
Takata, M., et al. (1998), 'Homologous recombination and non-homologous end-joining pathways of DNA double-strand break repair have overlapping roles in the maintenance of chromosomal integrity in vertebrate cells', *The EMBO journal,* 17 (18), 5497-508.
Takeuchi, T., et al. (2006), 'Structural relationship of curcumin derivatives binding to the BRCT domain of human DNA polymerase lambda', *Genes to cells : devoted to molecular & cellular mechanisms,* 11 (3), 223-35.
Teo, S. H. and Jackson, S. P. (1997), 'Identification of Saccharomyces cerevisiae DNA ligase IV: involvement in DNA double-strand break repair', *The EMBO journal,* 16 (15), 4788-95.
Terrados, G., et al. (2009), 'Characterization of a natural mutator variant of human DNA polymerase lambda which promotes chromosomal instability by compromising NHEJ', *PLoS One,* 4 (10), e7290.
Todaro, G. J. and Green, H. (1963), 'Quantitative studies of the growth of mouse embryo cells in culture and their development into established lines', *The Journal of cell biology,* 17, 299-313.
Tome, S., et al. (2013), 'MSH3 polymorphisms and protein levels affect CAG repeat instability in Huntington's disease mice', *PLoS genetics,* 9 (2), e1003280.
Tseng, H. M. and Tomkinson, A. E. (2002), 'A physical and functional interaction between yeast Pol4 and Dnl4-Lif1 links DNA synthesis and ligation in nonhomologous end joining', *The Journal of biological chemistry,* 277 (47), 45630-7.
van Loon, B. and Hubscher, U. (2009), 'An 8-oxo-guanine repair pathway coordinated by MUTYH glycosylase and DNA polymerase lambda', *Proceedings of the National Academy of Sciences of the United States of America,* 106 (43), 18201-6.
Vogel, H., et al. (1999), 'Deletion of Ku86 causes early onset of senescence in mice', *Proceedings of the National Academy of Sciences of the United States of America,* 96 (19), 10770-5.
Walker, J. R., Corpina, R. A., and Goldberg, J. (2001), 'Structure of the Ku heterodimer bound to DNA and its implications for double-strand break repair', *Nature,* 412 (6847), 607-14.

Watson, J. D. and Crick, F. H. (1953), 'The structure of DNA', *Cold Spring Harbor symposia on quantitative biology,* 18, 123-31.
Wells, R. D., et al. (2005), 'Advances in mechanisms of genetic instability related to hereditary neurological diseases', *Nucleic acids research,* 33 (12), 3785-98.
West, S. C. (2003), 'Molecular views of recombination proteins and their control', *Nature reviews. Molecular cell biology,* 4 (6), 435-45.
Williams, G. J., et al. (2014), 'Structural insights into NHEJ: Building up an integrated picture of the dynamic DSB repair super complex, one component and interaction at a time', *DNA repair,* 17, 110-20.
Wilson, D. M., 3rd and McNeill, D. R. (2007), 'Base excision repair and the central nervous system', *Neuroscience,* 145 (4), 1187-200.
Wilson, T. E. and Lieber, M. R. (1999), 'Efficient processing of DNA ends during yeast nonhomologous end joining. Evidence for a DNA polymerase beta (Pol4)-dependent pathway', *The Journal of biological chemistry,* 274 (33), 23599-609.
Wilson, T. E., Grawunder, U., and Lieber, M. R. (1997), 'Yeast DNA ligase IV mediates non-homologous DNA end joining', *Nature,* 388 (6641), 495-8.
Wimmer, U., et al. (2008), 'Control of DNA polymerase lambda stability by phosphorylation and ubiquitination during the cell cycle', *EMBO reports,* 9 (10), 1027-33.
Woo, R. A. and Poon, R. Y. (2004), 'Activated oncogenes promote and cooperate with chromosomal instability for neoplastic transformation', *Genes & development,* 18 (11), 1317-30.
Yan, C. T., et al. (2007), 'IgH class switching and translocations use a robust non-classical end-joining pathway', *Nature,* 449 (7161), 478-82.
Yaneva, M., Kowalewski, T., and Lieber, M. R. (1997), 'Interaction of DNA-dependent protein kinase with DNA and with Ku: biochemical and atomic-force microscopy studies', *The EMBO journal,* 16 (16), 5098-112.
Zhou, B. B. and Elledge, S. J. (2000), 'The DNA damage response: putting checkpoints in perspective', *Nature,* 408 (6811), 433-9.

APPENDIX